Train^{2}Wind

Training fellows in enTrainment in offshore Wind Power

A European Doctoral Network

Edited by: Mara Günther, Gregor Giebel and Haakon Lund
Duration: 2020–2024
Led by: DTU Wind Energy

Funded by the European Union

Cover
Photo of the Rødsand II offshore wind farm by Mikael Sjöholm.

Disclaimer
Funded by the European Union, project no. 861291. Views and opinions expressed are however those of the author(s) only and do not necessarily reflect those of the European Union or the European Climate, Infrastructure and Environment Executive Agency (CINEA). Neither the European Union nor the granting authority can be held responsible for them.

Acknowledgements
This deliverable was developed based on collective efforts from all partners of the Train²Wind project.

This project is funded by the European Union Horizon Europe Framework programme 2020 under grant agreement no. 861291.

Funded by the European Union

Summary

The Train^{2}Wind project started out of curiosity about how many wind turbines can be packed close together in the North Sea, giving consideration to effect of wake losses. The plans for buildout offshore, but especially in the North Sea were large and getting even larger, in the tens of GW. While wake modelling behind a single turbine has been studied since the 1980's, wind farm wakes and the effects of large wind farms only came into focus in the 2000s - 2010s. Wind farm wakes being thought of as independent of the development of the atmospheric boundary layer were investigated then, but for the very large wind farms coming, it is intuitively clear that there also should be an influence on the wider weather and wind resource patterns. Accordingly, Train^{2}Wind chose to concentrate on very extended wind farms or wind farm clusters, which extend with a large density of turbines for so long that the atmosphere reaches a new equilibrium.

A Marie Curie action allows to address a common problem from various angles. We found the necessary expertise in a relatively small consortium, consisting of the Technical University of Denmark (DTU), the Geophysical Institute at the University of Bergen (UiB), the Ecole Polytechnique Federal de Lausanne (EPFL), the Eberhard-Karls-University in Tübingen (EKUT) and the University of Copenhagen (UCPH). Additionally, we invited three of the largest offshore wind developers to the consortium (Vattenfall, Equinor and RWE), a company for vertical axis turbines (SeaTwirl) and Charles Meneveau from the University of Johns Hopkins University (JHU). In the end, we trained 13 PhD students and 6 short-term fellows. One of the fellows had the others as research topic, investigating the collaboration aspects between the students and groups from a humanities perspective (UCPH).

In the consortium, we chose expertise within wind and wind farm modelling with Large Eddy Simulations (LES) (DTU and EPFL), the mesoscale WRF model including wind farm parameterisations inside the model (DTU), built a small wind farm in a wind tunnel (EPFL), had an expert in wind speed observations from satellite (DTU), two groups performing lidar observations (UiB and DTU), and two groups with Uncrewed Aerial Systems (UAS) expertise (EKUT and UiB).

A major endeavour during the course of the Train^{2}Wind project was a planned experimental campaign at such a wind farm. Alas, the largest wind farms at the time were 40km long, and very far offshore, so that a campaign as the envisioned one was going to be very expensive. We therefore found an older wind farm in the South of Denmark, with easy access for the Danish, German and Norwegian partners. While the large planned offshore campaign including UAS and dedicated boats for the lidars eluded us due to permitting issues, and thereby the main goal of getting a definitive answer to the wind farm spacing question, Train^{2}Wind created progress for being able to investigate the research questions further, both from a conceptual and an experimental side. We were able to (for the first time) measure the wind with two lidars on a ship at many places inside and outside an offshore wind farm, aided by a scanning lidar from the substation for a shorter time period.

We also improved satellite based SAR image conversion to wind speeds, and developed a turbulence model as well as improved the wind farm parameterisation in weather models. The turbulence influence in a flow model was investigated, and the measurements of turbulence by UAS was shown to be able in a virtual environment. An improved analytical wake modelling framework was developed, and another one was used for wind farm control. We also improved modelling for vertical axis turbines. For the experimental side, we developed a particle measurement and a much faster hygrometer, a flying sonic anemometer and a motion controlled ship-borne lidar. The time for 5-hole probe calibration was cut from a day to 20 minutes using robotics. Using this, for the first time, Kelvin-Helmholtz billows were detected over a working wind farm. All those individual results and the trained fellows will bring the modelling and measurements of wind farm flows forward.

Authors and Affiliations

Technical University of Denmark - Wind and Energy Systems

Gregor Giebel
Dr.
Principal Investigator
grgi@dtu.dk

Tuhfe Göçmen
Dr.
Training Coordinator
tuhf@dtu.dk

Anna Maria Sempreviva
Emeritus
Training Coordinator
anse@dtu.dk

Jakob Mann
Prof. Dr.
Science Coordinator
jmsq@dtu.dk

Mikael Sjöholm
Dr.
Supervisor
misj@dtu.dk

Jake Badger
Dr.
Supervisor
jaba@dtu.dk

Søren Juhl Andersen
Dr.
Supervisor
sjan@dtu.dk

Nicolau Conti Gost
ESR
nicgo@dtu.dk

David Robert Verelst
Dr.
Supervisor
dave@dtu.dk

Charlotte Bay Hasager
Prof. Dr.
Supervisor
cbha@dtu.dk

Abdul Haseeb Syed
ESR
absy@dtu.dk

Oscar Manuel Garcia Santiago
ESR
osmasa@dtu.dk

Abdalmenem Owda
ESR
abow@dtu.dk

Emily Louise Hodgson
ESR
emlh@dtu.dk

Faegheh Pish
ESR
faepi@dtu.dk

University of Tübingen - Department of Geosciences

Jens Bange
Prof. Dr.
WP3 leader
jens.bange
@uni-tuebingen.de

Andreas Platis
PD Dr.
Supervisor
andreas.platis
@uni-tuebingen.de

Matteo Bramati
ESR
matteo.bramati
@uni-tuebingen.de

Vasileios Savvakis
ESR
vasileios.savvakis
@uni-tuebingen.de

Gabriela Miranda-Garcia
ESR
gabriela.miranda-garcia
@uni-tuebingen.de

Mosaab Sajidi
ESR
mosaab.sajidi
@uni-tuebingen.de

Nicholas Ceccon Libardi
ESR
nicholas.ceccon-libardi
@uni-tuebingen.de

University of Copenhagen - Department of Communication

Haakon Lund
Associate Professor
Supervisor
hl@hum.ku.dk

Morten Hertzum
Professor
Supervisor
mhz@ruc.dk

Frans van der Sluis
Associate Professor
Supervisor
frans@hum.ku.dk

Grischa Fraumann
ESR
grischa.fraumann@hamk.fi

Mara Günther
RA
mgr@hum.ku.dk

École Polytechnique Fédérale de Lausanne - Wind Engineering and Renewable Energy Laboratory

Fernando Porté-Agel
Prof. Dr.
WP1 leader
fernando.porte-agel@epfl.ch

Arslan Salim Dar
Dr.
Supervisor
arslan.dar@epfl.ch

Marwa Souaiby
ESR
marwa.souaiby@epfl.ch

Konstantinos Kotsarinis
ESR
konkotsa@stanford.edu

Guiyue Duan
ESR
guiyue.duan@epfl.ch

Guillem Armengol Barcos
ESR
garmengol@armen5.com

University of Bergen - Geophysical Institute and Bergen Offshore Wind Centre (BOW)

Joachim Reuder
Prof. Dr.
WP2 leader
joachim.reuder@uib.no

Shokoufeh Malekmohammadi
ESR
shokoufeh.malekmohammadi@uib.no

Mauro Ghirardelli
ESR
mauro.ghirardelli@uib.no

Contents

Introduction

Gregor Giebel, Tuhfe Göçmen, Jake Badger and Jakob Mann

The Train^{2}Wind project started out from an idea of figuring out how many wind turbines can be packed close together in the North Sea, giving consideration to effect of wake losses. The plans for buildout offshore, but especially in the North Sea were large and getting even larger, in the tens of GW. While wake modelling behind a single turbine has been studied since the 1980's [8], wind farm wakes and the effects of large wind farms, first modelled as increased surface roughness, only came into focus in the 2000s - 2010s [1, 3]. Gregor Giebel's own interest had shown already in GG's PhD, analysing smoothing and distribution effects of wind energy collection across Europe [6], but was renewed when, in his role as the convener of the wind power meteorology session at the European Geophysics Union General Assembly in Vienna, two talks were scheduled directly after each other: one by Lee Miller detailing from a planetary energy balance perspective that there are limits to the exploitation of wind energy [9], and another one by Christina Archer, who just had published one of the most noted global wind assessments [4]. Miller [9] based on first principles came to quite different and lower limits for wind power exploitation than the assessment integrated over Archers results [4]. The year after, Miller et al presented a poster juxtapositioning assessments based on global principles, and local assessments for the entire globe [2]. He worked out that the global resource assessments necessarily had higher results, since the local assessments were assuming single non-waked turbines, while the planetary scale assessments were taking a view of a global installation a high density of turbines which would reduce the wind significantly. It is worth noting that the different approaches to assess large scale wind resources, either coming from wind farms project scale and scaling-up or coming from more academic studies of global coverage were described in [10] and [12]. Furthermore the different approaches can be combined and bring increased confidence in the result obtained, as in the 2020 study of offshore resources in the German Bight [5].

The main research questions investigated in Train^{2}Wind can then be listed as:

- How large is "infinite", and is there a limit for installation / exploitation for "infinite" wind farms?
- How does the wind turbine atmospheric boundary layer (WTABL) develop?
- What factors influence that development?
- Can it be controlled?
- What is the influence of sea spray on the development?
- How does a network of heterogeneous European researchers collaborate and share information/data?

Accordingly, for Train^{2}Wind, we chose to concentrate on very extended wind farms or wind farm clusters, which extend with a large density of turbines for so long that the atmosphere reaches a new equilibrium. A good visualisation comes from Charles Meneveau's group [11], which we ended up inviting to Train^{2}Wind to be a host for two students:

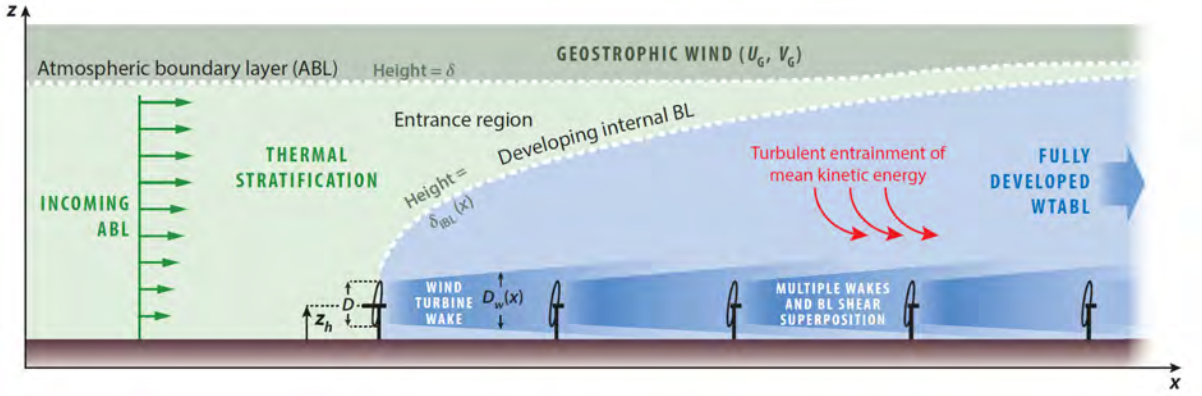

Figure 1: Various fluid mechanical flow phenomena in wind farms, including wakes, their superposition, and interactions with the atmospheric boundary layer (ABL), development of internal boundary layers, and, if a wind farm is large enough, the attainment of a fully developed wind turbine array boundary layer (WTABL) regime.

Conceptually, the disturbance of the surface layer grows in the flow going over the wind farm until it hits the Atmospheric Boundary Layer (ABL) height. At this stage, a new equilibrium is established, which Meneveau ([11]) calls a Wind Turbine Array Boundary Layer. However, the length at which this happens is uncertain. A survey among the participants of the kick-off meeting yielded a consensus around 100km. As the undisturbed wind entering the wind farm from the front conceptually is used up at this stage, all new energy comes into the wind farm from above through entrainment. The entrainment process in a very extended wind farm was therefore the main concept to be investigated.

A Marie Curie action allows to address a common problem from various angles. We found the necessary expertise in a relatively small consortium, consisting of ourselves (the Technical University of Denmark, DTU), the Geophysical Institute at the University of Bergen (UiB), the Ecole Polytechnique Federal de Lausanne (EPFL), the Eberhard-Karls-University in Tübingen (EKUT) and the University of Copenhagen (UCPH). Additionally, we invited three of the largest offshore wind developers to the consortium (Vattenfall, Equinor and RWE), a company for vertical axis turbines (SeaTwirl) and Charles Meneveau from the University of Johns Hopkins University (JHU).

In the consortium, we chose expertise within wind and wind farm modelling with Large Eddy Simulations (LES)(DTU and EPFL), the mesoscale WRF model including wind farm parameterisations inside the model (DTU), built a small wind farm in a wind tunnel (EPFL), had an expert in wind speed observations from satellite (DTU), two groups performing lidar observations (UiB and DTU), and two groups with Uncrewed Aerial Systems (UAS) expertise (EKUT and UiB). Additionally, we had one group looking at the collaboration aspects between the students and groups from a humanities perspective (UCPH).

A major endeavour during the course of the Train^{2}Wind project was a planned experimental campaign at such a wind farm. The problem was, the largest wind farms at the time were 40km long, and very far offshore, so that a campaign as the envisioned one was going to be very expensive. While there is some money allocated to the science in a Marie Curie action, it is more for a lab experiment and some consumables, and not enough for renting boats, getting people out on a hotel ship for several weeks and for the transport of expensive measurement equipment or getting extra UAS as well. Therefore, we had to find an offshore wind farm within range of the UAS we employed, preferably of the industry partners (Vattenfall, Equinor and RWE), and found an older one in the South of Denmark, with easy access for the Danish (DTU), German (Uni Tübingen) and Norwegian (Uni Bergen) partners. The Rødsand II wind farm became operational in 2010, consists of 90 turbines of 2.3 MW with rotor diameters of 93 m and is operated by RWE. The hub height is 68.5m, which by modern standards is a rather small wind farm, with a non-regular shape. It was already earlier the target of investigations during the EERA-DTOC project [7], where we tested wake models for the farm scale using the wake of the Nysted wind farm (the more regular looking one to the east) and the turbine power in the Rødsand II wind farm (the arc-shaped westerly one) as a measurement.

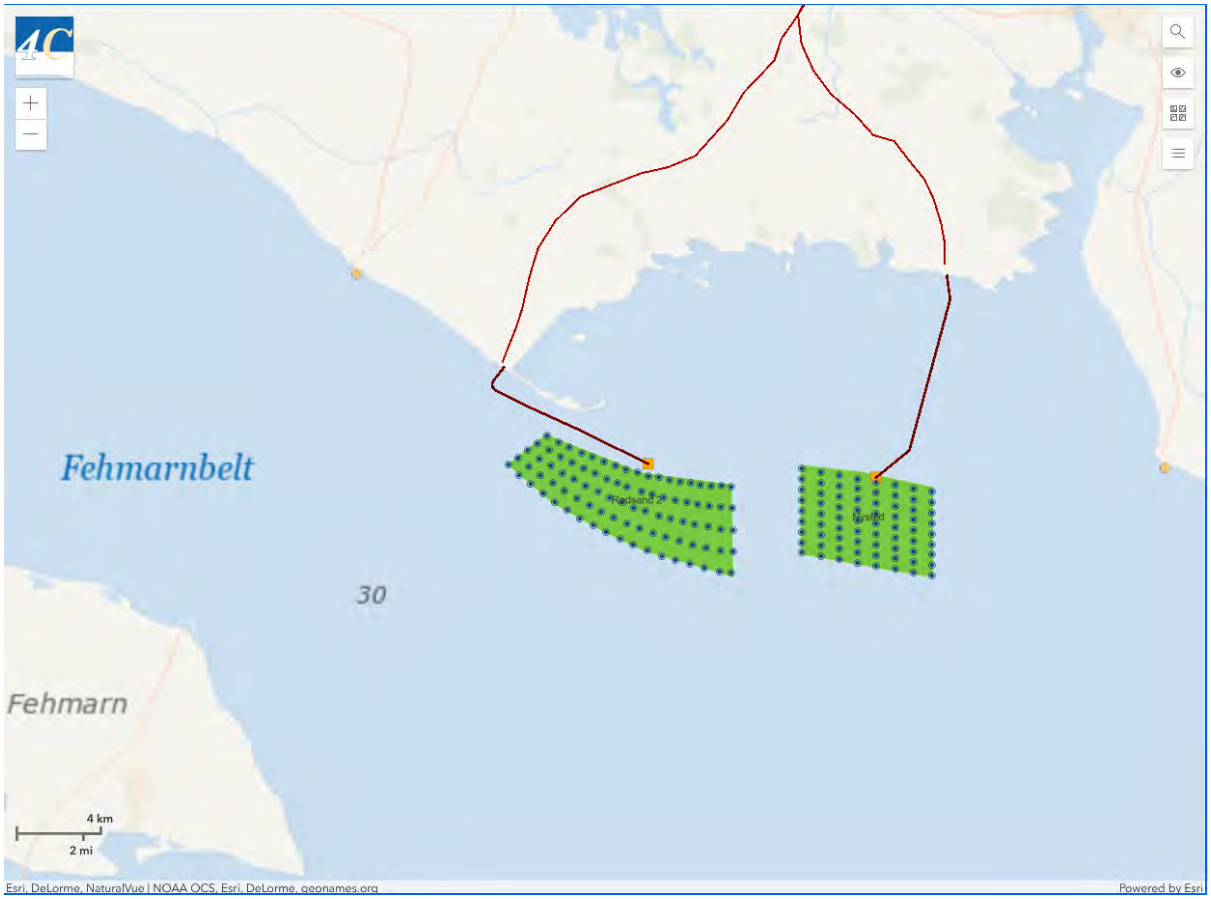

Figure 2: Rødsand II wind farm and Nysted wind farm as testing grounds. Source: 4COffshore.

Our plan was to put scanning lidars on the substation, to get a dedicated ship for a couple of vertically staring lidars to be sailed underneath the scanning lidar scans, and to have the

UAS using their 120km range to fly from the shore to the farm, make some passes in the lidar area, and then to return to the shore in a rather automated flight path Beyond Visual Line of Sight (BVLOS). The UAS were equipped with wind, pressure, humidity and temperature sensors and would have complemented the lidar measurements quite nicely. However, by the time we had defined the experiment, we did not manage to get the flight permits from the Danish Transport Authority. So we postponed the flight measurements by half a year (from one semester break in Tübingen to the next), and decided to at least have the lidars measuring from the boat deck of the Crew Transfer Vessel (CTV), which once a day brought technicians from Rødby harbour (the orange dot on the map to the west of Rødsand II) to several turbines in the wind farm and back in the evening. At the same time we wanted to get the scanning lidar installed on the substation and start measurements. Unfortunately, a week before DTU's technician was scheduled to do the scouting trip to the substation, someone blew up the NordStream pipelines, and Energinet (the Danish TSO owning the substation) decided to tighten security and not let other personnel get on the substation. So the installation of the scanning lidar also was delayed by several months, until Energinet opened up for visitors again. Despite the half year postponement, the Transport Authority still were not able to issue a flight permit in time for the planned measurements. We therefore decided to also forego the dedicated lidar ship, and just asked the CTV (RWE was very helpful throughout the experiment) to go a few times under the lidar track. A more detailed description of the dataset is forthcoming, and the data will be set free eventually.

Figure 3: The planned campaign at Rødsand II.

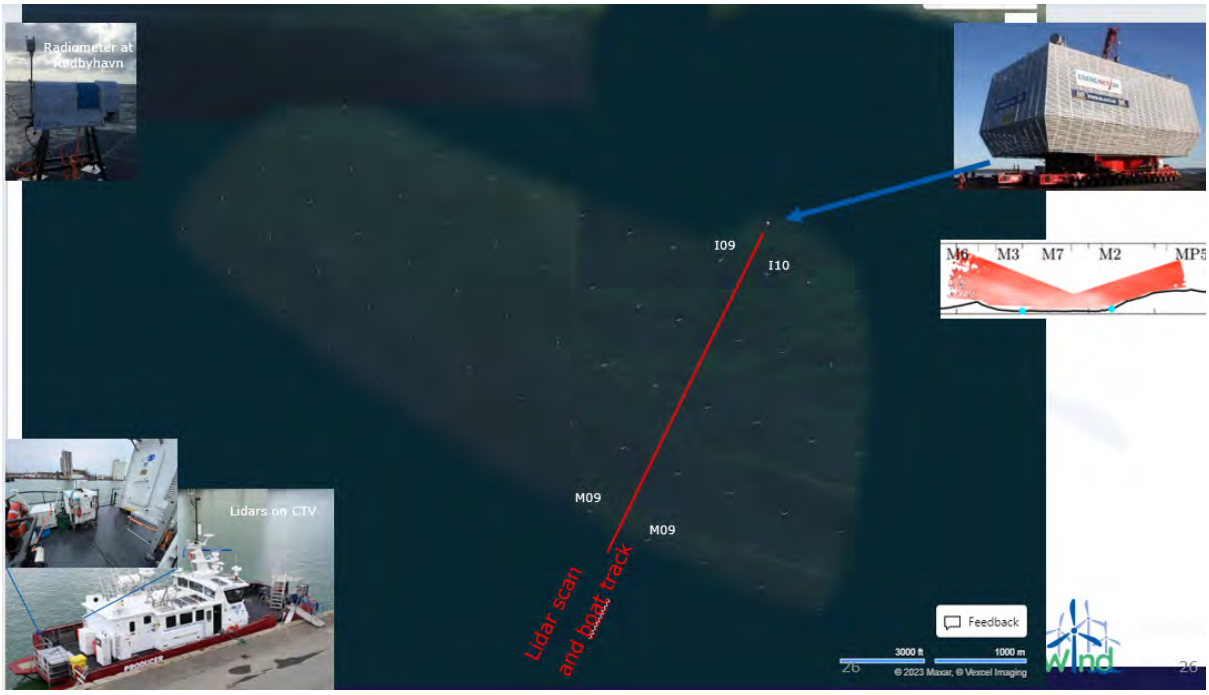

Figure 4: The actual measurements at Rødsand II.

In order to investigate the flow around and over wind farms, we employed 13 fellows aiming at a PhD. One fellow took his PhD in information science, with the other fellows being the subjects of investigation analysing how such a diverse group of people can collaborate. In the end, 2 PhD fellows decided to drop out of the program prematurely. We also employed 6 shorter-term (one year to 18 months) fellows for additional work, e.g. for modelling the vertical axis turbine and its wake. One works on vertical axis turbines with partner SeaTwirl, and tries to enable better tools for the design of the turbines, on the belief that a wind farm consisting of vertical axis turbines would have a significantly different wake and entrainment field. Another fellow looks into the possibility to control the wind farm wake and possibly steer it into a given direction. Two more students helped in the wind tunnel.

Training Activities in Train^{2}Wind

While the science in Train^{2}Wind was a unifying and for the involved scientists also satisfying endeavour, the main goal of a Marie Curie action was to train the fellows following three main training objectives:

- To give the fellows the necessary skills to execute their particular research project successfully,
- To give them a broad background in wind energy, so that they are able to frame their own project in the larger picture,
- To give them transferable skills for further personal development, including the employment of better research practices and efficient communication, dissemination, exploitation of research.

Train^{2}Wind Training Schools (TS) designed with these objectives in mind are summarised in the rest of this section. They aim to effectively provide fellows with a robust foundation in offshore wind energy research and by blending theoretical knowledge with practical assignments, the program is tailored to ensure that participants will develop the necessary skills to execute their research projects successfully, understand the broader context of their work within the wind energy sector, and acquire valuable transferable skills for their future careers in both industry and academia.

Training School 1 (TS1): Fundamentals of Offshore Wind Research

Coordinated by the Technical University of Denmark (DTU), the first training school, held online in February and March 2021, was a comprehensive introduction to key concepts in offshore wind research. The initial sessions held in its first part covered crucial topics such as wind farm-atmosphere interactions, microscale modeling, and offshore measurements using wind lidars, delivered by experts like Jakob Mann, Søren Juhl Andersen, Joachim Reuder, and Mikael Sjøholm. Interactive activities like Human Bingo helped participants network effectively. The second part of TS1 continued with discussions on relevant wind energy topics, including offshore measurements with unmanned aircraft systems, mesoscale modeling, wind tunnel challenges, and space-borne remote sensing, with contributions from Jens Bange, Andreas Platis, Jake Badger, Fernando Porte-Agel, and Merete Badger. Assignments during this period required fellows to pitch their projects through videos and blog posts, along with conducting literature reviews relevant to their research areas. The final session in March featured presentations of these pitches and blog posts, feedback sessions in breakout rooms, summaries of literature reviews, and discussions on potential collaborations.

Training School 2 (TS2): Enhancing Research and Publication Skills

The second training school, coordinated by the University of Copenhagen (UCPH) in June 2021, focused on research and publication skills. It began with an introduction to scientific paper writing by Mathias Stolpe from DTU and an overview of research metrics by Grischa Fraumann from UCPH. Subsequent sessions by Falco Hüser from the Royal Library covered open science tools related to publication, and Marianne Gauffriau discussed funding and responsible metrics. The second day concentrated on systematic methods for literature reviews, quality of evidence, and search standards, with sessions led by Lorna Wildgaard from the Royal Library and Haakon Lund from UCPH. Nikola Vasiljevic from DTU introduced machine-actionable metadata and open-source tools. Assignments during this period involved project work to apply the learned concepts. The final day of TS2 addressed diversity in research and engineering, presented by Lise Peitersen from DTU, and featured a lecture on the evolution of wind energy by Henrik Stiesdal from Stiesdal A/S. Students engaged in discussions about the future of wind energy and presented their systematic literature review projects, fostering a deeper understanding and collaborative spirit among the fellows.

Training School 3 (TS3): Data Management and Publication

The third training school, held in September 2021 and coordinated by DTU, focused on data management and publication, crucial for effective research dissemination. The sessions began with Anna Maria Sempreviva from DTU emphasizing the importance of taxonomies in making data FAIR (Findable, Accessible, Interoperable, Reusable) and introduced DTU Wind taxonomies. Afterwards, Signe Gadegaard from the DTU Library provided insights into data publication platforms like DTU Data and Zenodo, highlighting best practices for metadata, versioning, and citation. The hands-on sessions enabled participants to register and publish their data, ensuring they could apply theoretical knowledge practically.

Conclusion and Achievements

While the main goal of getting a definitive answer on how close you can space wind farms eluded us, as well as the large offshore campaign including UAS and dedicated boats for the lidars, Train^{2}Wind created progress for being able to investigate the research questions further, both from a conceptual and an experimental side. The main achievements of Train^{2}Wind are:

- 19 fellows were trained in the field of offshore wind energy, 4 of them already received a PhD for their work
- The collaboration of a large European network of researchers was investigated
- For the first time, two lidars were measuring wind profiles on a ship at many places inside and outside an offshore wind farm, aided by a scanning lidar from the substation for a shorter time period (UiB and DTU)
- Satellite based Synthetic Aperture Radar scans now yield a better conversion to hub height wind speeds (DTU and JHU)
- A dataset for further investigation based on the Lollex campaign is forthcoming
- The importance of the incoming turbulence length scales for wake development was demonstrated using DTU's LES tools
- A new 2D turbulence model for offshore flow improved the representativity of turbulence models for a wider range of frequencies
- Sampling of the turbulence using UAS in a virtual flow field provided by LES was investigated for the Flight Path Generator in combined work of DTU and EKUT
- An improved analytical wake modelling framework was developed at EPFL, being able to get better predictions in shorter time
- The parameterisation of wind farms in meteorological models was improved for both the near wake and the far wake, and implemented in WRF
- A much faster wake model using neural networks trained by RANS results was developed at DTU and used for wind farm control

- Wake control using cyclic yaw control, axial induction and tilt control was shown to be beneficial in EPFLs wind tunnel, also taking the influcence of thermal stability into account
- DTUs tools for modelling vertical axis wind turbines was improved doing LES experiments for training HAWC2
- Motion compensation of ship-borne lidars now allows to use them with accuracy similar to a fixed based lidar (UiB)
- For the first time, Kelvin-Helmholtz billows were detected over a working wind farm (UiB and RWE)
- For Uncrewed Aerial Systems, a novel 5-hole probe calibration robot was developed at EKUT, cutting the time for calibration from 1 day to 20 minutes
- A novel flying particle counter including an air dryer was developed at EKUT, able to sample dry and wet particles separately
- A research grade sonic anemometer was flown on a rope and on a boom by UiB as the novel SAMURAI UAS in an experiment in France
- A miniature chilled-mirror hygrometer able to fly on a UAS with one order of magnitude higher sampling rate (10Hz) was developed and demonstrated at EKUT

References

[1] David W. Keith et al. "The influence of large-scale wind power on global climate". In: *Proceedings of the National Academy of Sciences* 101 (46 2004), pp. 16115–16120.

[2] Lee M. Miller et al. "Two methods for estimating limits to large-scale wind power generation". In: *PNAS* 112 (36 2015), pp. 11169–11174.

[3] Sten T. Frandsen et al. "The making of a second-generation wind farm efficiency model complex". In: *Wind Energy: An International Journal for Progress and Applications in Wind Power Conversion Technology* 12 (5 2009), pp. 445–458.

[4] Cristina L. Archer and Mark Z. Jacobson. "Evaluation of global wind power". In: *Journal of Geophysical Research* 110 (2005).

[5] Agora Energiewende and Agora Verkehrswende. "Making the Most of Offshore Wind: Re-Evaluating the Potential of Offshore Wind in the German North Sea". In: *Environmental Research Letters* (2020).

[6] Gregor Giebel. "On the benefits of distributed generation of wind energy in Europe". PhD thesis. Carl von Ossietzky Universität Oldenburg, 2001.

[7] Kurt S. Hansen and Charlotte Hasager. "Validation of wake models for (two) wind farms". In: (2014).

[8] N.O. Jensen. "A note on wind generator interaction". In: *Risø National Laboratory* Risø-M No. 2411 (1983).

[9] F. Gans L. M. Miller and A. Kleidon. "Estimating maximum global land surface wind power extractability and associated climatic consequences". In: *Earth System Dynamics* 2 (1 2011).

[10] Jake Badger Patrick J. H. Volker Andrea N Hahmann and Hans E. Jørgensen. "Prospects for generating electricity by large onshore and offshore wind farms: Letter". In: *Environmental Research Letters* 12 (3 2017).

[11] Richard J.A.M. Stevens and Charles Meneveau. "Flow Structure and Turbulence in Wind Farms". In: *ANNUAL REVIEW OF FLUID MECHANICS* 49 (2017).

[12] Patrick J. H. Volker and Jake Badger. "Efficient large-scale wind turbine deployment can meet global electricity generation needs". In: *Proc Natl Acad Sci* 114 (2017).

Collaboration in a data intensive network of Ph.D-fellows - experiences from Train^{2}Wind

Grischa Fraumann, Frans van der Sluis, Morten Hertzum and Haakon Lund

Ph.D. projects within a specific Innovative Training Network (ITNs) are interconnected, necessitating collaboration across different organizations and fulfilling requirements set by both the host organization and the ITN. Collaboration often occurs during secondments, which are research training periods involving physical mobility. Unlike many other Ph.D. fellowships, MSCA funding supports these intersectoral and international mobility periods, which are considered crucial for every stage of research careers.

With the current development in the digitalization of the wind energy sector [3] Ph.D. fellows are increasingly embedded in data-intensive research environments, which involve processing large volumes of complex data from experiments or simulations. This reliance on data necessitates collaboration due to the varied competencies required, from data acquisition to validation and visualization, often beyond the capacity of individuals. Researchers must pool expertise, resources, and data access from multiple organizations. In wind energy, which relies on experimental data from wind farms and simulations, Ph.D. candidates must combine simulations, measurement campaigns, and data analysis while coordinating with various stakeholders, including wind farm developers and local authorities.

As a general phenomenon, scientific collaboration lacks a standard definition but generally means "joint effort toward a common goal." Sonnenwald defines it as interactions among scientists that facilitate task completion and shared goals [11]. Benefits of such collaboration include informal peer review and the ability to rely on the experience of senior researchers. However, challenges exist, such as demanding mobility requirements, conflicts within research alliances, and dependencies on team members. These challenges can overwhelm Ph.D. candidates, who may feel particularly burdened by the need to rely on others for the completion of their degrees. As part of the Train^{2}Wind project, we have studied collaboration within the project with a specific focus on the particular enablers and challenges for PhDs in wind energy.

These studies illustrate how the complexity and interdisciplinarity of data-intensive research make collaboration essential for the success of Ph.D. students and research networks.

Empirical Studies and Methods

Through three studies we gathered data on collaboration using early-stage interviews, late-stage interviews, and in-between observations at measurement campaigns. To date, there is limited research on data-intensive environments and Ph.D. fellows, particularly regarding how early-stage researchers such as Ph.D. fellows navigate these environments [10]. The

present study therefore provides unique insights into how Ph.D. fellows conceive collaboration in a data-intensive environment.

Based on early-stage interviews with 12 Phd students from the Train^{2}Wind Network we analyzed the expectations of PhD-students of collaboration in a data-intensive research environment. As an added benefit it was possible to interview 11 Ph.D fellows from 3 other similar networks adding more interview data about the expectation and experiences from PhD fellows towards collaboration. The interviews were framed with a background in the theory of remote collaboration (TORSC) [9] and gathered data from informants at various research organizations, and R&D firms in several countries. This study focuses on Ph.D. fellows' forward-looking expectations of collaboration, allowing a detailed analysis of the transition phase into a research environment. The interviews were conducted as remote video interview sessions and the collected audio files were subsequently transcribed and coded by the authors of this paper. The resulting codes were sorted into groups using card-sorting during in-person meetings [8, 6].

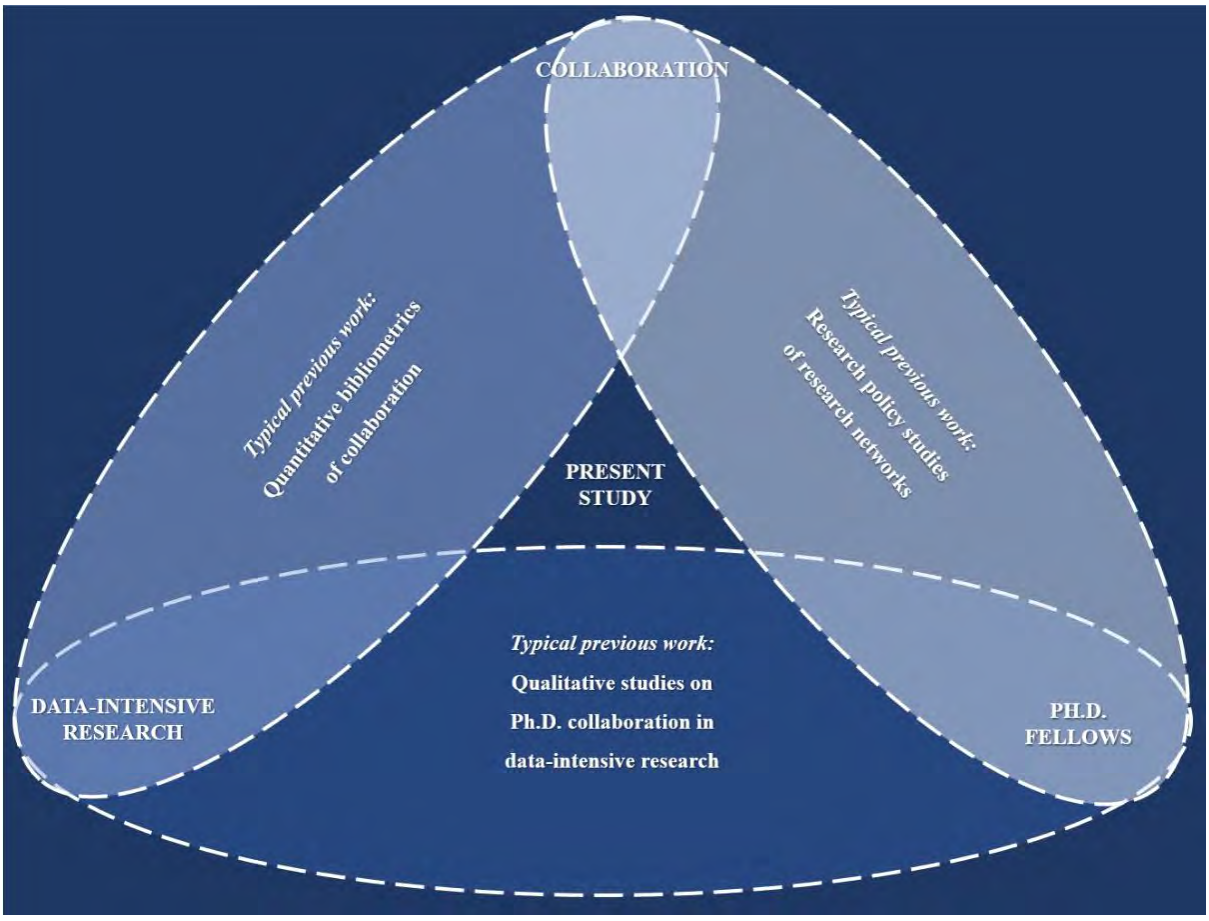

Figure 1: Position of the study. The present study combines three research topics (i.e., collaboration, Ph.D. fellows, and data-intensive research networks).

Framework for studying collaboration

A well established framework for studying collaboration is the Theory of Remote Scientific Collaboration (TORSC). TORSC was preferred as the theoretical framework because of its focus on collaboration in remote and technical environments [1, 7] Train^{2}Wind network can be characterized as relying heavily on remote collaboration due to its distributed structure with partners in several countries and it is to a high degree embedded in a highly technical environment. To guide the interviews with participating ESR, TORSC was used as a framework for developing an interview guide focusing on the following five key elements [9]:

Nature of the Work: Characteristics of the research, which in data-intensive environments can create communication bottlenecks due to the different expertise contributed by team members.

Common Ground: Mutual knowledge and shared understanding, which can be hindered by a lack of shared interests and common vocabulary.

Collaboration Readiness: Individual characteristics and motivations, which may be less developed in early-stage Ph.D. fellows, as their researcher role identity evolves over time within the network.

Organization and Management: The structure and management of collaboration, with known challenges in distributed collaborations and clearly defined roles in EU-funded projects.

Technology Readiness: Availability and proficiency in using the right technologies, which is generally less of an issue in data-intensive networks due to the high level of technical competence.

We derived four themes from our analysis of the collected data, each theme illustrating aspects of collaboration and the challenges experienced by the participating young researchers.

Collaboration is a balancing act

Research collaboration is inherently complex, requiring researchers to balance diverse priorities, collaborators, cultures, and interests [4]. This balancing act involves aligning different cognitive mindsets, managing multiple interdependent teams in a multiteam system, and reconciling various R&D goals between universities and firms [12, 2].

Ph.D. candidates in data-intensive research networks face specific balancing acts. They must balance the expectations and goals of their host university with those of the larger research network, often requiring the use of shared infrastructure and data. For instance, one interviewee highlighted the challenge of integrating knowledge from different facilities, while another emphasized the importance of cultural sensitivity in European projects.

Effective communication is crucial in these collaborations, especially given the reliance on remote interactions. Ph.D. candidates must navigate between local research group require-

ments and the broader network's objectives, balancing their focus on core Ph.D. elements with enriching opportunities from collaboration. This balancing act is further complicated by the need to evaluate the costs and benefits of collaborations in terms of time and resources, a significant challenge at the start of their Ph.D. journey.

Quotes from interviewees illustrate these challenges. One described how collaboration could add to their workload and distract from their primary research goals, while another stressed the importance of careful planning to meet deadlines for both collaborations and other projects. Time constraints, especially within the typical three-year Ph.D. duration, add to the complexity of producing high-quality research outputs while engaging with external collaborators.

An understanding of these balancing acts can feed into a better network organization and is crucial for successful training networks, given their specific focus on PhDs and collaboration.

Overall, Ph.D. candidates in data-intensive networks must balance project-network goals, focus versus enrichment, and timing versus benefits. This intricate process requires managing expectations from both their home institution and the broader network, making collaboration in such settings a true balancing act.

Experiences and expectations differ

Research collaboration, particularly in data-intensive research networks, involves navigating a complex balance of expectations and experiences. Ph.D. candidates often enter these collaborations with optimistic expectations, anticipating numerous opportunities to enhance their research. For example, respondents noted the supportive and encouraging nature of their professors and supervisors, who play a pivotal role in fostering collaborations by leveraging their networks and providing guidance. This optimism is rooted in the early stages of a Ph.D., where the focus is on planning and leveraging existing contacts and infrastructure facilitated by supervisors.

The positive outlook on collaborations is illustrated by interviewees' remarks on the beneficial role of supervisors and the encouragement to engage with external collaborators. Supervisors' involvement is crucial, especially in fields like wind-energy research, where access to infrastructure, data, and industry expertise is often managed through these established networks. For instance, respondents emphasized how supervisors initiate and support collaborations, ensuring that Ph.D. candidates can access necessary resources and expertise.

However, the reality of university-industry collaborations often presents challenges that temper initial expectations. Issues such as data sharing restrictions and limitations imposed by industrial partners can hinder the smooth execution of collaborative projects. Respondents highlighted difficulties in accessing valuable data sets that are not publicly available, which can significantly impact their research progress. These experiences underscore the

need for realistic expectations when engaging in industry collaborations, where proprietary data and internal restrictions can complicate the collaborative process.

The difference between expectations and actual experiences in collaborations is also influenced by prior experience in industry R&D settings. Ph.D. candidates with such backgrounds tend to have more pragmatic views on the availability and accessibility of data and infrastructure. Their firsthand experience with the constraints of industry collaborations helps them set more realistic goals and navigate potential challenges more effectively.

Overall, our analysis suggests that while Ph.D. candidates start with high expectations for collaborations, their experiences gradually shape a more balanced perspective. Supervision plays a critical role in managing these expectations, and prior industry experience helps in formulating realistic collaboration goals. As candidates progress through their Ph.D., they learn to balance their initial optimism with the practical realities of collaboration in a data-intensive research environment. This ongoing adjustment highlights the dynamic nature of research collaboration, where expectations and experiences continuously interact and evolve

Data shape collaboration

Networks can predefine research agendas, making collaboration a necessity rather than an option. This enforced collaboration is embedded in the network's structure, where roles, resources, and tasks are divided among members, as seen in respondents' reliance on data from other Ph.D. students for their projects. While such dependencies can create uncertainties, they also integrate diverse knowledge and perspectives, enriching the Ph.D. experience.

Ph.D. projects within ITNs (Innovative Training Networks) are often interlinked, with data dependencies set at the project proposal stage [5]. This structure, while potentially limiting individual research freedom, ensures a collaborative space that facilitates shared objectives and co-authored publications. For example, some respondents noted that their research questions depended on results from other Ph.D. students, highlighting the collaborative nature of their work.

Despite the predefined aspects, respondents viewed these structures as opportunities rather than constraints. The network's organizational structure and planned activities, such as meetings and secondments, provide additional collaboration opportunities, making the Ph.D. experience more enriching. The necessity of collaboration within the network, enforced through dependencies and predefined structures, ultimately supports a collaborative space that benefits the Ph.D. candidates by offering access to specialized knowledge and facilitating a structured yet enriching research environment.

Social events glue the network together

The COVID-19 pandemic significantly impacted collaborations within research networks by preventing most physical meetings, which are crucial for effective interaction among Ph.D. fellows. The enforced distance disrupted planned activities, such as physical meetings and common fieldwork, which were integral to the projects. This limitation was highlighted by our informants, who emphasized the need for frequent contact and social events to maintain a functional network.

The absence of in-person meetings created challenges for spontaneous interactions and informal problem-solving sessions, as expressed by respondents who missed the ease of face-to-face meetings. For example, one respondent noted, "it is much harder to get in contact with my colleagues in my [organization], and I really miss the possibility of this half hour of face-to-face meeting to solve some questions. [...] COVID is one of the problems that I think that still today we have to deal with" (Interviewee 19). This sentiment underscores the disruption caused by the pandemic, making it difficult to maintain the frequent contact necessary for successful collaboration.

The enforced physical distance stifled many collaborations, particularly within ITNs that started during the pandemic. Respondents reported that the shift to virtual meetings and online conferences hindered the natural flow of collaboration. For instance, one respondent shared, "[all of these ITNs started] during or under corona. [...] For a lot of these collaborations, I think it really stifled that, right? All of these conferences have been online. I've never met another [name of ITN] member and most of the ones that I do know are the ones from here at [name of organization]. I think that does block some of these collaborations" (Interviewee 21). This illustrates how the lack of physical interaction obstructed collaborative efforts.

Respondents also expressed a preference for in-person meetings over virtual ones, highlighting the human element and the ability to better gauge reactions and emotions face-to-face. One respondent mentioned, "[...] it's just very long Zoom meetings every now and then. [...] I mean, it's good. But anyway, I like in-person meetings more. I'm more comfortable with seeing the person, see how they feel, see how they react. It's more human for me" (Interviewee 7). The virtual format, while functional, failed to replicate the dynamics of in-person interactions.

Despite these challenges, respondents adapted by leveraging technologies to maintain continuous communication and share research data. Skills in using collaborative tools became essential, with respondents listing various websites and software used in their daily research practices. However, the extraordinary meeting restrictions during the pandemic added an extra layer of complexity to an already challenging environment, as respondents had to find alternative ways to communicate and collaborate over a distance.

Overall, the pandemic underscored the importance of social events and spontaneous interactions in gluing the network together. While technologies facilitated remote collaboration, the absence of physical meetings created barriers that affected the spontaneity and effec-

tiveness of interactions. This experience highlighted the crucial role of in-person meetings and social events in fostering a collaborative and cohesive research environment.

Perspective

The perspectives on collaboration evolve as candidates adjust their initial optimism to the realities of collaborative research, influenced by prior experiences and ongoing interactions within the network. Supervisors play a critical role in managing expectations and providing guidance, particularly in navigating the complexities of university-industry collaborations where data sharing restrictions can pose significant obstacles.

Despite the challenges, collaboration remains central to the Ph.D. experience, with networks often predefining research agendas and creating a structured space for shared objectives. While the pandemic disrupted physical meetings, highlighting the importance of social events for spontaneous interactions, candidates adapted by leveraging digital tools to maintain collaboration. Ultimately, successful collaboration in these networks requires a nuanced approach to balancing competing demands and leveraging the structured yet flexible environment provided by the network.

References

[1] M. J. Bietz, S. Abrams, D. Cooper, K. R. Stevens, F. Puga, D. Patel, G. M. Olson, and J. S. Olson. "Improving the Odds Through the Collaboration Success Wizard". In: *Translational behavioral medicine* 2.4 (2012), pp. 480–486.

[2] Gabrielle Cederholm. "Success Factors in University-industry Collaborations. A comparison of a research and development project". MA thesis. University of Gothenburg, 2015.

[3] A. Clifton, S. Barber, A. Bray, P. Enevoldsen, J. Fields, A. M. Sempreviva, L. Williams, and et al. "Grand challenges in the digitalisation of wind energy". In: *Wind Energy Science Discussions* 8.6 (2022), pp. 1–42.

[4] Jennifer Dusdal and Justin J W Powell. "Benefits, Motivations, and Challenges of International Collaborative Research: A Sociology of Science Case Study". In: *Science and Public Policy* 48.2 (2021), pp. 235–245.

[5] Mavrina E, Kimble L, Waury K, Gogishvili D, Gómez de San José N, Das S, and et al. "Multi-Omics Interdisciplinary Research Integration to Accelerate Dementia Biomarker Development (MIRIADE)". In: *Frontiers Neurologoy* (2022).

[6] Uwe Flick. *An introduction to qualitative research*. SAGE Publications Ltd, 2022.

[7] Magdelena Haman and Morten Hertzum. "Collaboration in a distributed research program: Islands of intensity in a sea of minimal interaction". In: *Journal of Documentation* 75.2 (2019), pp. 334–48.

[8] Conrad LY and Tucker VM. "Making it tangible: hybrid card sorting within qualitative interviews". In: *Journal of Documentation* 75.2 (2019), pp. 397–416.

[9] Judith S. Olson and Gary M. Olson. *Working Together Apart: Collaboration over the Internet*. Morgan and Claypool Publishers, 2014.

[10] Biswas R, Schiller A, Casolani C, Daoud E, Dode A, and et al. Genitsaridi E. "Doctoral Studies as part of an Innovative Training Network (ITN): Early Stage Researcher (ESR) experiences". In: *Open Research Europe [Internet]* (2021).

[11] Diane H. Sonnenwald. "Scientific collaboration". In: *Annual Review of Information Science and Technology* 41 (2007), pp. 643–81.

[12] Wanzenböck I Wuestman M Frenken K. "A genealogical approach to academic success". In: *PLOS ONE* 15.12 (2020).

Work Package 1

Modelling

Introduction

Fernando Porté-Agel

Optimal design and operation of wind farms requires accurate predictions of the complex two-way interactions between atmospheric boundary layer flow and wind farms. This is a non-trivial task considering the highly turbulent nature of the atmospheric boundary layer flow and the wide range of flow scales involved, from kilometers to millimeters. Specially challenging is the prediction of wind turbine wake flows, which are responsible for substantial power losses and fatigue loads in large wind farms. The interplay between atmospheric turbulence and wind turbine wakes affects their structure and dynamics, as well as their superposition in wind farms [1]. Their cumulative effect leads to the so-called wind farm wakes, which can extend several kilometers downwind, depending on the atmospheric conditions, thus affecting neighboring wind farms in high wind farm density regions such as the North Sea [2].

The main goal of the first workpage (WP1) of Train2Wind is the development and application of state-of-the-art modelling tools to improve our understanding of the multiscale interactions between atmospheric turbulence and wind farms. These efforts can be summarized as follows:

Using turbulence-resolving large-eddy simulation (LES), Hodgson et al. demonstrated the importance of the turbulence length scales of the incoming boundary layer flow on wind turbine wake development and thus power output. These results have implications for the way turbulence is represented in reduced-order models as well as the development of potential wind farm control strategies.

An improved parameterization of wind farms in mesoscales models was introduced by Garcia-Santiago et al.. The new parameterization improves the representation of the turbulence kinetic energy and subgrid-scale wake interactions. It was implemented into the Explicit Wake Parameterization and evaluated against high-resolution computational fluid dynamics methods.

The potential of machine learning for capturing steady-state wake effects in wind farms was investigated by Pish et al.. The tested feed-forward neutral networks predict output features with high degree of accuracy. The results also point to a limitation of the linear superposition model commonly used in analytical wind farm models.

An improved analytical wake modelling framework was proposed by Souaiby and Porté-Agel based on LES of wind farms of different sizes and configurations. The new framework gives more accurate wind farm power predictions and flow predictions, both inside and downstream of the wind farms, compared with existing analytical models commonly used for wind farm optimization.

The potential of different control strategies was studied using experiments at the EPFL boundary-layer wind tunnel. Specifically, Duan and Porté-Agel investigated cyclic yaw con-

trol (CYC) via wind-tunnel experiments. The results show that CYC can lead to considerable power gains in wind farms for a certain range of the control parameters (yawing amplitude and frequency). Barcos and Porté-Agel focused on axial induction and tilt control. The results show that axial induction is not effective for increasing global power production, while tilt control can lead to substantial power improvements. Finally, taking advantage of the temperature control system of the EPFL wind tunnel, Kotsarinis et al. demonstrated the effect of thermal stability on the structure of wind turbine wakes. All these experiments provide unique datasets for the validation of numerical models, from LES to analytical models.

References

[1] F Porté-Agel, M Bastankhah, and S Shamsoddin. "Wind-turbine and wind-farm flows: A review". In: *Boundary-Layer meteorology* 174.1 (2020), pp. 1–59. DOI: 10.1007/s10546-019-00473-0.

[2] J Schneemann, A Rott, M Dorenkamper, G Stenfeld, and M Kuhn. "Cluster wakes impact on far-distant offshore wind farm's power". In: *Wind Energy Science* 5 (2020), pp. 29–49.

Large Eddy Simulations of Energy Entrainment in Wind Turbine Wakes and Wind Farms

Emily Louise Hodgson, Søren Juhl Andersen, Niels Troldborg and Jens Nørkær Sørensen

Introduction

Wind turbines extract kinetic energy from the incoming wind, resulting in a wake region behind the turbine which has a lower velocity and higher turbulence intensity than the freestream flow. When turbines are grouped into wind farms, the turbines operating in wake flow have lower power production and increased structural fatigue. Therefore, accurately predicting and mitigating wake effects in wind farms is a topic of great importance, as it could lead to improved wind farm efficiency and power output. However, wind turbine wakes and wind farm flows are highly chaotic and complex, impacted by the prevalent atmospheric boundary conditions such as turbulence intensity, wind velocity and buoyancy [1, 2], as well as wind farm layout and density [3, 20]. Turbulence is an integral part of wind farm flow physics, as turbulent mixing governs the entrainment of energy into the wake region, and hence how rapidly the wakes recover [27, 4, 16]. In addition to turbulence intensity - a global quantity describing the total amount of velocity fluctuations in the flow - the dynamics and scales of turbulence also are important, and yet their interaction with wakes and wind farms remains poorly understood [19, 7]. Therefore, the aim of this work is to study the interaction between the dynamics of the inflow, wind turbine wakes and wind farms; specifically related to understanding the impact of freestream turbulent scales, both on wake development behind a single turbine and on energy entrainment into wind farms [15].

Numerical Modelling

Large Eddy Simulations (LES) in the DTU in-house flow solver EllipSys3D [21, 26] were used for all simulations in this work. LES is a high-fidelity, time-advancing and turbulence-resolving numerical tool, which can accurately model wind turbines and wind farm flows, given appropriate computational setup and grid resolution. For these studies, flows are generated in LES either using synthetic turbulence generated from the Mann Spectral Model [17, 18] imposed over a constant background flow, or by conducting precursor simulations to generate atmospheric boundary layer inflows, which can also include temperature and buoyancy effects. Turbines are modelled in LES using the actuator disc (AD) [22] or actuator line (AL) [25] method (as resolving the blade geometry is far too computationally expense), which use body forces applied in the CFD domain to model the effect of the wind turbine operation on the flow. In the actuator disc, forces are applied over a disc representing the rotor swept area; in the actuator line, forces are applied over three individual rotating lines, representing the individual blades.

Robust and reliable numerical tools are essential for producing relevant results and conclusions; therefore, the first part of this work consisted of three studies ([11, 13, 9]) which verified and validated the computational setup. Firstly, the coupling of the actuator disc and line to an aeroelastic tool [24] was verified, and the impact of flexibility on the blade loads was studied [11]; secondly, improvements were made to the aeroelastic-coupled actuator line and a validation was performed against fully resolved rotor simulations and measurement data [13]. Lastly, in a collaboration with EPFL, a comparison was conducted between non-neutral atmospheric boundary layer simulations and single wakes operating in those flows, and hence recommendations for grid resolution in order to obtain closely-matching results between different LES codes and AD setups were found [9].

Impact of Inflow Turbulent Scales on Wake Development

The second section of this work moved away from the validation and verification of tools, and towards addressing the primary aim - to investigate the influence of inflow turbulent scales on wake recovery and wind farm flows. Initially, work was conducted using an idealised inflow - a sinusoidal streamwise velocity [10]. A range of inflow Strouhal numbers ($St = fD/U$, where f is the frequency of the inflow fluctuations, D is the turbine diameter, and U is the mean freestream velocity) between $St = 0.25$ and $St = 0.14$ were studied, and flows with larger Strouhal numbers (hence shorter inflow time scales) showed a faster roll-up of the near wake into periodically shed vortex rings and hence a faster wake breakdown.

In a further study [14], a wider range of inflow Strouhal numbers was considered ($St = 0.05 - 0.5$) and a different technique was used to generate the inflows; using a single synthetic turbulence field, which was stretched or compressed such that the flow structures and turbulence intensity were identical, but the scales of the turbulence were different. The results from this study again demonstrated that shorter inflow integral time scales result in a faster breakdown of the tip vortices and transition to far wake turbulence, as can be seen in Figure 1. Hence, entrainment into the wake begins closer to the rotor, and the wake recovers quicker. This had a significant effect on the available downstream power output of subsequent turbines; an increase of 35% solely based on the difference between an inflow with Strouhal number $St = 0.48$ and $St = 0.12$. Therefore, these works demonstrated that the integral time scale of the freestream turbulence has a significant impact on the wake development behind a single turbine, independent of the turbulence intensity.

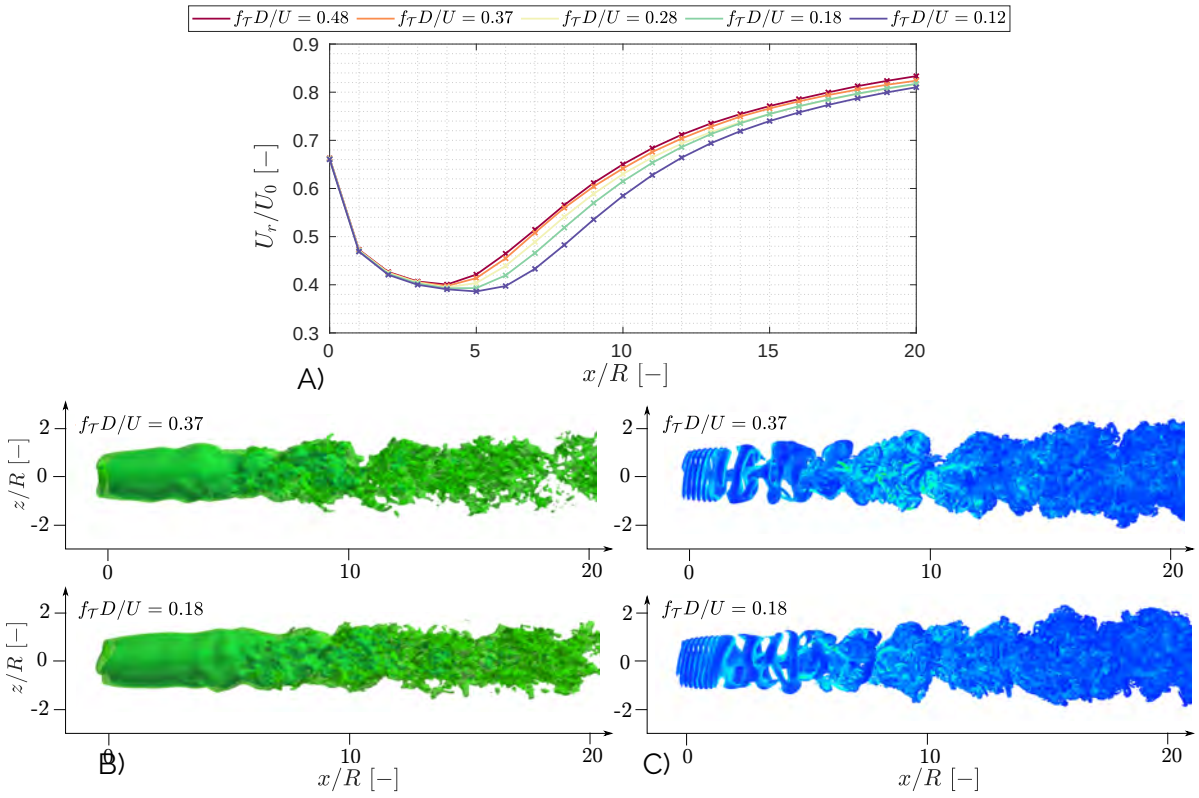

Figure 1: Wake flow under different inflow time scales: A) Normalised mean rotor-averaged velocity in the wake, U_r/U_0; B) Isosurfaces of streamwise velocity at $0.5U_0$ and $0.75U_0$ for $f_T D/U = 0.37$ and $f_T D/U = 0.18$; C) Q-criterion of velocity coloured by vorticity for $f_T D/U = 0.37$ and $f_T D/U = 0.18$. Reproduced from [14].

Energy Entrainment in Wind Farms

The final aim of this work was to extend the conclusion from single wakes into wind farm flows [12]. The same inflow methodology as [14] was used, with equivalent inflow Strouhal numbers of $0.625 - 0.17$ (expressed as length scales of $L_u = 3.2R$ and $L_u = 12.0R$ respectively), but applied to a row of 10 turbines with two spacings, $S_x = 8R$ and $S_x = 12R$. In the wake of the first turbine, very similar conclusions were found to the single turbine studies - shorter inflow integral scales led to a faster wake breakdown and recovery, and hence increased power output at the second turbine - a 42% difference for $S_x = 8R$ and a 18% difference for $S_x = 12R$. Over 4 turbines, the cumulative power gain was 8.6% and 6.0% respectively for the two spacings. In Figures 2 the mean velocity magnitude of two simulations is shown, along with a plot showing the difference between the two. Clearly, there is a much improved velocity recovery in the first wake, and also remaining somewhat through the first half of the farm, for the shorter integral time scale.

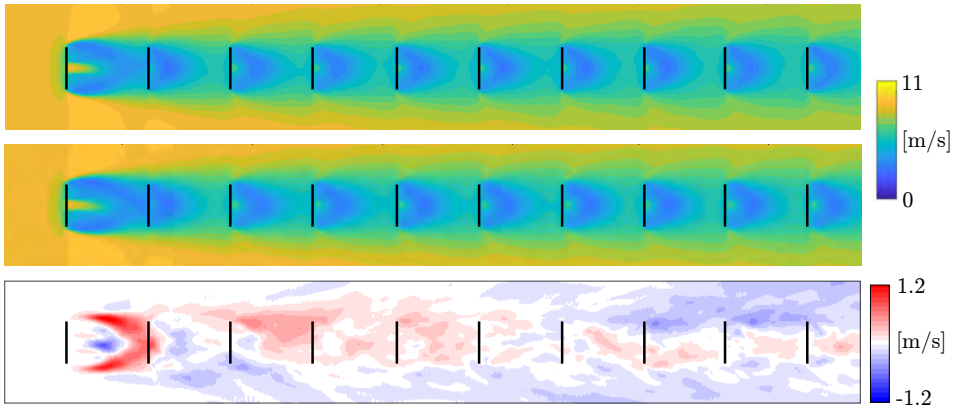

Figure 2: Mean velocity on an x - z plane through turbine centre for $S_x = 8R$: A) $L_u = 3.2R$; B) $L_u = 12.0R$; C) Difference between A) and B), $V_{L_u=3.2R} - V_{L_u=12.0R}$ (values greater than zero show where velocity in A) is greater than B)) Reproduced from [12].

The spectra, mean kinetic energy transport and scales of entrainment were also examined through the wind farm. Reflecting the results from a single wake and previous work, the first turbine was seen to break down the longer inflow scales and the second turbine inflow was dominated by smaller-scale wake-generated turbulence with a peak occurring at $St = 0.3 - 0.7$ [8, 6]. Further into the turbine row, scales associated with the turbine spacing appeared, in accordance with other previous work [3]. However, some limited influence of the very low-frequency inflow scales did persist even deep into the farm, as seen in the scales of entrainment and correlations of power signals from the turbines.

Conclusions

This work first performed extensive verification, validation and improvements of numerical tools: turbine modelling in LES; aeroelastic coupling of turbine models; non-neutral atmospheric boundary layer simulations; and single wakes. After validating the numerical modelling and providing recommendations for appropriate grid resolutions, the primary aim of the work was addressed - investigating whether inflow integral turbulent scales impact wind turbine wake development and recovery. First studying a single wake, it was seen that shorter integral time scales (in the range $St \approx 0.5$) led to a faster breakdown of tip vortices, and hence a shorter near wake length and earlier onset of energy entrainment into the wake, than long integral time scales (in the range $St \approx 0.1$). When considering a wind farm scenario, the impact was mainly felt in the wake of the first turbine, and hence the power output of the second, which increased by 42% and 18% respectively for $S_x = 8R$ and $S_x = 12R$, between the shortest and longest inflow integral scales. Over 4 turbines, the total power gain for the two spacings was 8.6% and 6.0% respectively. The second turbine experienced an inflow dominated by smaller-scale wake dominated turbulence, while deeper into the farm longer scales associated the spacing grew.

Overall, this work demonstrates that the integral time/length scales of freestream turbulence have a significant impact of the wake development behind turbines, and hence on wind farm flow and power output, mainly by impacting the farm entrance region. These

conclusions mean that turbulent scales should be considered in addition to turbulence intensity when characterising flows. Additionally, if these beneficial scales can be introduced into wind farms - either by layout design or dynamic control strategies [23, 5] - then wind farm efficiency and power output could be improved.

References

[1] Mahdi Abkar and Fernando Porté-Agel. "The Effect of Free-Atmosphere Stratification on Boundary-Layer Flow and Power Output from Very Large Wind Farms". In: *Energies* 6.5 (2013), pp. 2338–2361. ISSN: 1996-1073. DOI: 10.3390/en6052338. URL: https://www.mdpi.com/1996-1073/6/5/2338.

[2] Dries Allaerts and Johan Meyers. "Boundary-layer development and gravity waves in conventionally neutral wind farms". In: *J. Fluid Mech.* 814 (Mar. 2017), pp. 95–130.

[3] Søren J. Andersen, Jens N. Sørensen, and Robert F. Mikkelsen. "Turbulence and entrainment length scales in large wind farms". In: *Philosophical Transactions of the Royal Society A: Mathematical, Physical and Engineering Sciences* 375 (2091 Apr. 2017), p. 20160107.

[4] G. España, S. Aubrun, S. Loyer, and P. Devinant. "Spatial study of the wake meandering using modelled wind turbines in a wind tunnel". In: *Wind Energy* 14.7 (2011), pp. 923–937.

[5] Joeri A. Frederik, Bart M. Doekemeijer, Sebastiaan P. Mulders, and Jan Willem van Wingerden. "The helix approach: Using dynamic individual pitch control to enhance wake mixing in wind farms". In: *Wind Energy* 23 (8 Aug. 2020).

[6] Stefano Gambuzza and Bharathram Ganapathisubramani. "The influence of free stream turbulence on the development of a wind turbine wake". In: *Journal of Fluid Mechanics* 963 (2023), A19.

[7] "Grand challenges in the science of wind energy". In: *Science* 366 (6464 Oct. 2019), eaau2027.

[8] Michael Heisel, Jiarong Hong, and Michele Guala. "The spectral signature of wind turbine wake meandering: A wind tunnel and field-scale study". In: *Wind Energy* 21.9 (2018), pp. 715–731.

[9] E L Hodgson, M Souaiby, N Troldborg, F Porté-Agel, and S J Andersen. "Cross-code verification of non-neutral ABL and single wind turbine wake modelling in LES". In: *Journal of Physics: Conference Series* 2505.1 (May 2023), p. 012009.

[10] E. L. Hodgson, M. H. Aa Madsen, N. Troldborg, and S. J. Andersen. "Impact of Turbulent Time Scales on Wake Recovery and Operation". In: *Journal of Physics: Conference Series* 2265.2 (2022).

[11] E. L. Hodgson, S. J. Andersen, N. Troldborg, A. R. Meyer Forsting, R. F. Mikkelsen, and J. N. Sørensen. "A quantitative comparison of aeroelastic computations using flex5 and actuator methods in les". In: *Journal of Physics: Conference Series* 1934 (1 2021).

[12] E. L. Hodgson, N. Troldborg, and S. J. Andersen. "Impact of Freestream Turbulence Integral Length Scale on Wind Farm Flows and Power Generation". In: *TO BE SUBMITTED* (2024).

[13] Emily L. Hodgson, Christian Grinderslev, Alexander R. Meyer Forsting, Niels Troldborg, Niels N. Sørensen, Jens N. Sørensen, and Søren J. Andersen. "Validation of Aeroelastic Actuator Line for Wind Turbine Modelling in Complex Flows". In: *Frontiers in Energy Research* 10.May (2022), pp. 1–20.

[14] Emily L. Hodgson, Mads H Aa Madsen, and Søren J. Andersen. "Effects of turbulent inflow time scales on wind turbine wake behavior and recovery". In: *Physics of Fluids* 35.9 (Sept. 2023).

[15] Emily Louise Hodgson. "Large Eddy Simulations of Energy Entrainment in Wind Turbine Wakes and Wind Farms". English. PhD thesis. 2023.

[16] L. E.M. Lignarolo, D. Ragni, C. Krishnaswami, Q. Chen, C. J. Simão Ferreira, and G. J.W. van Bussel. "Experimental analysis of the wake of a horizontal-axis wind-turbine model". In: *Renew. Energy* 70 (2014), pp. 31–46.
[17] Jakob Mann. "The spatial structure of neutral atmospheric surface-layer turbulence". In: *Journal of Fluid Mechanics* 273 (Aug. 1994), pp. 141–168.
[18] Jakob Mann. "Wind field simulation". In: *Probabilistic Engineering Mechanics* 13 (4 Oct. 1998), pp. 269–282.
[19] Charles Meneveau. "Big wind power: seven questions for turbulence research". In: *Journal of Turbulence* 20.1 (Jan. 2019), pp. 2–20.
[20] Johan Meyers and Charles Meneveau. "Optimal turbine spacing in fully developed wind farm boundary layers". In: *Wind Energy* 15.2 (Mar. 2012), pp. 305–317.
[21] Michelsen. *Basis 3D—A Platform for Development of Multiblock PDE Solvers*. Tech. rep. Danmarks Tekniske Universitet, 1992.
[22] Robert Flemming Mikkelsen. English. PhD thesis. Jan. 2004. ISBN: 87-7475-296-0.
[23] W. Munters and J. Meyers. "Towards practical dynamic induction control of wind farms: analysis of optimally controlled wind-farm boundary layers and sinusoidal induction control of first-row turbines". In: *Wind Energy Science* 3.1 (2018), pp. 409–425.
[24] S. Øye. *Flex4 simulation of wind turbine dynamics*. Tech. rep. Lyngby, Denmark: DTU, 1996.
[25] Jens Nørkær Sørensen and Wen Zhong Shen. "Numerical modeling of wind turbine wakes". eng. In: *Journal of Fluids Engineering, Transactions of the ASME* 124.2 (2002).
[26] Niels N Sørensen. *General purpose flow solver applied to flow over hills*. Risø National Laboratory, 1995, 153 S (unknown). ISBN: 8755020798.
[27] L Vermeer, Jens Nørkær Sørensen, and A Crespo. *Wind Turbines Wake Aerodynamics*. 2003.

An improved wind farm parameterization in mesoscale models

Oscar M. Garcia-Santiago and Jake Badger

Introduction

Mesoscale modelling plays a crucial role in assessing wind resources by capturing atmospheric processes on scales from a few to several hundred kilometres. It effectively bridges the gap between global atmospheric patterns and local weather phenomena, integrating atmospheric dynamics with topography and surface characteristics to offer detailed insights into wind patterns over large areas. However, typical mesoscale models used in this context struggle with the direct representation of wind farms due to their kilometre-scale resolution, which is inadequate for capturing the finer dynamics at the scale of wind turbines.

Wind Farm Parameterizations (WFPs) are integrated into mesoscale models to address this scale discrepancy. These parameterizations strike a balance between the simplicity of engineering wake models and the complexity of atmospheric modelling, allowing for the simulation of wind farm clusters without excessive computational demands. By integrating WFPs, mesoscale models like the Weather Research and Forecasting [WRF; 15] model, can enhance our understanding of how wind farms affect local wind resources, neighbouring wind farms and regional climates [1, 8, 14]. Given the importance of the applications, these parameterizations must be as accurate as possible.

We present an improved wind farm parameterization that better represents the effects of wind farms on the atmosphere and has a better power modelling framework. The improvements are implemented into the Explicit Wake Parameterisation [EWP; 17], and the implementation is evaluated against high-resolution wake modelling using Computational Fluid Dynamics (CFD) methods.

Identifying opportunities for improvements

Several studies have compared WFPs based on wind speed, turbulent kinetic energy (TKE), and power output. However, without a reliable reference for validation, these comparisons are of limited use for identifying specific areas for improvement. Validating WFPs with actual measurements can highlight which parameterizations perform best under certain conditions. Still, there is no consensus on which WFP excels universally, as performance varies from case to case. Often, these variations stem from the mesoscale model's ability to fully capture the background flow, making it challenging to attribute performance errors directly to the WFPs or the underlying mesoscale model [3, 8].

To address the attribution challenge, this project also isolated the performance of various WFPs and evaluated them against Large-Eddy Simulation (LES) results under similar background conditions. Our findings [5] indicate that the spatial distribution of TKE is not well

captured, partly due to the limitations of using a single planetary boundary layer (PBL) scheme in the WRF model and how the WFPs handle TKE.

Another crucial aspect to improve is including subgrid-scale wakes in the WFPs. Turbines within these WFPs are represented as a number per grid cell, which assumes no wake effects within the cell. This assumption can lead to inaccuracies, as turbines are often not perfectly aligned to avoid wake effects, resulting in overestimated wind turbine impacts in these WFPs. These unaccounted inter-turbine wake interactions are unresolved subgrid features that need proper consideration. Parameterizations have been developed to account for these subgrid effects [9, 10, 13]. However, these WFPs perform better when the wind farm is enclosed in a single grid cell. When the wind farm is divided into multiple grid cells, it is essential to consider the wake effects at the grid cell scale (grid-scale wakes) and the subgrid-scale wakes, as mentioned above.

Developing an improved wind farm parameterization

In the following, we present the improvements to the wind farm parameterizations, specifically to the EWP, based on the aforementioned results and studies.

Turbulent kinetic energy treatment

We have developed and integrated a new turbulence model, the Latent Kinetic Energy (LKE) method, into the existing explicit wake parameterization. By using the tracer capabilities of the WRF model, the LKE method provides a "memory" of turbulence evolution, enhancing the accuracy of TKE representation downstream. This new model effectively replicates the spatial development of the TKE downstream (Fig. 1), as observed in LES with actuator disc (LES-AD) reference. The LKE model is compatible with any PBL scheme within the WRF model that incorporates TKE in its equations, providing better results than the standard WFP, commonly known as the Fitch parameterization [4], under these PBL schemes. The improved representation of the spatial structure of TKE impacts the wind speed wake recovery (Fig. 2), as the explicit source of TKE enhances mixing on the downstream wake. In summary, the LKE method implemented in the EWP, better represents the effects of wind farms on the atmosphere using mesoscale models.

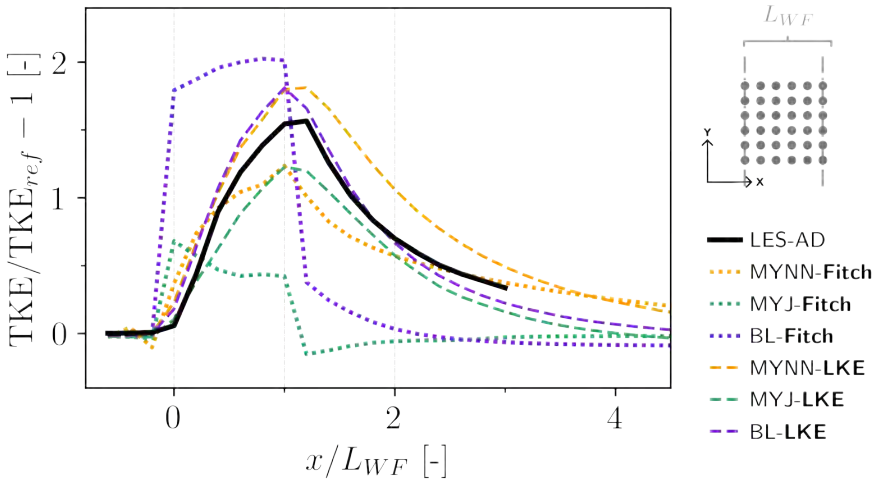

Figure 1: Comparison of the streamwise added TKE using the LKE method (dashed lines) and the Fitch parameterization (dotted lines) using the MYNN [11], the MYJ [6] and BouLac [2] PBL scheme, with LES-AD (solid line) as the baseline. The vertical grey lines represent the front and last row of the analysed wind farm, depicted for reference at the top rightmost of the panel.

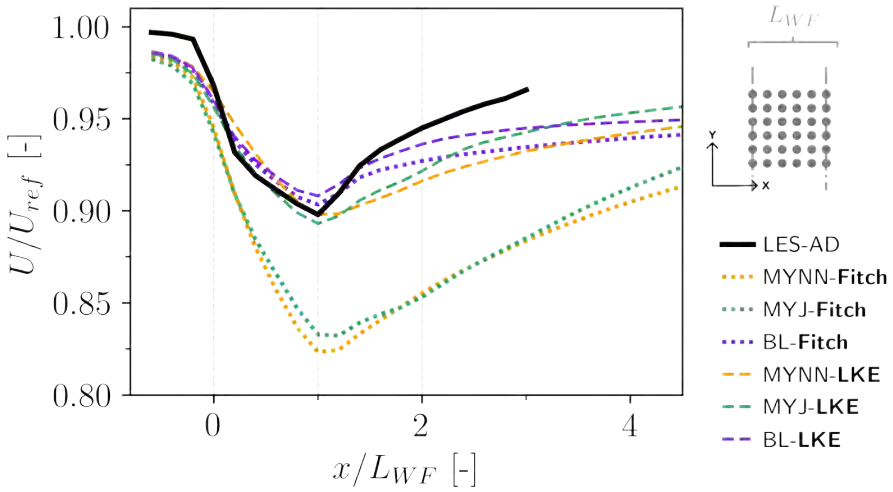

Figure 2: Similar to Fig. 1, but for the hub-height wind speed.

Subgrid scale wake interactions

The typical WFPs do not consider subgrid-scale wakes, which result in nearly uniform power output across different wind directions at a specific wind speed, as shown in Fig. 3a. To address this, we have developed a novel approach that integrates subgrid wake effects into the EWP and accounts for grid-scale wakes. This enhancement uses precalculated thrust and power curves from various engineering wake models, allowing for flexible, case-specific applications. By including subgrid-scale interactions, our method successfully captures the directional variation in power output, as demonstrated in Figs. 3b and 3c, mirroring results from high-resolution Reynolds-Averaged Navier-Stokes (RANS) simulations for an offshore wind farm.

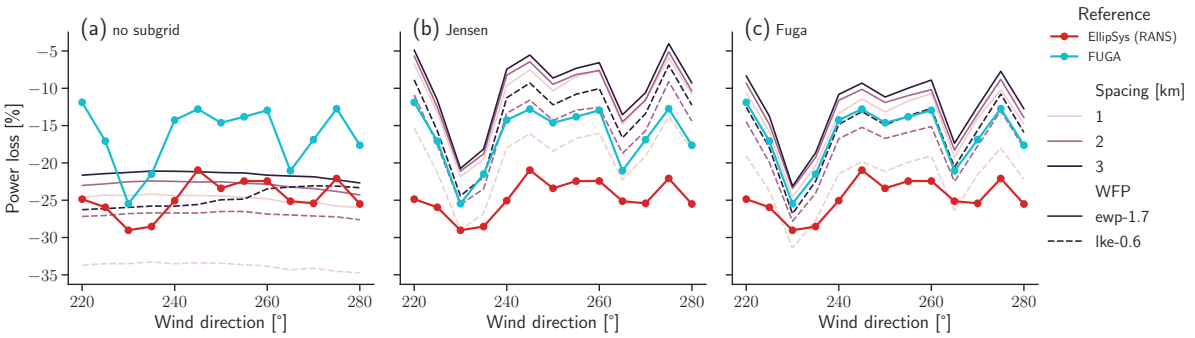

Figure 3: Power loss variation due to wind direction-layout interaction from EWP (ewp-1.7) and EWP with the LKE method (lke-0.6) under three grid spacings showing the effects of (a) not using subgrid information and using the information from the (b) Jensen [7] and (c) Fuga [12] model. Simulations from high-resolution RANS [EllipSys; 16] and Fuga are shown for reference.

References

[1] Naveed Akhtar, Beate Geyer, Burkhardt Rockel, Philipp S. Sommer, and Corinna Schrum. "Accelerating Deployment of Offshore Wind Energy Alter Wind Climate and Reduce Future Power Generation Potentials". In: *Sci Rep* 11.1 (June 2021), p. 11826. ISSN: 2045-2322. DOI: 10.1038/s41598-021-91283-3. (Visited on 09/14/2023).

[2] P. Bougeault and P. Lacarrere. "Parameterization of Orography-Induced Turbulence in a Mesobeta–Scale Model". In: *Mon. Wea. Rev.* 117.8 (Aug. 1989), pp. 1872–1890. ISSN: 1520-0493, 0027-0644. DOI: 10.1175/1520-0493(1989)117<1872:POOITI>2.0.CO;2. (Visited on 11/15/2023).

[3] Jana Fischereit, Roy Brown, Xiaoli Guo Larsén, Jake Badger, and Graham Hawkes. "Review of Mesoscale Wind-Farm Parametrizations and Their Applications". In: *Boundary-Layer Meteorol* 182.2 (Feb. 2022), pp. 175–224. ISSN: 1573-1472. DOI: 10.1007/s10546-021-00652-y. (Visited on 07/06/2022).

[4] Anna C Fitch, Joseph B Olson, Julie K Lundquist, Jimy Dudhia, Alok K Gupta, John Michalakes, and Idar Barstad. "Local and Mesoscale Impacts of Wind Farms as Parameterized in a Mesoscale NWP Model". In: *Mon. Wea. Rev.* 140.9 (Sept. 2012), pp. 3017–3038. ISSN: 00270644. DOI: 10.1175/MWR-D-11-00352.1. (Visited on 01/17/2020).

[5] Oscar García-Santiago, Andrea N. Hahmann, Jake Badger, and Alfredo Peña. "Evaluation of Wind Farm Parameterizations in the WRF Model under Different Atmospheric Stability Conditions with High-Resolution Wake Simulations". In: *Wind Energy Science* 9.4 (Apr. 2024), pp. 963–979. ISSN: 2366-7443. DOI: 10.5194/wes-9-963-2024. (Visited on 04/22/2024).

[6] Zaviša I. Janjić. "The Step-Mountain Coordinate: Physical Package". In: *Mon. Wea. Rev.* 118.7 (July 1990), pp. 1429–1443. ISSN: 1520-0493, 0027-0644. DOI: 10.1175/1520-0493(1990)118<1429:TSMCPP>2.0.CO;2. (Visited on 11/15/2023).

[7] N. O. Jensen. *A Note on Wind Generator Interaction*. Tech. rep. 2411. Risø National Laboratory, 1983. (Visited on 04/01/2024).

[8] J. K. Lundquist, K. K. DuVivier, D. Kaffine, and J. M. Tomaszewski. "Costs and Consequences of Wind Turbine Wake Effects Arising from Uncoordinated Wind Energy Development". In: *Nat. Energy* 4.1 (Jan. 2019), pp. 26–34. ISSN: 2058-7546. DOI: 10.1038/s41560-018-0281-2. (Visited on 09/10/2023).

[9] Yulong Ma, Cristina L. Archer, and Ahmad Vasel-Be-Hagh. "Comparison of Individual versus Ensemble Wind Farm Parameterizations Inclusive of Sub-Grid Wakes for the

WRF Model". In: *Wind Energy* 25.9 (2022), pp. 1573–1595. ISSN: 1099-1824. DOI: 10.1002/we.2758. (Visited on 06/12/2023).

[10] Yulong Ma, Cristina L. Archer, and Ahmadreza Vasel-Be-Hagh. "The Jensen Wind Farm Parameterization". In: *Wind Energy Science* 7.6 (Dec. 2022), pp. 2407–2431. ISSN: 2366-7443. DOI: 10.5194/wes-7-2407-2022. (Visited on 06/12/2023).

[11] Mikio Nakanishi and Hiroshi Niino. "Development of an Improved Turbulence Closure Model for the Atmospheric Boundary Layer". In: *J. Meteorol. Soc. Jpn. Ser. II* 87.5 (2009), pp. 895–912. DOI: 10.2151/jmsj.87.895.

[12] S. Ott, J. Berg, and M. Nielsen. *Linearised CFD Models for Wakes*. Tech. rep. Risø-R-1772. Risø, 2011.

[13] Yang Pan and Cristina L Archer. "A Hybrid Wind-Farm Parametrization for Mesoscale and Climate Models". In: *Boundary-Layer Meteorol* 168.3 (Sept. 2018), pp. 469–495. ISSN: 15731472. DOI: 10.1007/s10546-018-0351-9. (Visited on 03/05/2020).

[14] S C Pryor, T J Shepherd, P J H Volker, A N Hahmann, and R J Barthelmie. ""Wind Theft" from Onshore Wind Turbine Arrays: Sensitivity to Wind Farm Parameterization and Resolution". In: *J. Appl. Meteorol. Clim.* 59.1 (2020), pp. 153–174. DOI: 10.1175/JAMC-D-19-0235.1.

[15] C. Skamarock, B. Klemp, Jimy Dudhia, O. Gill, Zhiquan Liu, Judith Berner, Wei Wang, G. Powers, G. Duda, Dale Barker, and Xiang-yu Huang. *A Description of the Advanced Research WRF Model Version 4.3*. Tech. rep. NCAR/TN-556+STR). NCAR/UCAR, 2021. (Visited on 12/14/2022).

[16] N. N. Sørensen. "General Purpose Flow Solver Applied to Flow over Hills". PhD thesis. Roskilde, Denmark: Risø National Laboratory, 1994.

[17] P. J.H. Volker, J. Badger, A. N. Hahmann, and S. Ott. "The Explicit Wake Parametrisation V1.0: A Wind Farm Parametrisation in the Mesoscale Model WRF". In: *Geosci Model Dev.* 8.11 (2015), pp. 3715–3731. ISSN: 19919603. DOI: 10.5194/gmd-8-3715-2015.

Generalization of single wake surrogates for multiple and farm-farm wake analysis

Faegheh Pish, Tuhfe Göçmen and Paul van der Laan

Introduction

Wind farm efficiency is influenced by atmospheric turbulence and wake interactions from preceding turbines. Optimal performance necessitates effective control strategies, encompassing collective/individual pitch (and/or torque) control, yaw control, and innovative techniques, significantly boosting energy capture. Wake effects are crucial, impacting downstream turbines and reducing overall energy extraction. For this purpose, the study of wind farm flow control (WFFC) holds significant relevance in this context. In this study, a Deep Neural Network predicts downstream flow features of a wind turbine under diverse control scenarios, including varying thrust coefficient and yaw control. A feed-forward neural network models the deficit and added turbulent intensity of a single wake, trained using Computational Fluid Dynamics (CFD) simulations as reference data. Linear superposition establishes the wind farm flow field, allowing examination of downstream effects. Another feedforward neural network encompasses wind farm physics such as blockage and wake recovery in and around wind turbine arrays which are overlooked by the single wake model. The methodology employed in this study yields results that are more time-efficient compared to traditional CFD models while maintaining a higher level of accuracy (ideally) than the engineering models, especially when implemented for WFFC without calibration.

Methodology

First, a comprehensive range of three-dimensional single wakes of a DTU 10MW is simulated using PyWakeEllipSys[6], which is a RANS wind farm flow model in which the wind turbine is implemented as an actuator disk (*AD*) to simulate the wake effects within a wind farm or behind a turbine. Inflow conditions are based on the atmospheric surface layer modeled using the k-ε-f_P turbulence model[3] on flat terrain, varies from 3% to 30%. Turbine is controlled using the thrust coefficient (CT) covering the range from 0.1 to 0.92, corresponding to inflow wind speed (U_∞) from 20 to 4,m/s, respectively. Additionally, turbine is yawed within the range of $+30°$ (clockwise) to $-30°$ (counterclockwise) with a step of $5°$. The results are used to train two different models to predict deficit (ΔU) and TI_{add}. For this purpose, a Feedforward Neural Network (FFNN) is utilized. To find the optimal set of hyperparameters for the best model, a comprehensive grid search is conducted.

The wind farm flow is modeled as the outcome of linear superpositioned method [2, 4], incorporating surrogate single wakes. The prediction of the initial single wake is based on identical inputs used in the RANS simulations. Subsequent single wakes, corresponding to the specified number of turbines, are generated with updated inputs. To evaluate this approach, CFD simulations were conducted for a series of five similar wind turbines with

varying internal distances of $3D$, $5D$, and $8D$. Subsequently, residuals were computed by comparing the RANS wind farm with the superimposed ANN model. These residuals indicate the absence of wind farm effects, such as blockage and wake recovery, which are considered as correction term. This forms a new dataset for predicting the correction of the components of the linear superposition surrogate model. Therefore, two additional FFNNs are employed to model the correction of ΔU and TI_{add} in a wind farm. It should be noted that this approach is comparable to similar methodology on point-wise weighted (linear) summation of the wakes performed by Bastankhah (2020)[5]. However, the trained corrected superimposition followed here is performed on 3D domain (for all the nodes in the 3D grid), for the entire flow in and around the wind farm.

Results and discussion

The single wake surrogate model is able to predict the ΔU and TI_{add} precisely in less than 3 second, the highest error of the models are 3.9% and 1.2% respectively among all the cases. Emphasizing the robustness of the models, the comparison with RANS data is specifically has been done for the strongest wake scenario, which is influenced mainly by the CT, under a high yaw angle. Examining U, the maximum error is approximately 0.8%. This discrepancy is in the near wake close to the turbine, where the non-linearity of the wake flow is more prominent. For the TI the maximum error is approximately 0.32%.

Ensuring the single wake surrogate model predicts accurately, the model is used to simulate a wind farm (contains 5 turbines). The wind farm comparison between the superimposed surrogate single wake and the RANS wind farm is studied to analyse the performance of the linear superimposed ANN models. For this purpose, a wind farm with 4D internal spacing of turbines and only first one is yawed ($-28°$) has been chosen. The inflow has TI of 4% with low speed to set the turbine at high CT of 0.814 (strong wake effects). The study reveals significant errors of approximately 31.5% and 7% for U and TI, respectively. The high error is behind the more downstream turbines (third and the rest). This notable discrepancy arises from the absence of wind farm physics, such as blockage effects [1] and wake recovery, which are not present in the superimposed ANN single wake model. As more turbines are added to the farm, the combined effects intensify, making the superimposed surrogate model less accurate in its predictions. This inadequacy becomes more pronounced in low inflow TI scenarios, due to slower wake recovery. Therefore downstream turbines experience reduced incoming velocity due to the coherent and enduring wake, intensifying the blockage effect. In conditions of high inflow TI, increased mixing and dispersion occur in the wake, facilitating a faster recovery. This accelerated wake recovery, in turn, mitigates the blockage effect, leading to a reduced TI_{add} downstream. Consequently, the wake in the wind farm in high inflow TI closely resembles that of a single wake for each turbine, particularly when factoring in the CT (lower CT values contribute to more closely aligned results). Moreover, the stronger wake leads to a higher TI_{add}. Additionally, increase in internal turbine spacing, and decreasing the CT the impact of blockage becomes less pronounced due to the extended duration for the wake to recover. The superimposed model aligns more closely with the wind farm results in high TI cases. The analysis reveals that the majority of

cases exhibit high errors (up to 60%) for both U and TI, and only approximately 28% of cases showing errors below 10% for U and 25% below 2.5% for TI. Given these significant errors, it underscores the imperative need for the application of the correction model. To address the unaccounted wind farm physics, two correction models (one for deficit and another for TI_{add}) are introduced to rectify the absence of this phenomenon in the flow. The corrected superimposed model effectively captures the trends in the flow behavior within and around the wind farm, resulting in a substantial decrease of U maximum error from 31.5% to 4.2% (for strong case, which mentioned before). Similarly, for TI, the correction model demonstrates its capability by reducing the maximum error from 7% to 1.1%. As mentioned before, superimposed ANN surrogates have high error and only some portion of cases has error below 10%, while the corrected superimposed ANN model was able to bring this higher error to maximum 10% for U and 3% for TI.

Conclusion

In this article, the potential of machine learning, namely the feed-forward neural networks, has been investigated for capturing the (steady-state) wake effects within wind farms, using extensive RANS database. It was demonstrated that the models predict output features with a high degree of accuracy. It was shown that the linear superposition model is incapable of accurately capturing the farm's physics, indicating a need for correction model.

References

[1] A Meyer Forsting et al. "A wind-tunnel investigation of wind-turbine wakes in yawed conditions". In: *Journal of Physics: Conference Series* (2015).

[2] Ewan Machefaux et al. "An experimental and numerical study of the atmospheric stability impact on wind turbine wakes". In: *Wind Energy* (2015).

[3] Van der Laan M P et al. "An improved k-ε model applied to a wind turbine wake in atmospheric turbulence". In: *Wind Energy* (2015).

[4] P.B.S. Lissaman. "Energy effectiveness of arbitrary arrays of wind turbines". In: *Journal of Energy* (2012).

[5] Bastankhah M and Porté-Agel. "A wind-tunnel investigation of wind-turbine wakes in yawed conditions". In: *Journal of Physics: Conference Series* (2015).

[6] *PyWakeEllipSys*. `https://topfarm.pages.windenergy.dtu.dk/cuttingedge/pywake/pywake_ellipsys/v3.10/index.html`.

An improved analytical framework for flow prediction inside and downstream of wind farms

Marwa Souaiby and Fernando Porté-Agel

Introduction

Large Eddy Simulation (LES) is an accurate, yet complex and costly numerical tool, as opposed to analytical models, which are fast but less reliable [3, 10]. Hence, improving the existing low-cost analytical models would provide an attractive alternative in the applications of the fast-growing wind energy sector.

This study [11] presents a comprehensive evaluation of available analytical wake models and proposes an enhanced modelling framework for flow prediction inside and downstream of finite-size wind farms, using LES data obtained from the implementation of the WIRE-LES code [1, 9, 15].

Simulations are performed for the no-farm, finite-size wind farm and infinite wind farm cases. Sixteen different finite size wind farm cases are considered, where their size is varied: from 9 rows up to 36 rows, and two different layouts are modeled: aligned and staggered. The no-farm case acts as a precursor simulation generating the inflow to the wind farms, with a hub height mean wind velocity (M_∞) of 7.75 m/s and an ambient flow streamwise turbulence intensity (I_0) of 10%. The infinite wind farm cases have wind turbines placed over the whole domain and, owing to the periodic boundary conditions in both horizontal directions, they represent the infinite regime of the modelled wind farms.

All cases consider a Conventionally Neutral Boundary Layer (CNBL) with a weak free atmosphere stratification level fixed at $\Gamma = 1\ K/km$. The flow is driven by a geostrophic wind $G = 10\ m/s$ and the Coriolis parameter used is $f_c = 1.195 \times 10^{-4}\ rad/s$. In the no-farm and infinite wind farm cases, the initial temperature profile starting from the reference temperature $\theta_0 = 293\ K$ is kept constant vertically up to $100\ m$ and then follows the set lapse rate Γ. The surface roughness is set to $z_0 = 0.05\ m$. The cases are initialized with a constant streamwise wind velocity of $10\ m/s$. Additionally, to stimulate the development of turbulence inside the Atmospheric Boundary Layer (ABL), small random perturbations are added to the initial wind velocity and temperature fields at the lowest $100\ m$ of the domain. All the simulations are run for a long enough duration to guarantee that quasi-stationary conditions are achieved.

Large-eddy simulations

The LES results reveal a clear effect of wind farm size, layout and density on the flow in the wind farm exit and wind farm wake regions. For the typical size range of existing and planned wind farms, and for a particular layout, increasing the wind farm size leads to a reduction in the spanwise-averaged mean wind speed at any given distance relative to the wind farm exit. For the largest considered wind farms, the flow and power output deep

inside the wind farm show less variability with farm size and become closer to those found in infinite wind farms, albeit not reaching them. As expected, increasing wind farm density leads to a decrease in wind speed, thus power output per turbine, deep inside the wind farms and in their wakes. As for the effect of changing the layout, fully aligned configurations, characterized by relatively shorter streamwise and longer spanwise effective inter-turbine distances, produce larger spanwise flow heterogeneity than their staggered counterparts. This explains the fact that they lead to larger power losses while yielding larger spanwise-averaged wind speed in the wind farm exit and wake region.

Analytical wake models

The following analytical models are evaluated against the LES data: the Park model [6], the TurbOPark model [8], the framework of Niayifar and Porté-Agel (2016)[7], and the momentum conserving framework of Zong and Porté-Agel (2020) [16]. All the tested models tend to over-predict the wake recovery behind the turbines inside and downstream of the wind farms for all the considered sizes and layouts. As a result, the power output over the wind farm rows is not well predicted. Our results show that an important factor contributing to the overestimation of the wake recovery by some of the analytical models is the assumption of a linear or quasi-linear wake expansion rate. Analysis of the LES data reveals that this linear relationship is not valid at relatively long distances downwind of wind turbines, which is consistent with the findings of Vahidi and Porté-Agel (2022) [13] for a single turbine.

Proposed analytical framework

To address the aforementioned wake recovery overestimation, we propose a new analytical framework extending the recently developed model [12] for stand-alone wind turbines, which does not rely on the linear wake expansion assumption, to the flow prediction inside and downstream of wind farms. The proposed framework depends on estimating the near-wake length and turbulence intensity within a wind farm, crucial for prescribing the non-linear growth rate. In this context, various methods for calculating the near-wake length [14, 2, 13], turbulence intensity [4, 5] and its superposition are assessed against the LES data.

Near-wake length

For the near-wake length, three different methods from Vermeulen (1980) [14], Bastankhah and Porté-Agel (2016) [2], and Vahidi and Porté-Agel (2022) [13] are tested. The latter method [13], is found to yield the most accurate predictions at the first row and within the wind farms, when turbines are in unwaked and waked conditions, respectively. This is achieved by applying a distinct expansion region length in each condition, namely $x_0 = 1D$ and $x_0 = 0.5D$, respectively.

Turbulence intensity variation within wind farms

For the added turbulence intensity by a single turbine, it is shown that the relation of Frandsen (2007) [5] is more accurate than the relation of Crespo and Hernández (1996) [4]. Furthermore, the study establishes the necessity of adopting a cumulative superposition method-

ology to account for the combined effect of the added turbulence intensity from all the wind turbines upstream. Additionally, it is recommended to normalize the standard deviation of wind velocity with the local wind speed within the wind farm instead of using the undisturbed flow velocity at the wind farm inlet.

Results

Compared with LES (Figure 1), the proposed analytical modelling framework yields improved power estimates and wind speed predictions both inside and downstream of wind farms with respect to the other tested analytical wake models. It is important to note that the proposed analytical framework applies the momentum conserving superposition method [16] to superpose the single turbine wakes within wind farms since this superposition technique shows the best results in the analytical wake models analysis. The improved framework also exhibits robustness by achieving the same level of accuracy in the wake prediction for all considered cases regardless of the wind farm size, density, and configuration.

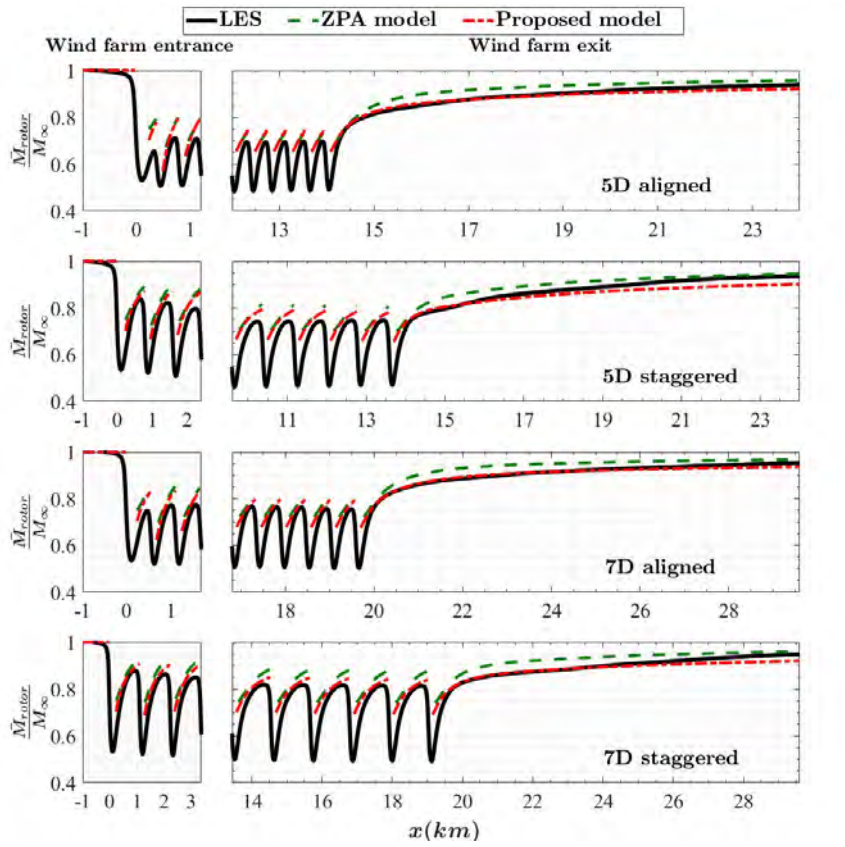

(a)

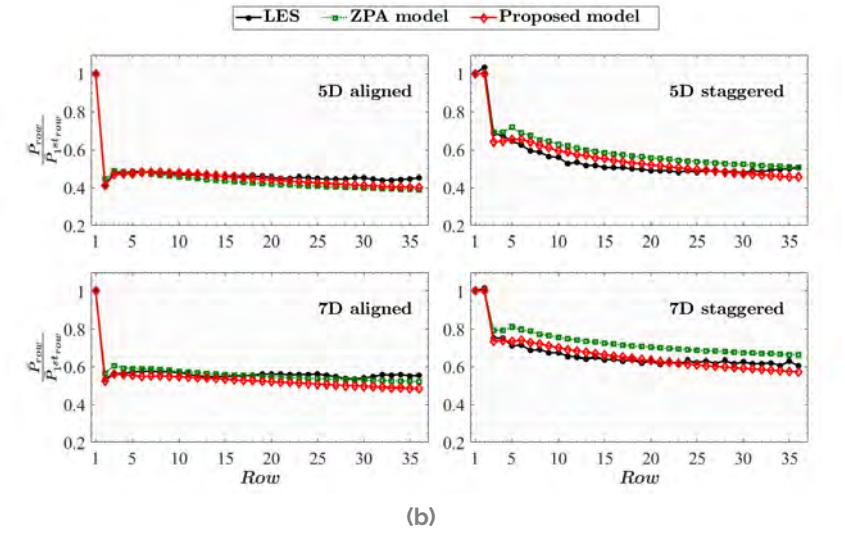

(b)

Figure 1: (a) Rotor-averaged wind velocity variation near the entrance and exit of the 36 rows wind farms of different configurations and their wake region, (b) and the normalized row power output of the 36 rows wind farms of different configurations, as simulated by LES and predicted by the proposed model and the ZPA model [16].

Conclusion

This study evaluates available analytical wake models for flow prediction inside and downstream of wind farms of different sizes and layouts using LES, and introduces an enhanced analytical framework. The proposed framework consistently yields more accurate power estimates and flow predictions inside and downstream of finite-size wind farms with different sizes and configurations. In future work, we aim to study the effects of surface-layer thermal stratification on wind farm wakes and assess the ability of different analytical wake models (including the newly developed framework) to predict those impacts.

References

[1] John David Albertson. "Large eddy simulation of land-atmosphere interaction". English. PhD thesis. TA - TT -, 1996. DOI: LK-https://worldcat.org/title/40720104.

[2] M. Bastankhah and F. Porté-Agel. "Experimental and theoretical study of wind turbine wakes in yawed conditions". In: *Journal of Fluid Mechanics* 806 (2016), pp. 506–541.

[3] S. P. Breton, J. Sumner, J. N. Sørensen, K. S. Hansen, S. Sarmast, and S. Ivanell. "A survey of modelling methods for high-fidelity wind farm simulations using large eddy simulation". In: *Philosophical Transactions of the Royal Society A: Mathematical, Physical and Engineering Sciences* 375 (2017).

[4] A. Crespo and J. Hernández. "Turbulence characteristics in wind-turbine wakes". In: *Journal of Wind Engineering and Industrial Aerodynamics* 61 (1996), pp. 71–85.

[5] Sten Tronæs Frandsen. "Turbulence and turbulence-generated structural loading in wind turbine clusters". English. Risø-R-1188(EN). PhD thesis. 2007. ISBN: 87-550-3458-6.

[6] I. Katic, J. Hojstrup, and N.O. Jensen. "A Simple Model for Cluster Efficiency". In: *EWEC'86. Proceedings*. Ed. by W. Palz and E. Sesto. Vol. 1. Rome: Raguzzi, A., 1986, pp. 407–410.

[7] Amin Niayifar and Fernando Porté-Agel. "Analytical modeling of wind farms: A new approach for power prediction". In: *Energies* 9 (2016), pp. 1–13.

[8] Nicolai Gayle Nygaard, Søren Trads Steen, Lina Poulsen, and Jesper Grønnegaard Pedersen. "Modelling cluster wakes and wind farm blockage". In: *Journal of Physics: Conference Series* 1618.6 (2020).

[9] F. Porté-Agel, C. Meneveau, and M. Parlange. "A scale-dependent dynamic model for large-eddy simulation: Application to a neutral atmospheric boundary layer". In: *Journal of Fluid Mechanics* 415.July 2000 (2000), pp. 261–284.

[10] Fernando Porté-Agel, Majid Bastankhah, and Sina Shamsoddin. *Wind-Turbine and Wind-Farm Flows: A Review*. Vol. 174. Springer Netherlands, 2020, pp. 1–59.

[11] Marwa Souaiby and Fernando Porté-agel. "An improved analytical framework for flow prediction inside and downstream of wind farms". In: *Renewable Energy* 225.March (2024), p. 120251.

[12] Dara Vahidi and Fernando Porté-Agel. "A New Streamwise Scaling for Wind Turbine Wake Modeling in the Atmospheric Boundary Layer". In: *Energies* 15.24 (Dec. 2022), p. 9477.

[13] Dara Vahidi and Fernando Porté-agel. "A physics-based model for wind turbine wake expansion in the atmospheric boundary layer". In: *Journal of Fluid Mechanics* (2022), pp. 1–28.

[14] P.E.J. Vermeulen. "An experimental analysis of wind turbine wakes". In: *3rd International Symposium on Wind Energy Systems*. Jan. 1980, pp. 431–450.

[15] Yu Ting Wu and Fernando Porté-Agel. "Large-Eddy Simulation of Wind-Turbine Wakes: Evaluation of Turbine Parametrisations". In: *Boundary-Layer Meteorology* 138 (2011), pp. 345–366.
[16] H Zong and F Porté-Agel. "A momentum-conserving wake superposition method for wind farm power prediction". In: *Journal of Fluid Mechanics* 889 (2020).

A wind-tunnel study on cyclic yaw control towards wind farm power improvement

Guiyue Duan and Fernando Porté-Agel

Introduction

In wind energy research, wind tunnel experiment is a cost-efficient method to help understand the pros and cons of wind farm control strategies and their mechanisms of power improvement. The present study investigates a new control strategy, the cyclic yaw control (CYC), in wind farm models consisting of multiple small-scale modeled wind turbines (i.e., the WiRE-01 miniature wind turbines [1]). The effects of control parameters, i.e., the yaw amplitude and the Strouhal number, on wind farm power performance and wake characteristics are examined [2].

Setup and methods

The experiments are conducted in the closed-loop atmospheric boundary-layer (ABL) wind tunnel (Figure 1(a)) of the WiRE laboratory at EPFL, Switzerland. A neutral boundary layer flow (Figure 1(c)) naturally develops along the 28m long, 2.6m wide and 2.0m high wind tunnel test section. The WiRE-01 miniature wind turbine used in this study is a three-blade horizontal wind turbine with a rotor diameter (D) of 15cm and a hub height of 12.5cm. The blades feature a low-Reynolds-number airfoil [1, 3], in order to have power and thrust coefficients comparable to utility-scale turbines. As presented in Figure 1(d), the power and thrust coefficients are around 0.35 and 0.80, respectively, at the optimal tip-speed ratio (TSR) of 3.6. In wind farm models, all individual wind turbines are operating at this optimal TSR. CYC is applied to the most upstream wind turbine in the farm by imposing a sinusoidal temporal variation of its yaw angle [2]. The control equation for CYC is written as

$$\gamma(t) = \gamma_{max} \sin\left(2\pi \frac{St \cdot U_{hub}}{D} t\right), \tag{1}$$

where the yaw angle γ at time t is decided by the yaw amplitude γ_{max} and the Strouhal number St, i.e., a reduced frequency given by $St = fD/U_{hub}$, where f is the yaw frequency and U_{hub} is the mean streamwise inflow velocity at the hub height of the wind turbine. In this study, γ_{max} and St are tested in ranges of $0-35°$ and $0-0.35$, respectively. To also reveal how CYC affects wind farm power performance through dynamic wake steering, wake flows in wind farms are measured via the particle-image velocimetry (PIV) technique. Details of the PIV setup can be found in the work of Duan et al. [2].

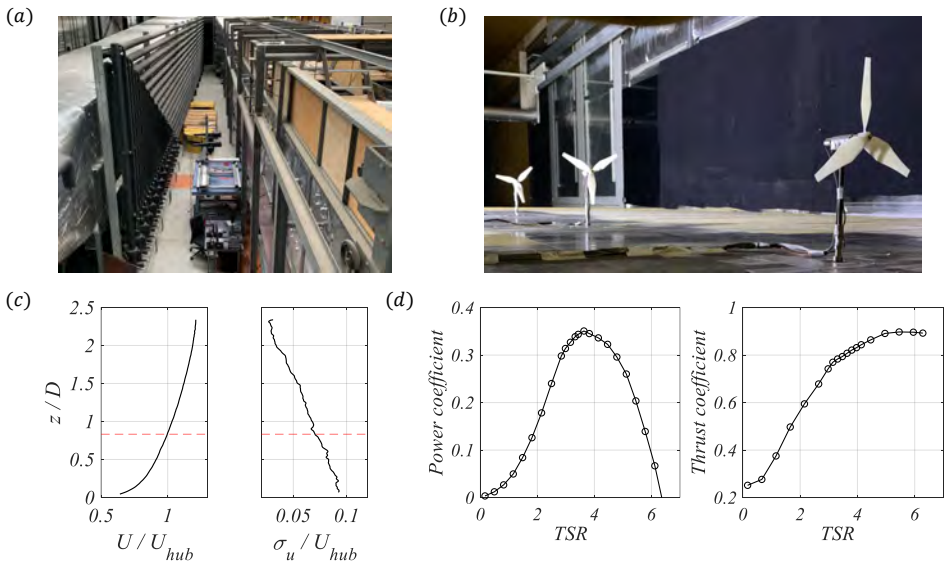

Figure 1: (a) A general overview of the WiRE ABL closed-loop wind tunnel; (b) A three-turbine wind farm model in the test section; (c) The inflow condition: normalized mean streamwise velocity and turbulence intensity; and (d) The power and thrust curves of the WiRE-01 miniature wind turbine.

Power performance and wake flow

Power measurements are conducted in wind farms (fully aligned with $5D$ streamwise spacing) comprising various numbers of wind turbines with different combinations of γ_{max} and St. As presented in Figure 2(a), in principle, CYC causes the power decrease for a single wind turbine while leading to the power increase of wind farms in a wide range of γ_{max} and St combinations. With more wind turbines in the wind farm, CYC can be more efficient in improving power production: the maximum power gain increases from 10% for 2 turbines to 32% for 8 turbines. This proves the potential CYC in wind farms, especially in large wind farms with many rows of wind turbines. In addition, it is found that the power gain is more dependent on both γ_{max} and St. With more wind turbines, the optimal power gain tends to appear at a slightly higher or constant γ_{max} but a lower St. This indicates that for wind farms with more wind turbine rows, CYC can be applied at a lower yaw speed. Wake flow information obtained from PIV measurements reveals that CYC can accelerate the wake recovery for all individual wind turbines (as shown in Figure 2(b)) and thus lead to more available power downstream, which eventually improves the power performance of wind farms.

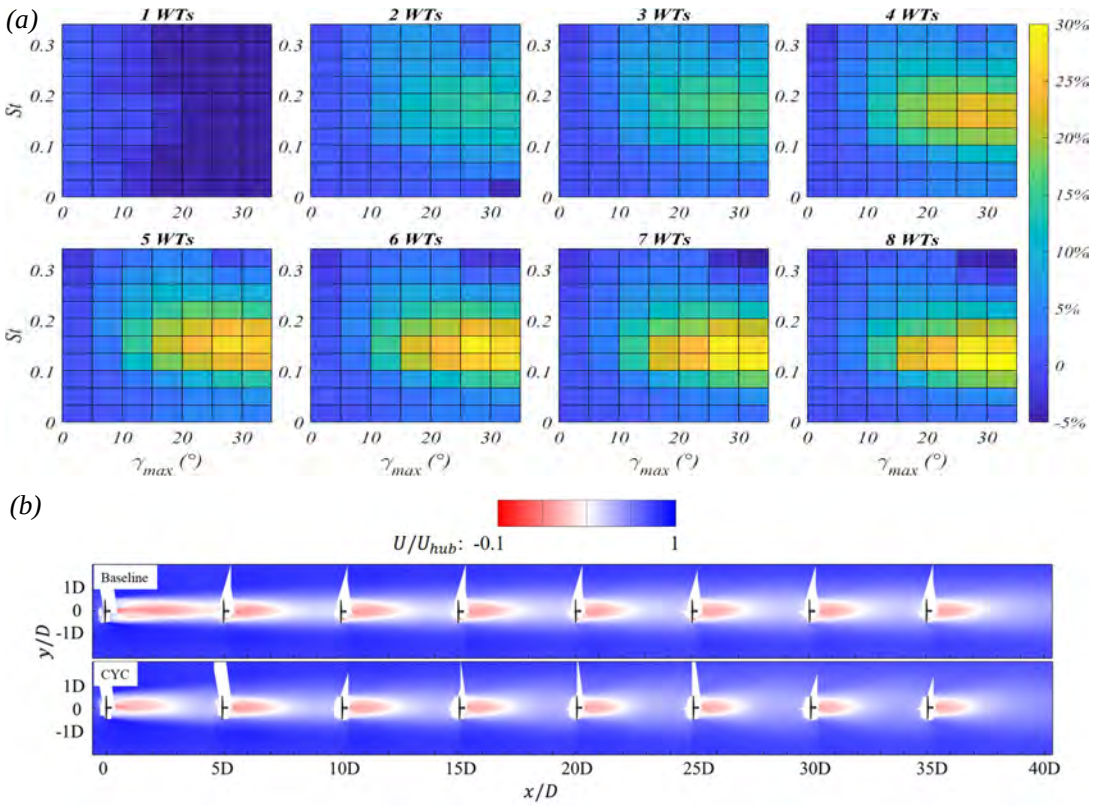

Figure 2: (a) Power gain of wind farms comprising various numbers of wind turbines (WTs) when applying CYC with different combinations of γ_{max} and St; and (b) normalized mean streamwise wake velocity distribution at the hub-height horizontal-streamwise plane in the 8-turbine wind farm for the baseline case and the optimal CYC case.

Conclusion

The application of cyclic yaw control (CYC) strategy in wind farms is investigated via wind tunnel experiments with the WiRE-01 miniature wind turbines. Results from power measurements show that CYC can lead to considerable power gain in wind farms, depending on γ_{max} and St. The efficiency increases when there are more rows of turbines in the wind farm. Wake measurements reveal that the power improvement is due to a faster wake recovery caused by CYC. This study proves that CYC can be a potential strategy for power benefits. However, the results still need to be verified with numerical and field data, and the effects on loading also need to be evaluated.

References

[1] Majid Bastankhah and Fernando Porté-Agel. "A new miniature wind turbine for wind tunnel experiments. Part I: Design and performance". In: *Energies* 10.7 (2017), p. 908.

[2] Guiyue Duan, Arslan Salim Dar, and Fernando Porté-Agel. "A wind tunnel study on cyclic yaw control: Power performance and wake characteristics". In: *Energy Conversion and Management* 293 (2023), p. 117445.

[3] Tristan Revaz, Mou Lin, and Fernando Porté-Agel. "Numerical framework for aerodynamic characterization of wind turbine airfoils: Application to miniature wind turbine WiRE-01". In: *Energies* 13.21 (2020), p. 5612.

Enhancing Wind Farm Performance through Axial Induction and Tilt Control: Insights from Wind Tunnel Experiments

Guillem Armengol Barcos and Fernando Porté-Agel

Introduction

Static axial induction control and tilt control are two strategies that have the potential to increase power production in wind farms, mitigating wake effects and increasing the available power for downstream turbines. The results of a study which looks into these two techniques experimentally through wind tunnel experiments are described next [1]. Experiments are conducted in the boundary layer wind tunnel at the WiRE laboratory of EPFL, using the miniature wind turbine WIRE-01 [2, 3], with a rotor diameter D of $15cm$.

Axial Induction Control

The effect of modifying the axial induction factor of upstream turbines on the overall power is tested in a wind farm comprising two, three and five wind turbines. The rotational speed of the upstream turbines is modified in increments of 4.5% of their optimal value (i.e., 100 rpm) down to an 82% of it, whereas the last turbine is always operated at an optimal tip speed ratio (i.e., TSR). For the five-turbine case, to limit the studied cases and examine the cumulative effect of the strategy, the downstream turbines are operated either as far from their optimal points as the upstream ones or closer (i.e., as a percentage). The excluded scenarios are considered less promising since this technique aims to enhance wind farm power production by increasing the available power for downstream turbines. Therefore, downrating upstream turbines is more likely to be advantageous, as there are more turbines downstream that can benefit from it. The turbine inter-spacing (i.e., S_x) in the three cases is $7D$, and the turbines are placed in one column under full wake conditions. A scheme of the setup placed in the wind tunnel can be seen in Figure 1.

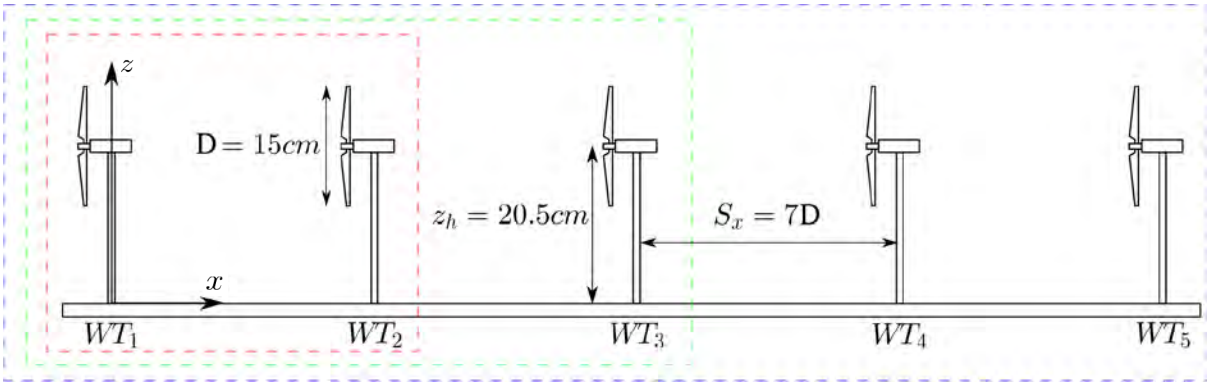

Figure 1: Sketch of the wind farms in the axial induction control experiments (not to scale).

The axial induction factor can be modified by adjusting the TSR or the pitch angle, but these

methods differ. Changing the pitch angle uniformly alters the axial induction factor and angle of attack (AoA) across the entire blade. In contrast, operating outside the optimal TSR causes non-uniform changes in these factors, varying the velocity deficit across the rotor. In fact, reducing the AoA via the pitch angle (i.e., pitch to feather) reduces the thrust coefficient [6], but reducing the AoA through the rotational velocity (i.e., higher TSR) increases it. This difference is theoretically explained in [1].

Figure 2 shows the normalized overall power extraction with respect to the baseline case (i.e., operating all turbines at optimal TSR) for the three scenarios. In the plots, the color of the circles represents the percentage of derating of each turbine. Cases where the upstream turbines increase their TSR are not included, as the power extraction of downstream turbines did not increase in such situations. It can be seen that only very few cases exhibited slight enhancements in overall power production (i.e., less than 0.5%). Moreover the overall power gradually diminishes as the upstream turbines are further downrated, indicating that additional downrating of the wind farm would not yield increased power production. Notably, the purple dots are predominantly clustered on the left side of the plot. In conclusion, employing static axial induction control through the TSR is not an effective technique for augmenting global power production. Nevertheless, given the marginal overall losses observed in most configurations, this strategy could be contemplated for other objectives, such as load distribution balancing within a wind farm.

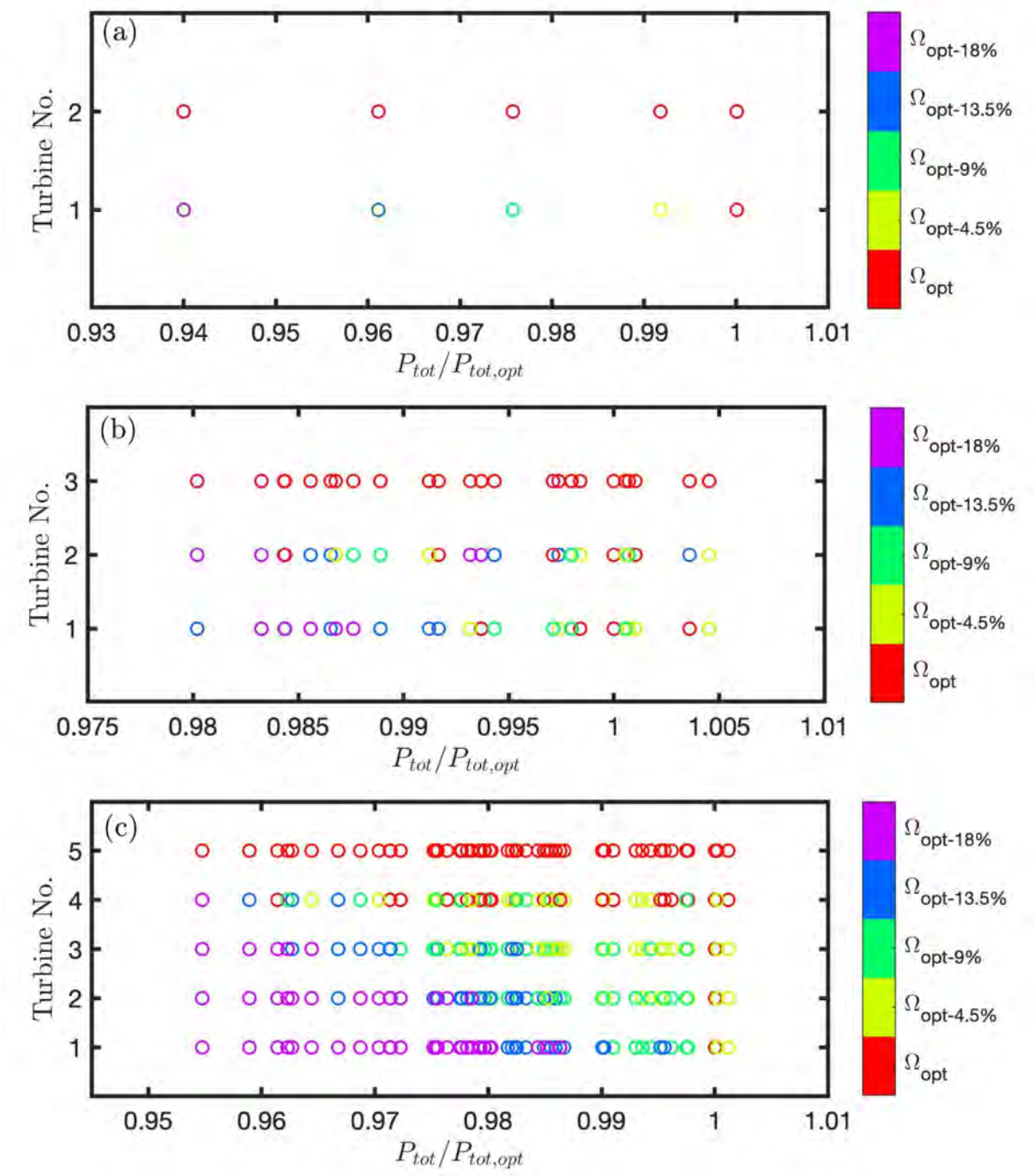

Figure 2: Normalized wind farm power extraction $P_{tot}/P_{tot,opt}$ for a wind farm comprising two (a), three (b) and five (c) wind turbines. Different colors indicate the difference (in percentage) between the operating TSR and the optimal value

Tilt Control

The ability of tilt control to enhance global power production is tested in a two-turbine wind farm, tilting the upstream turbine forward and backward up to an angle of $\gamma = 25°$ in increments of $5°$ (i.e., eleven tilt angles). Additionally, the impact of turbine spacing (i.e., S_x) and turbulence intensity (i.e., TI) on the strategy is analyzed. In this regard, experiments are

conducted by placing the turbines at distances of $5D$ and $7D$ and two levels of streamwise turbulence intensity, $\sigma_{Uthti} = 6.6\%$ and $\sigma_{Utlti} = 8.9\%$. A scheme of the setup placed in the tunnel can be seen in Figure 3.

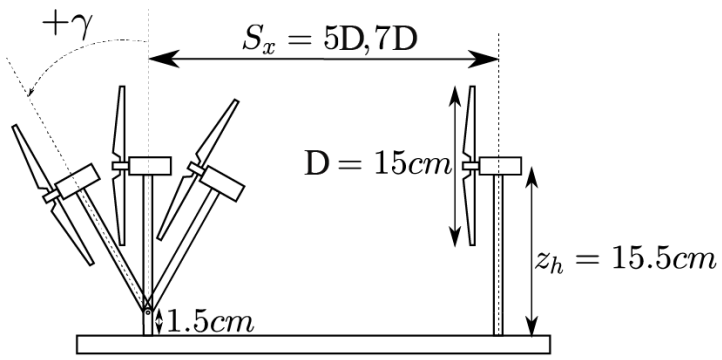

Figure 3: Sketch of the wind farm in the tilt control experiments (not to scale).

The power extraction for each of the two turbines and the combined cluster for the four setups can be seen in Figure 4. Data is normalized with respect to the combined power of both turbines in the baseline case of each configuration (i.e., no tilt applied). When the upstream turbine is tilted backward, although the power extraction of the downstream turbine gradually increases with the tilt angle, the gain is significantly smaller compared to the reduction of the upstream one, resulting in relatively similar losses, in percentage, across all four configurations. The overall power extraction gradually decreases with the tilt angle, meaning that further tilting of the upstream turbine would result in even lower output. Thus, backward tilting is seen as ineffective, regardless of the turbulence intensity level and turbine inter-spacing distance. Regarding forward tilting, significant increments in overall power extraction can be observed. In fact, the increments in power (e.g., 16.5% and 10.9%) surpass those of other wake mitigation techniques using only two turbines under full wake conditions [5, 4]. The highest increments are seen for low TI levels and S_x distances. Higher TI levels enhance turbulent mixing and vertical entrainment, and higher S_x distances allow the wake to recover. Therefore, the power losses caused by the upstream wake decrease with high TI levels and S_x distances, leaving less room for improvement using wake mitigation techniques. Tilt control is seen to be more sensitive to the TI level than to the S_x distance since the increase in both percentagewise is comparable (i.e., from 6.6% to 8.9%, and from $5D$ to $7D$), but an increase in the TI results in a higher reduction in power gain.

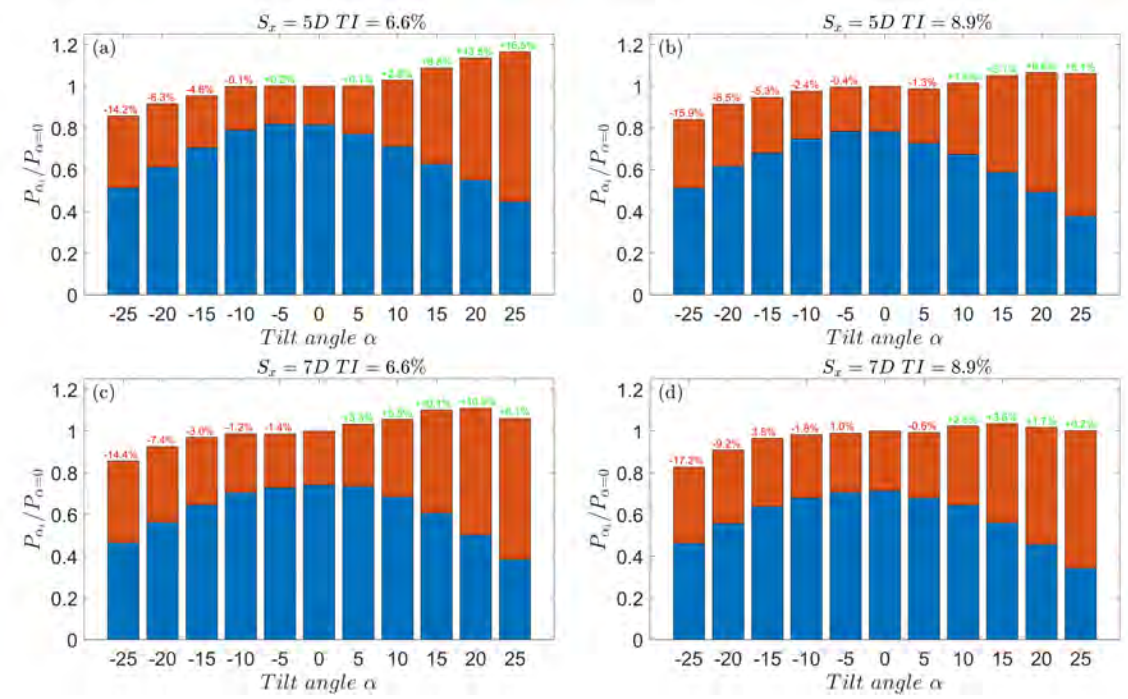

Figure 4: Normalized power of the upstream turbine (blue) and the downstream turbine (orange) for the four configurations. (a) $S_x = 5D$ and $TI = 6.6\%$; (b) $S_x = 5D$ and $TI = 8.9\%$; (c) $S_x = 7D$ and $TI = 6.6\%$; (d) $S_x = 7D$ and $TI = 8.9\%$. The sum of both represents the overall power production.

The flow dynamics in the two-turbine wind farm under tilt control are also analyzed, tilting the upstream turbine ($\gamma = 0, +10, +20, -20°$). Figure 5 displays contour plots of the normalized mean streamwise velocity deficit along with the trajectory of the wake's center (i.e., where the highest streamwise velocity deficit is encountered) for $S_x = 5D$. The deflections of both wakes increases with the increase in the tilt angle due to increased vertical component of the thrust force and, therefore, because of the conservation of momentum, increased induced vertical velocity in the wake. Similarly (i.e., due to reduced thrust in the streamwise direction) lower streamwise velocity deficit values are encountered as the tilt angle increases. Forward tilt angles deflect the wake toward the ground, and the wake deflection is characterized by an initial decrease down to $x/D = 3$, especially for $\gamma = +20°$, after which the wake is redirected because of floor blockage. In downward deflection, the flow above the turbine, characterized by high speed and low turbulence intensity, is pulled into the wake space increasing the available power significantly for the downstream turbine. In contrast, backward tilt angles induce a consistent upward deflection of the wake, which results in higher secondary steering due to higher vertical velocities and inclination angles experienced by the downstream turbine. Moreover, the downstream turbine experiences a low-speed, highly turbulent flow from below the turbine's rotor level due to upward wake deflection. In conclusion, the dissimilarity between positive and negative tilt angles, both looking at the power extraction and flow across the wind farm, becomes apparent due to the shear within the incoming boundary layer.

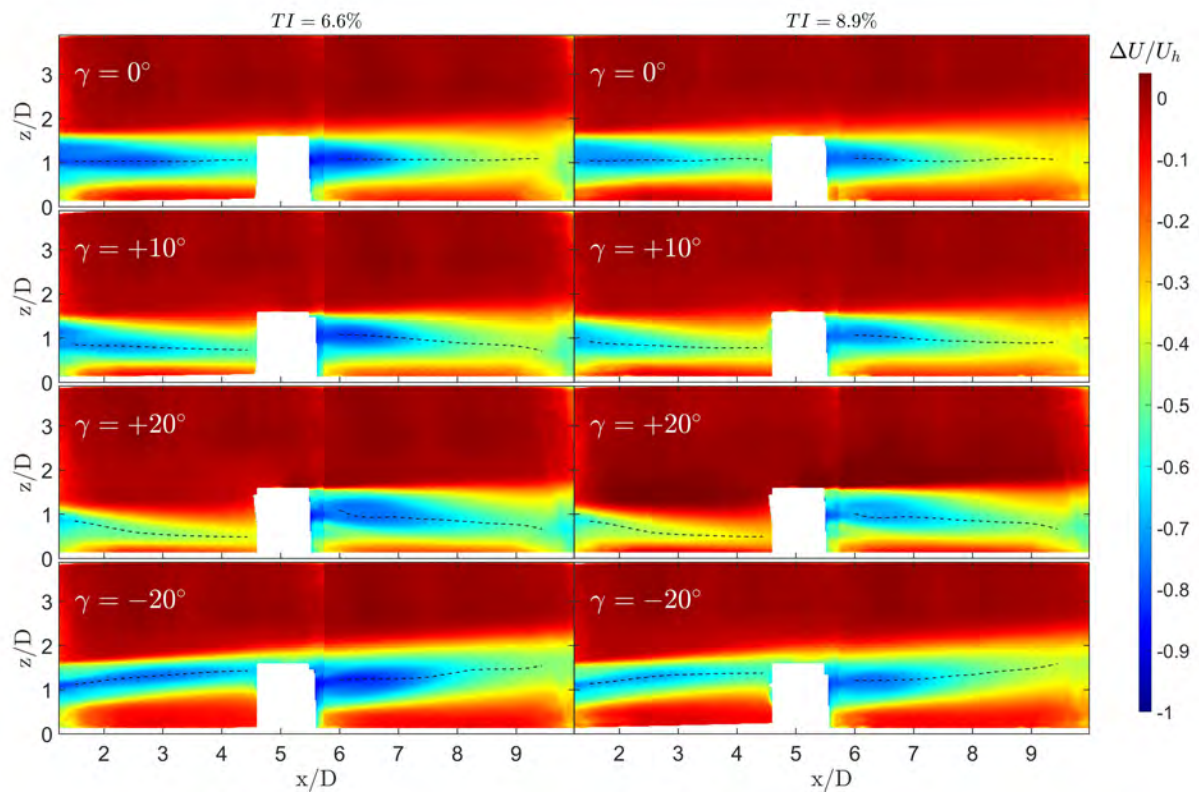

Figure 5: Contour plots of the normalized mean streamwise velocity deficits under different tilt angles in the two-turbine wind farm ($S_x = 5D$). The black dashed lines represent the center of the wake.

Both the turbulent and mean momentum fluxes exhibit very similar patterns in the wake of the upstream turbine, with noticeable distinctions between positive and negative tilt angles. For positive tilt angles, a single prominent peak emerges, aligning with the location of maximum shear (i.e., between the wake and the outer flow above the turbine). Conversely, for negative tilt angles, both the turbulent and mean momentum fluxes display two peaks: the upper one is associated with the high shear between the wake and the outer flow, whereas the lower peak originates from the airflow beneath the turbine, which is drawn into the wake space. This lower peak dominates the entire wake, indicating that for a negative tilt, wake recovery is primarily driven by the low energetic flow occupying the wake space, rather than the high shear between the wake and the flow above the turbine.

The streamwise velocity, vertical velocity and available power (derived from flow measurements) vertical profiles at the position of the hypothetical third wind turbine are shown in 6. These quantities also exhibit opposite trends between positive and negative tilt angles due to secondary steering, which refers to the deflection of the downstream turbine's wake. This phenomenon arises from the increased vertical component of velocity in the wake of the tilted turbine, which influences the downstream turbine's wake trajectory. Secondary steering is reduced for positive tilt angles as the ground redirects the wake flow and reduces its vertical component. At the position of the hypothetical third wind turbine, forward tilt angles result in significantly lower available power in the lower half of the rotor compared to the

baseline case. This contrasts with the increase in available power observed at the upper half of the rotor because of enhanced entrainment. Backward tilt angles yield the opposite effect. They lead to increased available power in the lower half of the rotor, approximately doubling the power at the bottom tip compared to the baseline case, while the available power decreases in the upper half. The negative peak in the streamwise velocity and, consequently, power, could potentially be displaced out of the rotor plane through increased secondary steering. This outcome emphasizes the importance of cumulative wake deflection through the gradual reduction of the tilt angle, which has the potential to significantly increase the power gains using tilt control in a wind farm with more turbines.

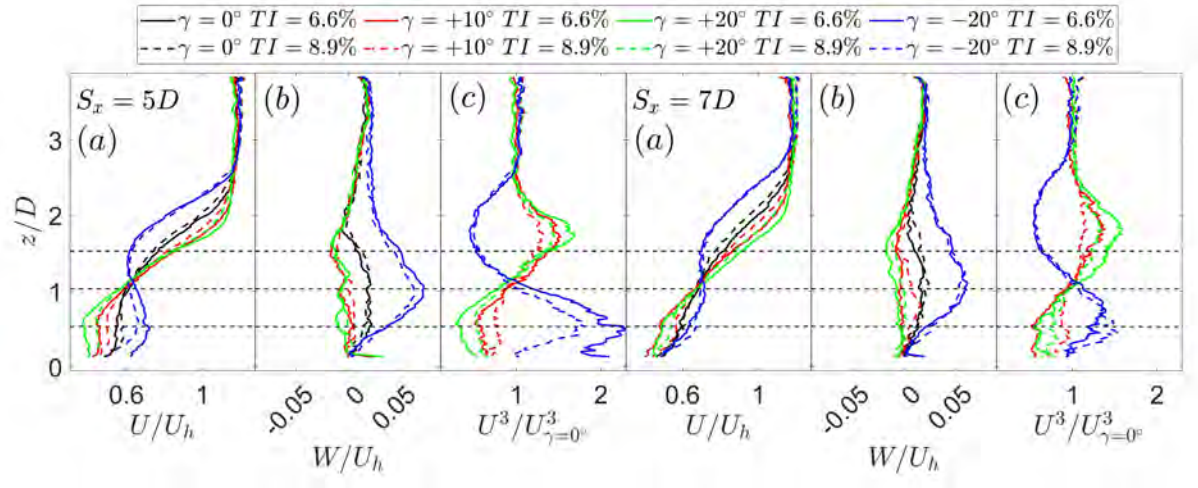

Figure 6: Vertical profiles of normalized streamwise velocity (a), normalized vertical velocity (b), and normalized available power (c) experienced by a hypothetical third turbine. The black dashed lines represent the rotor's top tip, hub height, and bottom tip.

References

[1] Guillem Armengol Barcos and Fernando Porte-Agel. "Enhancing Wind Farm Performance through Axial Induction and Tilt Control: Insights from Wind Tunnel Experiments". In: *Energies* 17.1 (2023).

[2] Majid Bastankhah and Fernando Porte-Agel. "A new miniature wind turbine for wind tunnel experiments. Part I: Design and performance." In: *Energies* 10.7 (2017).

[3] Majid Bastankhah and Fernando Porte-Agel. "A new miniature wind turbine for wind tunnel experiments. Part ii: Wake structure and flow dynamics." In: *Energies* 10.7 (2017).

[4] Majid Bastankhah and Fernando Porte-Agel. "Experimental and theoretical study of wind turbine wakes in yawed conditions." In: *Fluid Mechanics* 806 (2016).

[5] Majid Bastankhah and Fernando Porte-Agel. "Wind farm power optimization via yaw angle control: A wind tunnel study." In: *Renewable and Sustainable Energy* 11.2 (2019).

[6] Tristan Revaz, Mou Lin, and Fernando Porté-Agel. "Numerical framework for aerodynamic characterization of wind turbine airfoils: Application to miniature wind turbine WiRE-01". In: *Energies* 13.21 (2020), p. 5612.

A wind tunnel study of wind turbine wakes in convective, neutral and stable boundary layers

Konstantinos Kotsarinis, Arslan Salim Dar and Fernando Porté-Agel

Introduction

The variation of the thermal stratification of earth's atmosphere throughout the day, affects the development of wind turbine wakes, which strongly influences the performance and lifetime of the wind turbines [3]. A neutral boundary layer forms when the temperature gradient from the earth to the atmosphere is zero. Negative temperature gradients result in a convective boundary layer, which leads to a faster recovery of the wind turbine wake compared to neutral conditions and positive temperature gradients result in a stable boundary layer, which has a slower wake recovery than neutral conditions [2]. Wind tunnel experiments offer the opportunity to thoroughly analyse the flow field around wind turbines under a variety of precisely controlled and repeatable conditions. The present study investigates the structure of the wind turbine wake in a thermally convective, neutral and stable boundary layer.

Experimental Setup

A series of experiments were carried in the $28m \times 2.6m \times 2m$ test section of the closed-loop atmospheric boundary layer wind tunnel of the Wind Engineering and Renewable Energy Laboratory (WiRE) laboratory at EPFL. In order to generate the convective and stable boundary layer conditions, a temperature control system was employed for both the air and the wind tunnel floor, capable of reaching temperatures from $-10\ ^{\circ}C$ up to $100^{\circ}C$. In particular, 32 temperature control aluminum tiles along $12.8m$ of the test section are used for floor heating/cooling and 16 heat exchangers equally spaced along the height of the wind tunnel for airflow heating/cooling. The absolute humidity of the wind tunnel was maintained at 5 g/kg during the experiments with the help of an air dehumidifier. The WiRE-01 miniature three-bladed horizontal axis wind turbine [1] was used in this study.

The boundary layer developed naturally along the test section and all the measurements were performed at a location where the boundary layer was fully developed. The mean flow temperature was acquired using a K-type thermocouple averaging over 60 s for a range of heights and a sampling rate of 1kHz. In order to characterize the wake of the wind turbine, two-dimensional two-component Particle Image Velocimetry system was deployed. The field of view of the measurements was set up to be 3D $\times$ 5D in a vertical plane through the center of the wind turbine rotor. A pulsed 425 mJ dual-head Nd:YAG laser was used for the illumination of the tracing particles and a sCMOS camera (2560 $\times$ 2160 pixels) to capture 1000 pair images at a sampling rate of 10 Hz. In order to obtain the velocity fields, a two step analysis is conducted. In the first step, the interrogations window reduction starts with a window size of 64 $\times$ 64 pixels and in the second step a size of 32 $\times$ 32 pixels is used. The

correlation is obtained by two passes through each of the windows sizes while keeping an overlap of 75 % between neighboring windows.

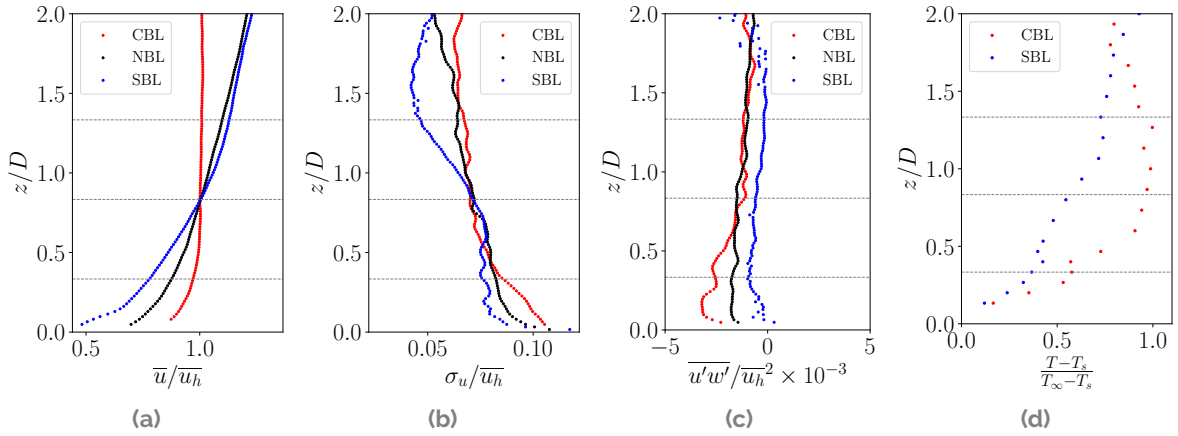

Figure 1: Boundary layer characteristics for Convective (red) Neutral (black) and Stable (blue) conditions: (a) normalized mean streamwise velocity, (b) normalised streamwise turbulence intensity (c) normalized mean vertical momentum flux (d) Normalised mean temperature (e) Richardson number. The dashed grey lines denote the rotor projected area.

Figure 1 presents a summary of the boundary layer characteristics for the convective, neutral and stable conditions. The mean streamwise velocity $\overline{u}$, the standard deviation of the streamwise velocity σ_u are normalised by the mean velocity at the height of the rotor hub $\overline{u_h}$ and the vertical momentum flux $\overline{u'w'}$ by its square. The mean temperature is normalised using the surface temperature T_S and the freestream temperature T_∞. A strong temperature gradient is evident for both the stable and convective conditions, but the slope corresponding to the convective case is larger compared to the slope of the stable case closer to the surface. This leads to higher uniformity in a lower distance from the surface for the convective boundary layer compared to the stable boundary layer due to higher turbulent mixing. On the other hand the stable boundary layer has a stronger mean flow shear compared to the neutral boundary layer whereas the convective boundary layer has a weaker mean flow shear compared to the neutral boundary layer. Both turbulence intensity and vertical momentum fluxes are slightly larger for the convective boundary layer but remain within the same order of magnitude for all the cases. Finally, the bulk of the flow has a Richardson number of approximately 0.2 for the stable case and -0.3 for the convective case. The Richardson number can be obtained as $Ri_B = \frac{g\delta\Delta T}{\overline{T}U_\infty^2}$,where g is the gravitational acceleration, δ is the boundary layer height, ΔT is the temperature at the surface and the height of interest, $\overline{T}$ is the mean temperature and U_∞^2 is the freestream velocity.

Results and Discussion

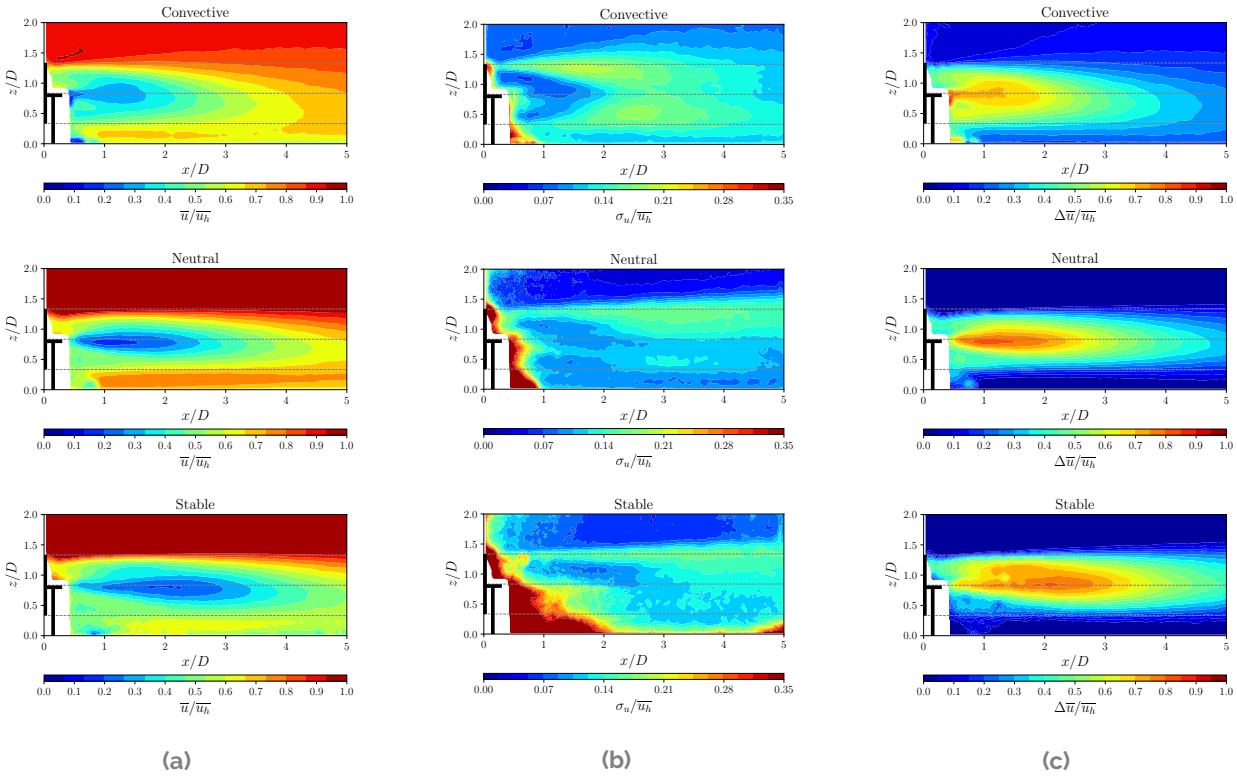

Figure 2: PIV measurements of the model wind turbine wake: (a) normalized mean streamwise velocity, (b) normalised streamwise turbulence intensity (c) normalized mean vertical momentum flux for the Convective (top), Neutral (middle) and Stable (bottom) boundary layer conditions.

The flow field around the wind turbine model is shown in Figure 2. The convective boundary layer conditions lead to an increase in normalised mean streamwise velocity compared to the neutral boundary layer conditions, whereas the stable boundary layer conditions lead to a decrease of the mean velocity compare to the neutral conditions. The stronger wake created in the stable conditions becomes even more evident in the plots showing the boundary layer deficit in velocity caused by the wind turbine model. The convective conditions as expected lead to a smaller velocity deficit compare to the neutral conditions and due to entrainment, the wake recovers in less than 4 D back to a velocity approximately equal to 80% of the freestream. On the other hand, the stable conditions result in a significant increase in the velocity deficit and the wake is not able to recover to a velocity higher than 50 % of the freestream even at 5 D. This can have a significant impact on the interactions of wind turbines in a wind farm. Finally, despite the similarity of the turbulence intensity distributions of the 3 boundary layers, the wind turbine induced turbulent intensity flow fields showcase important differences both in their scale and structure. In the neutral case, a region with increased turbulence intensity is evident at the top of the rotor tip that propagates for the full field of view of the PIV measurements. This region becomes wider for distances over 2 D after the turbine. The stable case flow field is also characterized by a similar region of increased turbulence intensity, but interestingly the convective case has

a second region of increased turbulence at the bottom of the rotor tip as well. These two regions start merging after 2 D creating an elevated mean value of of turbulence intensity but with a more uniform distribution downstream the wind turbine.

In Figure 3 we compare the normalized maximum streamwise velocity deficit between the three investigated conditions. It is clear that the peak values for the neutral and convective cases are before 2 D, whereas for the stable case the peak of the maximum deficit curve occurs after 2 D, indicating a slower recovery.

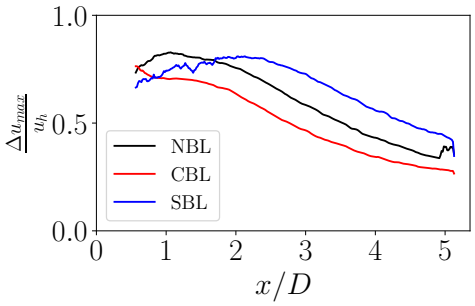

(a)

Figure 3: Comparison of the normalized maximum streamwise velocity deficit for the Convective (red) Neutral (black) and Stable (blue) conditions.

Conclusion

The present study highlights the significant impact of thermal stability on wind turbine wake behavior and performance. Convective boundary layer conditions, characterized by increased turbulent mixing, facilitate faster wake recovery compared to neutral conditions. Conversely, stable boundary layer conditions, marked by stronger mean flow shear, result in a slower wake recovery and a larger velocity deficit, which could affect the interactions of turbines within a wind farm. Despite similar turbulence intensity distributions among the boundary layers, the induced turbulence flow fields show notable differences, particularly in the convective case, which features distinct regions of increased turbulence intensity. These findings underscore the importance of considering thermal stratification effects in optimizing wind turbine performance and layout within wind farms.

References

[1] Majid Bastankhah and Fernando Porté-Agel. “A new miniature wind turbine for wind tunnel experiments. Part I: Design and performance”. In: *Energies* 10.7 (2017), p. 908.

[2] Giacomo Valerio Iungo and Fernando Porté-Agel. “Volumetric lidar scanning of wind turbine wakes under convective and neutral atmospheric stability regimes”. In: *Journal of Atmospheric and Oceanic Technology* 31.10 (2014), pp. 2035–2048.

[3] Fernando Porté-Agel, Majid Bastankhah, and Sina Shamsoddin. “Wind-turbine and wind-farm flows: a review”. In: *Boundary-layer meteorology* 174.1 (2020), pp. 1–59.

Work Package 2

Remote Sensing

Introduction

Mikael Sjöholm, Joachim Reuder, Charlotte Bay Hasager, and Jakob Mann

From an experimental point of view, the lower half of the offshore marine atmospheric boundary-layer has to date been difficult to measure with meteorological masts and towers, as they cannot be built arbitrarily high, and even a 100-m mast offshore costs more than 10 million euro. Today, however, we have agile high-resolution remote sensing lidars (light detection and ranging), that can reach and measure details several hundreds of meters up into the atmospheric boundary-layer, and at measurement distances of several kilometers. A comprehensive overview of lidar technology for offshore wind energy applications can be found in [1].

The lidar technology relies on laser beams that are sent out into the atmosphere, reflected by aerosols notionally travelling with the overall wind speed, and collected again, analysing the Doppler shift due to the aerosol travelling velocity. Wind profiling lidars use a limited number of differently oriented beams (nowadays typically 5) to measure the altitude dependence of wind speed and direction above the lidar. Scanning lidars have steerable heads able to conduct essentially any trajectory. Both types of lidars have been utilized in the targeted Train2Wind measurement campaign Lollex [2], where several lidars from DTU and UiB were used in and around the Rødsand 2 wind farm off the coast of Lolland. One scanning wind lidar system was installed on the transformer platform of the wind farm, mainly performing RHI (range height indicator) scans along one specific transect through the farm. In addition, one lidar wind profiler and one scanning lidar in vertical stare mode, were installed on a crew transfer vessel (CTV) as platform of opportunity, providing about 6 months of continuous data inside and around the Rødsand wind farm. This approach provided a novel and unique data set for the detailed characterization of wind farm flow which has been analyzed by UiB.1.

A deeper understanding of the low-frequency wind fluctuations prevalent in the marine atmosphere has been gained by the work done by DTU.4 that has developed a novel 2D turbulence model based on a two-dimensional spectral tensor, operating within a two-dimensional domain to allow the evaluation of two-point statistics which together with a high-frequency wind turbulence model for smaller scales, effectively can represent the broad frequency range relevant for offshore wind farms.

A more area based approach is available from Synthetic Aperture Radar (SAR) mounted on satellites. Wind maps retrieved from satellite SAR show the offshore wind speed variation with spatial resolutions down to a few meters. Wakes of large offshore wind farms can therefore be resolved at high spatial detail. Previous work based on SAR has shown a velocity deficit up to 100 km downstream of large offshore wind farms compared to the freestream velocity. SAR wind fields are thus very valuable for validation of wake models. DTU.3 has improved the conversion from the raw SAR observations to a wind map at hub height, using Sentinel-1 SAR observations from Copernicus, and compared it to numerical

results.

For better understanding the interaction of the wind fields with vertical axis turbines, a coupled near and far-wake model for the aerodynamic modelling of vertical-axis wind turbines has been developed by DTU.ra.1. The coupled model yields much more realistic aerodynamic loads and power than the original Actuator Cylinder model thanks to the aerodynamic coupling of the different blade sections which effectively adds 3D effects. Its computational cost remains low compared to higher fidelity models (free-wake codes, CFD...) which allows it to be used extensively as an engineering model, hence it is implemented in the HAWC2 software.

References

[1] Joachim Reuder, Etienne Cheynet, Andy Clifton, Marijn Floris van Dooren, Julia Gottschall, Jasna B. Jakobsen, Jakob Mann, Jose Palma, David Schlipf, Mikael Sjøholm, Juan-Jose Trujillo, Ludovic Thobois, Ines Würth, and Alberto Zasso. *Recommendation on use of wind lidars*. Tech. rep. Bergen, Norway, 2021, pp. 1–33. DOI: 10.5281/zenodo.4672351. URL: http://doi.org/10.5281/zenodo.4672351..

[2] Train2Wind. *Experimental campaign at the offshore wind farm Rødsand 2 , Denmark "Lolland Experiment (LOLLEX) - Project Description*. Tech. rep. Train2Wind Technical Report, 2023, 17pp.

Satellite Synthetic Aperture Radar (SAR) data analyses for offshore wind energy and coastal applications

Abdalmenem Owda and Charlotte Hasager

Introduction

DTU Wind and Energy Systems possess a large satellite Synthetic Aperture Radar (SAR) archive of ocean surface wind maps. The PhD study aims to utilize and improve the reliability of such data for offshore wind energy and coastal applications. SAR data has global coverage. They are independent of atmospheric conditions as they can be observed through rain and clouds. During the day and night, SAR data is retrieved. At each overpass of the polar-orbiting satellites with SAR sensors on board, valuable data is collected. A classical output from SAR is spatially high-resolution ocean surface wind fields. The wind speeds are retrieved at 10 m height. Another output from SAR is wave parameters. These two parameters are central in studying offshore wind energy and coastal applications. Furthermore, a novel approach to derive the ocean aerodynamic roughness length is developed and tested in the study.

Research objectives

The ocean wind retrieval is based on the physical principle of the normalized radar cross section (NRSC) observed by the SAR, a function of the short waves at the sea surface. The short waves are generated from the near-instantaneous ocean wind speed. The geophysical model functions relate the NRSC values and the wind speed in a non-linear equation. This equation includes wind direction, satellite viewing geometry, and the SAR wavelength. The first research objective was to eliminate false wind speed due to objects on the ocean that impact the NRSC compared to NRSC values at an ocean surface without objects. The objects can be ships and wind turbines, among others. The research presented a dedicated method to remove anomalous pixels in areas with, e.g., ships without altering the retrieved wind speed in the open ocean [3]. The study showed improved wind retrieval after implementing the method. Furthermore, the presented implementation in [3] preserves the offshore wind farm wakes and can be used to update the global wind turbine databases.

The second research objective was to quantify the horizontal variation in wind speed in coastal zones for several large offshore wind farms. Firstly, the variation in wind speed using a series of SAR wind maps recorded before the wind farms were installed showed significant wind speed gradients, both for sites near the coastline and further away. Furthermore, the study indicated a large wind speed up for winds flowing from land towards the sea, while some stagnation in wind speed was noted for winds flowing from sea to land. The latter relates to the blocking from the adjacent land masses. Secondly, the same variation in wind speed gradient was investigated after the wind farms were installed. Wind farm wakes were also found in those cases. The challenge was to disentangle what wind speed variation

should be ascribed to the wind farm wake and what should be ascribed to the natural wind speed gradient [2]. Interestingly, the wind farm capacity appears to be related to the wake extension and its intensity [2].

The results reported in [2] are from the North Sea and the Kattegat Strait. A brief study on wind farm wakes, and coastal wind speed gradients in the South China Sea with a large wind farm in the study area showed different results, most likely due to oceanic processes impacting the ocean surface [1].

The third research objective focused on ocean wave retrieval in the coastal zone. The method is well developed for open ocean and was tested here in the coastal zone. The results comparing SAR-derived wave height and wave period to ocean buoy data near the US coastlines proved successful [4]. The next step was to extend this analysis to include wave model data for comparison. The results were comparable to the buoy data. The advantage of the model-based comparison was the larger number of collocated samples for the statistics than the buoy comparison. Finally, based on satellite SAR, novel and innovative research was undertaken to retrieve the aerodynamic roughness length over the ocean. Two challenges had to be overcome. The first is the cut-off effect due to the viewing geometry from the satellite SAR used, in this case, Sentinel-1 Interferometric Wide mode data, and the pixel size available. The second is to relate the SAR values to the environment in the study, again the US coastline. Both challenges were overcome [4, 5]. A wave dispersion schema was used for the first challenge, while an empirical method to fit the parameters to the environment was used for the latter challenge. The study highlights the possibility of using SAR remote sensing data for global mapping of roughness length, including coastal effects of local variability in sea state and wind field gustiness.

References

[1] Abdalmenem Owda and Merete Badger. “Wind speed gradients and wakes mapped using SAR for a study area in south-east China”. In: *IGARSS 2022 - 2022 IEEE International Geoscience and Remote Sensing Symposium*. Kuala Lumpur, Malaysia, 2022.

[2] Abdalmenem Owda and Merete Badger. “Wind speed variation mapped using SAR before and after commissioning of offshore wind farms”. In: *Remote Sensing* 14.6 (2022).

[3] Abdalmenem Owda, Jørgen Dall, Merete Badger, and Dalibor Cavar. “Improving SAR wind retrieval through automatic anomalous pixel detection”. In: *International Journal of Applied Earth Observation and Geoinformation* 122.103444 (2023).

[4] Abdalmenem Owda, Andrey Pleskachevsky, Merete Badger, Xiaoli Guo Larsén, and Dalibor Cavar. “Normalized roughness length estimation using derived sea state parameters from SAR”. In: *Proceeding of IEEE International Symposium on Geoscience and Remote Sensing (IGARSS)*. Pasadena, CA, USA, 2023.

[5] Abdalmenem Owda, Andrey Pleskachevsky, Xiaoli Guo Larsén, Merete Badger, Dalibor Cavar, and Charlotte Bay Hasager. “Evaluation of SAR-based sea state parameters and roughness length derivation over the coastal seas of the USA”. In: *IEEE Journal of Selected Topics in Applied Earth Observations and Remote Sensing* 17 (2024), pp. 9415–9428.

Large-scale coherent structures in the marine atmosphere

Abdul Haseeb Syed and Jakob Mann

Introduction

Several features of the marine atmosphere differ from the land-atmosphere and make it favorable for extracting wind energy. Although more costly, offshore wind energy projects provide a higher capacity factor than their onshore counterparts. This implies that wind resources are more abundant and reliable in the seas. The wind on the land is affected by obstructions such as cities, forests, and mountains, which is not the case offshore. Land also has a lower heat capacity than water, suggesting it heats up and cools down more quickly. This effect contributes to the diurnal and seasonal variation of land temperatures and, eventually, wind patterns. Over the seas, the temperature change is more gradual, resulting in consistent and more reliable winds. Another defining feature of the marine atmosphere is its low wind turbulence. The turbulence in the surface layer (the lowest 10% of the atmospheric boundary layer) is often generated by roughness elements or obstructions—the absence of these rough elements causes less turbulence in the winds over water.

The interaction between wind turbines and the atmosphere constitutes one of the three "grand challenges" in wind energy science presented by [1, 7]. The atmospheric flow contains a spectrum of scales ranging from planetary or synoptic scales ($10^5 - 10^7$ m), which influence global climate patterns, to mesoscales ($10^3 - 10^5$ m) impacting local weather systems and wind resource, and finally microscales (<10^3 m) where the energy dissipation processes occur. These scales impact wind power systems on different levels. Microscales are primarily responsible for the loads, fluctuations in power production, and wake flow characteristics of individual wind turbines. On the other hand, mesoscales play a significant role in influencing wind resources at a certain location, wind farm energy output, and characterizing wake flow from large wind farms.

Historically, most research efforts were focused on modeling and characterizing the microscales [2, 3] since their size corresponded to typical onshore wind power system components. Flow at scales larger than microscales was usually ignored or modeled as a mean background flow. Moreover, the flow models presented were more representative of the onshore wind and less of the offshore wind conditions. Modern offshore wind power systems feature turbines with rotor diameters approaching 250 m and large wind farms spanning tens of km. At such large spatial scales, the influence of mesoscales on the dynamic response of an individual wind turbine, especially a floating turbine, or the overall performance of a wind farm can not be disregarded.

In this project, a model is developed for low-frequency wind fluctuations and coherences in the marine atmosphere. The model can describe the two-dimensional nature of large-scale coherent structures in the wavenumber domain.

Highlights

- We present a model [5] to characterize low-frequency wind fluctuations prevalent in the marine atmosphere. The 2D turbulence model is based on a two-dimensional spectral tensor, operating within a two-dimensional domain to allow the evaluation of two-point statistics. Together with a high-frequency wind turbulence model for smaller scales, it can effectively represent the broad frequency range, including the spectral gap. The energy spectrum formulation used in the model resembles the von Kármán spectrum, featuring a well-defined length scale. Additionally, an anisotropy parameter is incorporated into the 2D turbulence model, which indicates spectral distortion in the wavenumber domain.
- The 2D turbulence model is validated against in-situ measurements from the FINO1 platform and remote sensing measurements from the Hywind Scotland floating offshore wind farm [5]. The 2D turbulence model accurately captured the one-point auto- and two-point cross-spectra at low frequencies down to 1 hr^{-1} at both sites. Fig. 1 exhibits the 2D and 3D turbulence models fitted on the measured spectra observed at FINO1 under neutral atmospheric conditions for $\overline{U} = 13.5$ ms^{-1}.

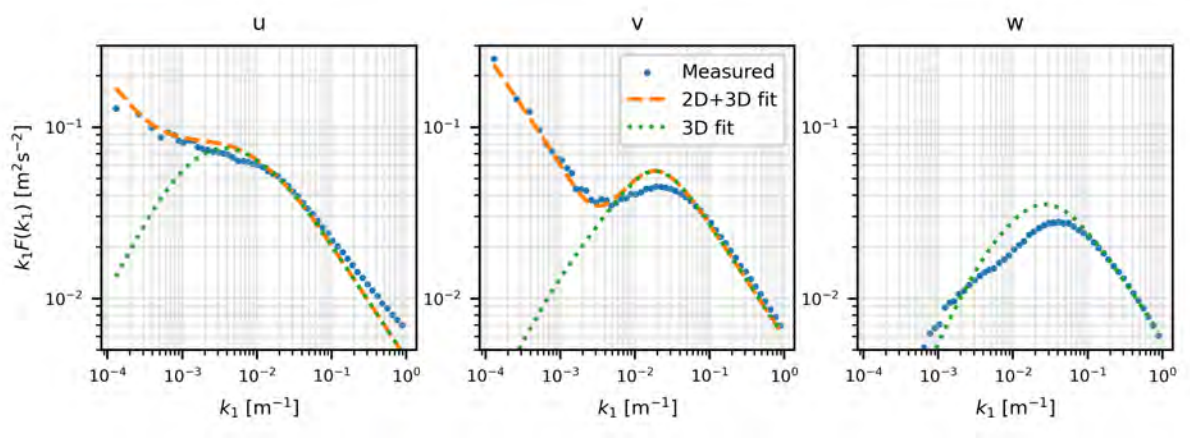

Figure 1: Wind velocity spectra measurements (blue dots) for $\overline{U} = 13.5$ ms^{-1} at $z = 81$ m from FINO1 under neutral atmospheric conditions. The 3D turbulence model (Mann spectral model) is fitted (green dotted lines) as well as the 2D+3D turbulence model (orange dashed lines) for u and v components

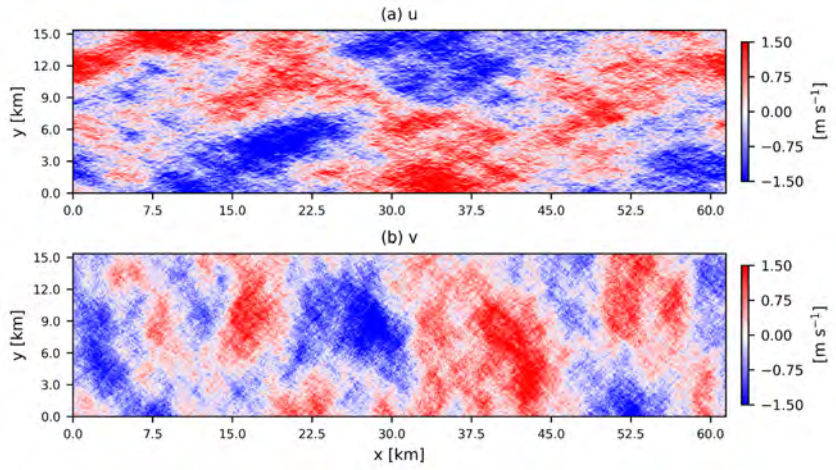

Figure 2: Simulated low-frequency fluctuations of longitudinal u and transverse v wind components. One can easily spot the large-scale coherent structures in the simulated wind field.

- The 2D turbulence model finds application in generating synthetic wind fields, particularly for evaluating loads in large offshore wind turbines. A method for generating synthetic wind fields based on the low-frequency wind turbulence model is detailed in the thesis. The simulation method follows the framework proposed by [4], generating two-dimensional wind fields from the velocity spectral tensor. Assuming statistical independence between low-frequency and high-frequency turbulence, these two wind fields can be superposed to achieve a comprehensive spectral representation of longitudinal and lateral wind velocity components. The auto- and cross-spectra obtained from the simulated wind fields are validated against the modeled relations, and excellent agreement was found. Furthermore, the program to generate the wind fields containing 2D turbulence is open-source and available to the research community [6].

References

[1] "Grand challenges in the science of wind energy". In: *Science* 366 (6464 Oct. 2019), eaau2027.
[2] J. C. Kaimal, J. C. Wyngaard, Y. Izumi, and O. R. Coté. "Spectral characteristics of surface-layer turbulence". In: *Quarterly Journal of the Royal Meteorological Society* 98.417 (1972), pp. 563–589.
[3] J. Mann. "The spatial structure of neutral atmospheric surface-layer turbulence". In: *J. Fluid Mech.* 273 (1994), pp. 141–168.
[4] Jakob Mann. "Wind field simulation". In: *Probabilistic engineering mechanics* 13.4 (1998), pp. 269–282.
[5] Abdul Haseeb Syed and Jakob Mann. "A model for low-frequency, anisotropic wind fluctuations and coherences in the marine atmosphere". In: *Boundary-Layer Meteorology* 190.1 (2024), p. 1.
[6] Abdul Haseeb Syed and Jakob Mann. "Simulating low-frequency wind fluctuations". In: *Wind Energy Science Discussions* 2023 (2023), pp. 1–16.

[7] P. Veers, K. Dykes, S. Basu, A. Bianchini, A. Clifton, P. Green, H. Holttinen, L. Kitzing, B. Kosovic, J. K. Lundquist, J. Meyers, M. O'Malley, W. J. Shaw, and B. Straw. "Grand Challenges: wind energy research needs for a global energy transition". In: *Wind Energy Science* 7.6 (2022), pp. 2491–2496. DOI: 10.5194/wes-7-2491-2022. URL: https://wes.copernicus.org/articles/7/2491/2022/.

A coupled near and far-wake model for the aerodynamic modelling of vertical-axis wind turbines

Nicolau Conti Gost and David Verelst

Introduction

Vertical-axis wind turbines could have a niche in offshore wind farms due to their lower center of gravity which could reduce the substructure costs, which are one of the top contributors to offshore wind levelized cost of energy. On top of that, their lower susceptibility to inflow direction and turbulence compared to horizontal-axis wind turbines and their faster wake recovery rate allows for a reduced spacing in wind farms and therefore a higher wind farm power density [1].

The main focus of this work is to improve the aerodynamic modelling of vertical-axis wind turbines so as to include 3D effects to an existing 2D induction model but keeping the computational cost low as it is meant to be used in fully coupled aeroelastic simulations. This is needed to be able to consider a large amount of load cases as required by design load certification standards. The new model is implemented in HAWC2, DTU's leading aero-hydro-servo-elastic software for simulation of wind turbines which is extensively used in both academia and industry.

Model description

The model consists in the coupling of a lifting-line model for the near-wake contribution of induction to the original Actuator Cylinder model [2] (Madsen, 1982) for the far-wake contribution of induction.

The Actuator Cylinder model computes the induced velocities on a cylinder coinciding with the surface swept by the blades of a vertical-axis wind turbine by solving Euler equations with blade forces acting as external forces. It is a pure 2D model as it solves each slice of rotor in the z-direction separately, so there is no aerodynamic coupling between different blade sections. It also assumes an infinite number of blades, as blade loads are applied across the cylinder and not only at blade actual locations.

The lifting-line model [4] computes the velocities induced by the vorticity trailed by a blade due to spanwise variation of bound circulation. For the case of a vertical-axis, the wake is assumed to be straight. Since the induced velocities depend on the strength of the trailed vortices which in turn depend on the induced velocities, both values have to be iterated to equilibrium at every time step. It solves each blade separately so the different blade sections of a blade are aerodynamically coupled, but the different blades are not.

At each time step, the Actuator Cylinder model computes the far-wake induction in the first place and then the lifting-line model computes the near-wake induction. Both inductions are added up straight away to compute the total induction as their sources are independent

and do not overlap; the far-wake induction is caused by shed vorticity (generated by time variation of bound circulation) and the near-wake induction is caused by trailed vorticity (generated by spatial variation of bound circulation).

Both models benefit from the coupling; thanks to the lifting-line model the far-wake induction from different blade sections are coupled, and thanks to the Actuator Cylinder model the near-wake inductions of each blade are also coupled to the other blades.

Results and Conclusions

After the development and implementation of the coupled model in the HAWC2 code, its performance has been tested for a wide range of turbine geometries and operating points. There are a few conclusions to be remarked after evaluating the results:

- The coupled model adds 3D effects and effectively works as a tip loss correction, inducing greater velocities towards the blade tips where the aerodynamic loading is null. This yields lower aerodynamic loads towards the blade tips compared to the original Actuator Cylinder model, which in turn leads to a decrease of power production.
- Thanks to the aerodynamic coupling of different blade sections, bound circulations and therefore aerodynamic loads are influenced by other blade sections. This leads to much more realistic results than the original Actuator Cylinder model, especially in non-uniform inflow and for blades with varying properties (chord, twist, profile...) across their span.
- The 3D effects of the coupled model make the power coefficient depend on the turbine aspect ratio ($AR = \frac{H}{R}$) since it increases as aspect ratio increases. This allows for a much more accurate design of vertical-axis wind turbines because structural limitations prevent blades from being as long as aerodynamics would suggest, so the coupled model yields a more accurate power production for the low aspect ratios that structural limitations will impose.
- Similarly to [3], the coupled model was compared against the original Actuator Cylinder model but applying a global modification to the polars to correct them based on the blades finite aspect ratio. Results in uniform inflow showed a close match for integral parameters (power, thrust) but large deviations in local values across the blade (velocities, forces). Even integral parameters were greatly different for non-uniform inflow, so this cheaper approach is not enough to model 3D effects as accurately as the coupled model.
- Due to the inherent limitations of lifting line theory, the near-wake induction might not converge for situations where the gradient of lift coefficient with respect to angle of attack $\frac{dCl}{d\alpha}$ is negative. This corresponds to the stall region of aerodynamic profiles, which in vertical-axis turbines can happen for low tip speed ratios. The current best solution has been thought to be de-activating the lifting-line model in such conditions

and keeping the near-wake induction from the previous time-step, but it still remains a weak point of the coupled model.

- The increase of simulation time with respect to the original Actuator Cylinder model is moderately low thanks to the efficient implementation of the vortex integral as a decrement from its value at the previous time step plus an increment from the current time step and a relaxation factor that eases the convergence of the near-wake induction. This allows the coupled model to be used extensively in fully coupled aeroelastic simulations.

  To sum up, the coupled far-wake and near-wake model yields much more realistic aerodynamic loads and power than the original Actuator Cylinder model thanks to the aerodynamic coupling of the different blade sections which effectively adds 3D effects. Its computational cost remains low compared to higher fidelity models (free-wake codes, CFD...) which allows it to be used extensively as an engineering model, hence it is implemented in HAWC2 software. Further performance comparisons against CFD are planned to be made and described in a future journal publication.

References

[1] Ming H., V. P. Yugandhar, Sciacchitano A., and Ferreira C. "Experimental study of the wake interaction between two vertical axis wind turbines". In: *Wiley* (2023).

[2] H. A. Madsen. "The Actuator Cylinder: A flow model for vertical axis wind turbines". In: *Institute of Industrial Constructions and Energy Technology, Aalborg University Centre* (1982).

[3] Pirrung. G. R., Blondel F., Galinos C., Paulsen U. S., and Madsen H. A. "Dynamic tip loss modelling for H-VAWTs". In: (2017).

[4] Pirrung. G. R., Riziotis V., Madsen H. A., Hansen M., and Kim T. "Comparison of a coupled near- and far-wake model with a free-wake vortex code". In: *Wind Energ. Sci* (2017).

Ship-based lidar measurements and motion compensation

Shokoufeh Malekmohammadi and Joachim Reuder

Introduction

The use of lidars in wind energy covers a wide range of applications, from wind resource assessment before establishing a wind farm to monitoring the actual wind conditions during wind farm operation for control purposes [6]. Compared to the traditionally used mast-mounted cup or sonic anemometers, it has been proven that the wind lidars are flexible, robust and affordable instruments. For this reason, the interest in using these devices for the characterization of the wind has progressively grown in the last few years. The employment of lidars in offshore areas can be achieved under different configurations, such as their installation in wind turbine nacelles or in floating platforms like buoys or ships. Ship-based lidars are an innovative technology that, compared with other measurement systems, provide benefits like an easier maintenance, flexibility to measure in deep water areas and their capabilities to provide highly reliable wind data within a wide spatial extent. It is, however, essential to overcome specific challenges in order to establish a reliable and reproducible method for deploying this technology within the wind energy sector. One of the main challenges is a detailed understanding of the motion induced errors on the lidar wind retrievals, and determining the optimal approach to counteract them.

Previous literature has investigated different ways to take the motion effects out of the measurements, either by means of mechanical compensation systems [3, 9, 1, 11], i.e active or passive stabilized instrument platforms, or through the implementation of post-processing motion compensation algorithms [10, 4]. Applying complete motion correction or compensation methods has been shown to be a promising solution for removing the motion effect from the ship-based lidar wind measurements. There are a few lidars that provide off-the-shelf an integrated motion compensation algorithm, such as a specific version of the WindCube v2 offshore. However, this motion compensation system corrects only for the error induced by angular motions (which might be sufficient for floating lidar deployed on buoys), but is not able to compensate for translatory motions that are relevant for ship based deployments. Therefore, the detailed understanding of the motion compensation algorithms and performance of the different available lidar devices under various motion scenarios and atmospheric conditions is of high relevance. In addition, being able to compare the performance of various lidars at different situations, provides the opportunity to optimize the setup for the execution of measurement campaigns using ship-based lidar systems in the future.

Methodology

As an attempt to fill this knowledge gap, we studied the motion effect on several commercially available wind lidars onshore and offshore in different scenarios and climates.

First, we investigated the effect of motion on lidars installed on a moving platform, with two corresponding ground-based lidars serving as reference instruments. The aim of this experiment, referred to as the Grimstad experiment, was to distinguish between systematic errors and motion-induced errors, and to compare the performance of two wind profiling lidars, WindCube V1 and ZX300 (formerly known as ZephIR 300). The setup and positioning of the lidars for the Grimstad experiment are illustrated in Figure 1.

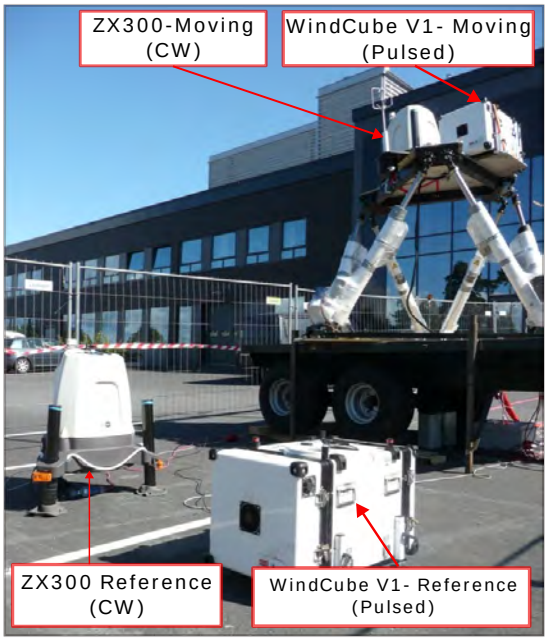

Figure 1: Grimstad experiment: A WindCube V1 and a ZX300 were mounted on a large 6-degree-of-freedom motion platform, side-by-side with an identical set of lidars as reference.

Second, we installed one WindCube V2 offshore and ZX300 onboard the Norwegian research icebreaker R/V Kronprins Haakon, during the cruise JC3 of the Nansen Legacy project [5] in February/March 2022. During this campaign, the wind lidars retrieved wind data up to 300 m height for three weeks in the Barents Sea and the Arctic Ocean as illustrated in Figure 2. We used further sensors in conjunction with these wind lidars to obtain high-resolution motion information, such as tilting, ship position, and ship speed. The aim of this study was to further understand the reliability and accuracy of these instruments under different motion and weather conditions with considering some of the most relevant parameters such as the wind speed and direction, turbulence, pitch, roll, or ship speed over ground.

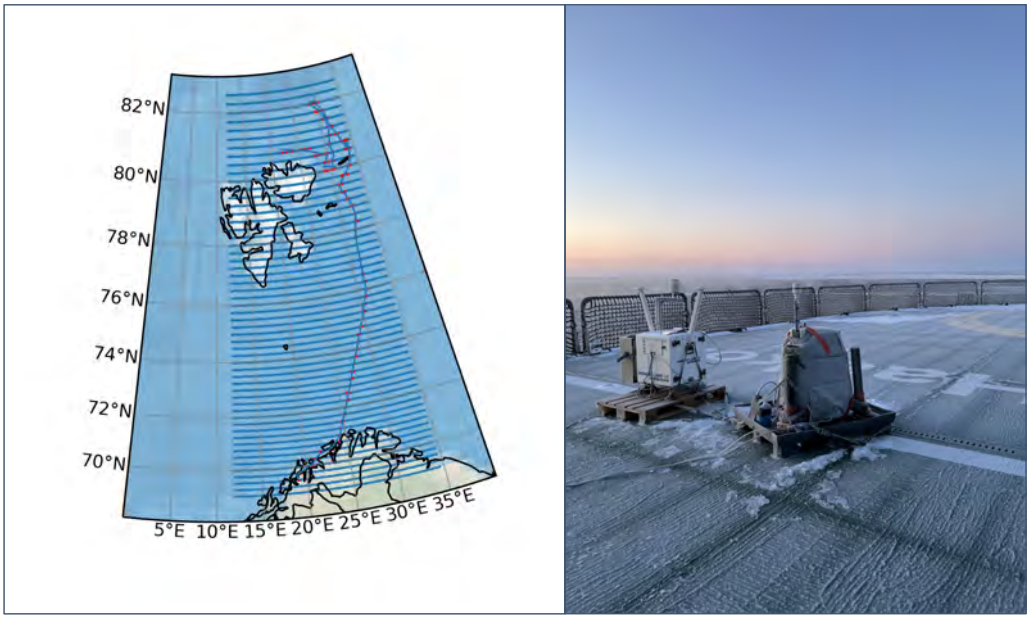

Figure 2: Nansen Legacy experiment: Ship track during the campaign (left), the dotted lines indicate the periods when the systems were not operating. Lidars positioning and setup on the helicopter deck on board R/V Kronprins Haakon (right).

Third, we designed and carried out the Lollex campaign in the period September 2022 to August 2023, as a collaborative effort between Train2Wind and the RWE group [8]. The campaign took place in the area of the Rødsand 2 wind farm (Denmark) operated by the RWE group [7]. In this campaign we installed two types of wind lidars, a WindCube V2 offshore as a vertical profiling lidar and a scanning WindCube 100S, oerated in vertical stare mode, onboard a crew transfer vessel (CTV) as an observational platform of opportunity.

These two instruments were deployed on the stern side of the CTV (see Figure 3). Over the course of a typical working day, the CTV commuted within the wind farm from the morning until the evening, transporting personnel and equipment for the maintenance and repair of individual wind turbines. Hence, wind velocity data within the wind farm was collected for nearly twelve hours per day. As the vessel returned to the harbour in the evening, the lidars continued to measure, allowing the collection of data outside the wind farm.

In this study, we utilized the ship-based lidar setup to characterize vertical velocity fluctuations within and around the offshore wind farm. Our lidar systems were also capable of capturing significant atmospheric events above the wind farm. For instance, the lidar successfully recorded the characteristics of vertical wind associated with the formation and evolution of Kelvin-Helmholtz billows (KHBs) in the atmospheric boundary layer.

Figure 3: Lollex experiment: Temporary installation of lidars onboard the CTV. The WindCube V2 lidar wind profiler (left) and WindCube 100S scanning wind lidar (right) were installed on the stern side in the back of the vessel.

Results and Conclusion

Our study demonstrated that ship-based or buoy-based lidars have significant potential for wind energy applications. Figure 4 compares the reference lidar and moving lidar of each type (WindCube V1 and ZX300) under two scenarios (no motion and yaw motion) in the Grimstad experiment. Panels (a) and (c) display the wind speed differences, while panels (b) and (d) show the correlation between the lidars at two heights of interest (85 m and 145 m from the surface). The WindCube V1 results are shown in blue, and the ZX300 results are shown in orange. When stationary, the wind speed differences between the lidars do not exceed 0.15 m.s^{-1} for the ZX300 and 0.5 m.s^{-1} for the WindCube V1. However, under yaw motion, the ΔU ranges from 0.1 to 0.5 m.s^{-1} for the ZX300 and 0.18 to 1 m.s^{-1} for the WindCube V1. The correlation between the lidars also decreases significantly when exposed to motion, with a more pronounced drop for the WindCube V1 at 145 m from the surface, where it reaches 0.2 m.s^{-1}.

Our findings indicate that the older WindCube profiler, known as WindCube V1, exhibits higher random and systematic errors and is more susceptible to errors when exposed to motion compared to the ZX300 (Figure 4). However, the ZX300 may also exhibit high errors under motion, depending on the frequency of the motion.

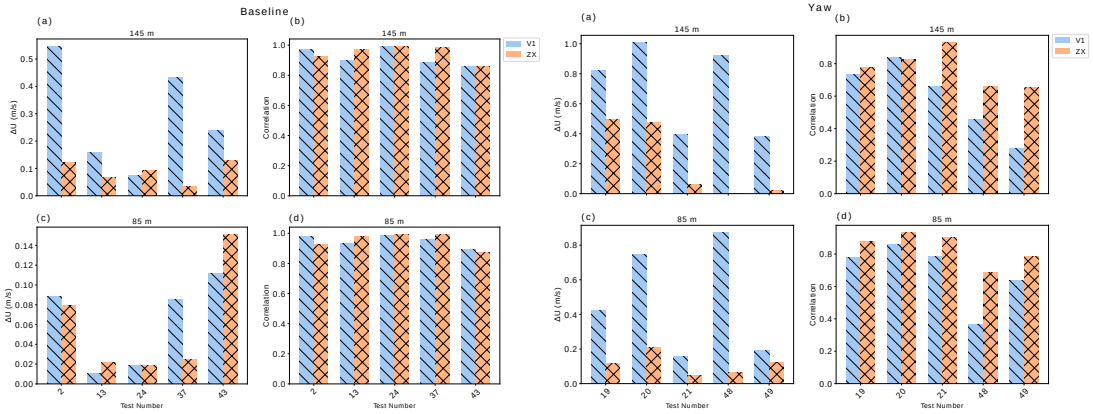

Figure 4: Left: Comparison of lidars in case of no motion (baseline); Wind speed difference between reference and moving lidars at 145 m (a) and 85 m (c). Correlation between reference and moving lidars at 145m (b) and 85m (d). WindCube V1 is shown in blue and ZX300 in orange. Right: Comparison of lidars in case of periodic yaw motion.

Furthermore, the comparison between wind speed measurements by ZX300 and WindCube V2 in the ship-based setup in the Arctic is presented in Figure 5. The left panel in this figure shows wind speed measurements at three heights from the lidar surface: 40 m, 100 m, and 200 m. The lidars demonstrate good agreement in their measurements even under conditions of motion and very low temperatures (-10 to -25 °C). However, the WindCube V2 exhibits greater variability compared to the ZX300, with this variability increasing significantly at 200 m. Due to the WindCube V2's more scattered data, a full motion correction (accounting for all rotations and translational motions) was applied to its results. The comparison of the corrected results with ERA5 reanalysis data [2] is shown in Figure 5 right panel. The results indicate that, after applying motion correction, the WindCube V1 lidar data reached a good agreement with the ERA5 reanalysis data throughout the campaign.

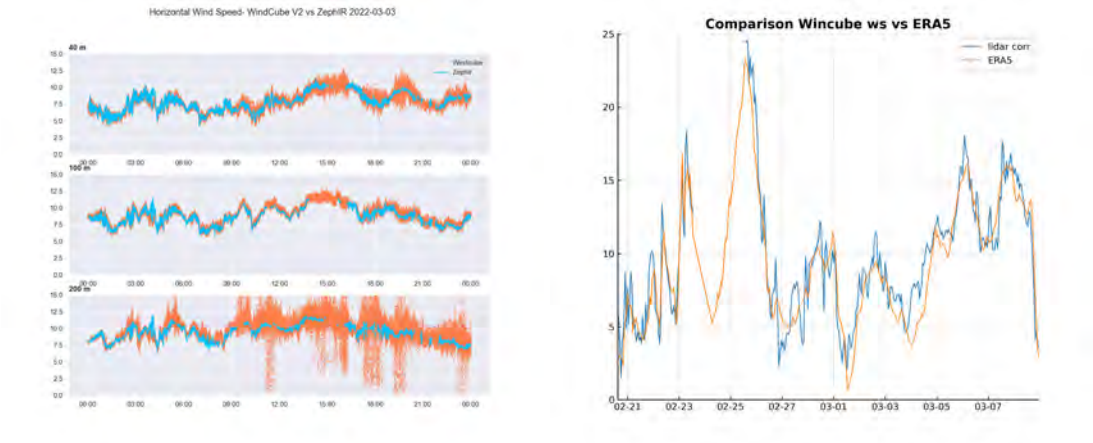

Figure 5: Left : Wind speed measurement comparison between ZX300 (blue) and WindCube V2 (orange) at 40, 100, and 200 m on 2022-03-03. Right : Wind speed measurement comparison between WindCube V2 (orange) after applying motion correction at 100 m and ERA5 reanalysis (blue) during the campaign.

Moreover, the Nansen legacy campaign results demonstrated that ship-based lidar mea-

surements are highly effective for wind assessment in the Arctic. The lidar instruments proved to be reliable and robust even in extreme weather conditions. This indicates that lidar technology has great potential for wind measurements in high latitude regions like Svalbard, where there is an ongoing transition to renewable energy sources.

Lastly, the Lollex campaign results encompass nearly one year of data from in and around the Rødsand 2 wind farm and are currently under analysis. As an initial step in our analysis, we observed that our lidars not only captured wind speed with high accuracy but also can be utilized to investigate structures and layering within the atmospheric boundary layer, exemplified by the detection of KHBs.

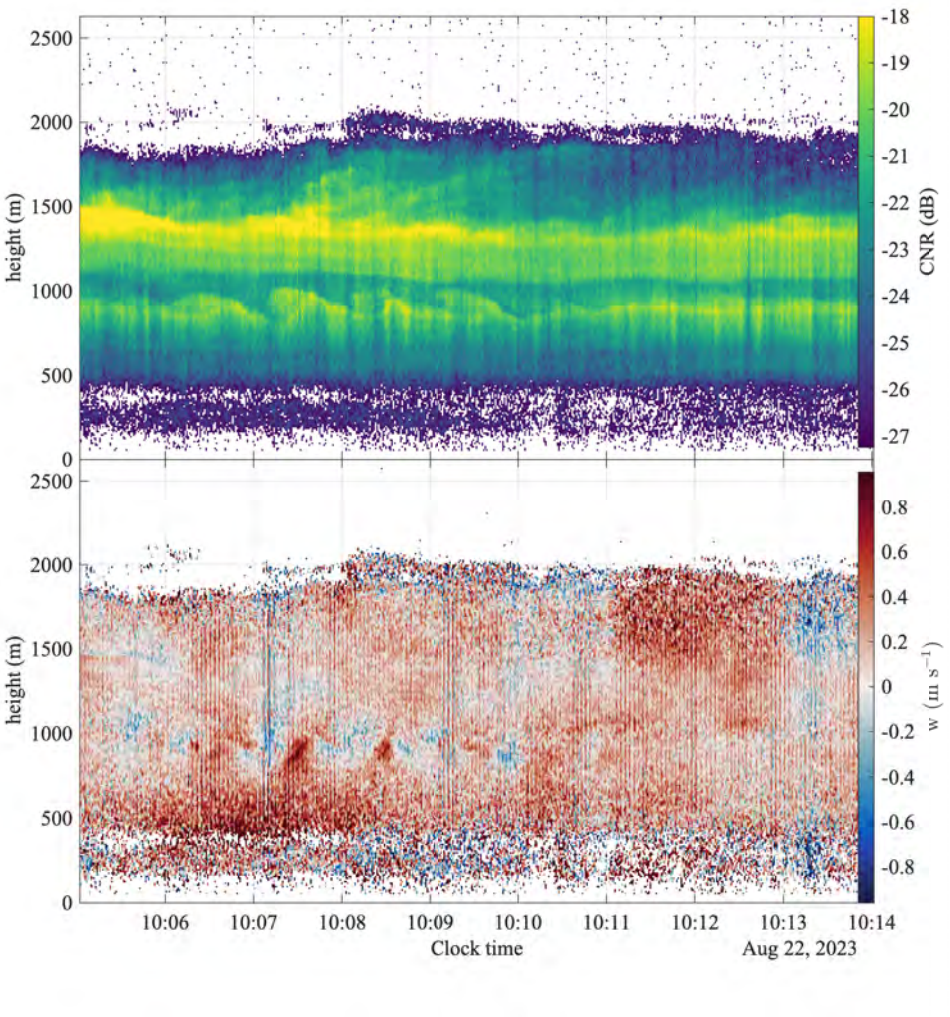

Figure 6: KHBs observed on 2023-08-22 between 10:06 and 10:11 at heights around 600 m and 1000 m above the surface. Time series of the CNR (top panel) and vertical velocity component (bottom panel) recorded by the WindCube 100S in vertical stare mode.

Figure 6 shows about 10 minutes of data (1 Hz resolution) from the WindCube 100S scanning lidar in vertical stare mode from 2023-08-22. The upper panel displays a time-height cross sections of the carrier-to-noise ratio (CNR) and the lower panel shows the corresponding plot for the vertical wind component measured by the lidar. The CNR plot shows a highly dynamic multi-layer structure, including a KHB event lasting for several minutes before dissipating again. These billows are more visually evident in the CNR plot, although the upward and downward vertical velocities are also clearly detectable in the vertical wind plot. This phenomenon was detected multiple times in the measurements, and we analyzed the characteristics of these events in a manuscript currently under review. Our findings indicated that KHBs enhance the vertical mixing of momentum above the wind farm, thereby contributing to velocity deficit recovery in the wake zone.

This campaign demonstrated the potential of using a scanning Doppler wind lidar system in a combination of vertical stare and DBS mode to study the marine atmospheric boundary layer. This setup proved efficient in capturing wind speed details and detecting significant atmospheric events that are usually hard to identify such as KHBs.

Nonetheless, there are some limitations regarding using ship-based lidars. This includes limited space onboard, power supply access, and the need for regular maintenance, especially for the scanning lidar, which is not designed for offshore use. Moreover, condensation, full memory, and internet issues can arise. Therefore, careful planning before such campaigns, calibration, and maintenance are of high importance.

References

[1] P. Achtert, I. M. Brooks, B. J. Brooks, B. I. Moat, J. Prytherch, P. O. G. Persson, and M. Tjernström. "Measurement of wind profiles by motion-stabilised ship-borne Doppler lidar". In: *Atmospheric Measurement Techniques* 8.11 (2015), pp. 4993–5007. DOI: 10.5194/amt-8-4993-2015.

[2] H. Hersbach, B. Bell, P. Berrisford, S. Hirahara, A. Horányi, J. Muñoz-Sabater, J. Nicolas, C. Peubey, R. Radu, D. Schepers, A. Simmons, C. Soci, S. Abdalla, X. Abellan, G. Balsamo, P. Bechtold, G. Biavati, J. Bidlot, M. Bonavita, G. De Chiara, P. Dahlgren, M. Dee D.and Diamantakis, R. Dragani, J. Flemming, R. Forbes, M. Fuentes, L. Geer A.and Haimberger, S. Healy, R. J. Hogan, E. Hólm, M. Janisková, S. Keeley, P. Laloyaux, P. Lopez, C. Lupu, G. Radnoti, P. de Rosnay, I. Rozum, F. Vamborg, S. Villaume, and J.-N. Thépaut. "The ERA5 global reanalysis". In: *Quart. J. Royal Meteorol. Soc.* 146.730 (2020), pp. 1999–2049.

[3] R J Hill, W A Brewer, and S C Tucker. "Platform-motion correction of velocity measured by Doppler lidar". In: *Journal of Atmospheric and Oceanic Technology* 25.8 (2008), pp. 1369–1382. DOI: 10.1175/2007jtecha972.1.

[4] Felix Kelberlau, Vegar Neshaug, Lasse Lønseth, Tania Bracchi, and Jakob Mann. "Taking the Motion out of Floating Lidar: Turbulence Intensity Estimates with a Continuous-Wave Wind Lidar". In: *Remote Sensing* 12.5 (2020), p. 898. DOI: 10.3390/rs12050898.

[5] Angelika HH Renner, Rolf Gradinger, Andreas Altenburger, Pernille Amdahl, Karoline Barstein, Pedro Duarte, Jørn Dybdahl, Kristian Lampe Gjemdal, Lucie Goraguer, Amalie Gravelle, et al. "JC3 Winter gaps cruise: Cruise Report". In: *The Nansen Legacy Report Series* 33 (2022).

[6] Joachim Reuder, Etienne Cheynet, Andy Clifton, Marijn Floris van Dooren, Julia Gottschall, Jasna B. Jakobsen, Jakob Mann, Jose Palma, David Schlipf, Mikael Sjøholm, Juan-Jose Trujillo, Ludovic Thobois, Ines Würth, and Alberto Zasso. *Recommendation on use of wind lidars*. Tech. rep. Bergen, Norway, 2021, pp. 1–33. DOI: 10.5281/zenodo.4672351. URL: http://doi.org/10.5281/zenodo.4672351..

[7] RWE Group. *Rødsand 2 Wind Farm*. https://se.rwe.com/en/projects-and-locations/wind-farm-rodsand/. Online; accessed 2024. 2024.

[8] Train2Wind. *Experimental campaign at the offshore wind farm Rødsand 2 , Denmark "Lolland Experiment (LOLLEX) - Project Description*. Tech. rep. Train2Wind Technical Report, 2023, 17pp.

[9] Sara C. Tucker, Christoph J. Senff, Ann M. Weickmann, W. Alan Brewer, Robert M. Banta, Scott P. Sandberg, Daniel C. Law, and R. Michael Hardesty. "Doppler Lidar Estimation of Mixing Height Using Turbulence, Shear, and Aerosol Profiles". In: *Journal of Atmospheric and Oceanic Technology* 26.4 (2009), pp. 673–688. ISSN: 1520-0426. DOI: 10.1175/2008JTECHA1157.1.

[10] G. Wolken-Möhlmann, J. Gottschall, and B. Lange. "First Verification Test and Wake Measurement Results Using a SHIP-LIDAR System". In: *Energy Procedia* 53 (2014), pp. 146–155. DOI: 10.1016/j.egypro.2014.07.223.

[11] Rolf Zentek, Svenja H. E. Kohnemann, and Günther Heinemann. "Analysis of the performance of a ship-borne scanning wind lidar in the Arctic and Antarctic". In: *Atmospheric Measurement Techniques* 11.10 (2018), pp. 5781–5795. DOI: 10.5194/amt-11-5781-2018.

Work Package 3

Airborne Measurements

Introduction

Jens Bange

Uncrewed aircraft systems (UAS) have various civil applications and are also widely used for movies and advertising. However, most users use UAS only 'out of the box' and are not familiar with the complex technology behind e.g. energy and power management, autopilot systems that enable stable and safe flight, and the data transfer in the background.

The most important objective of the Train^{2}Wind project was to train young scientists in UAS and to explore the technological possibilities and deployment scenarios. The project experimented with open-source autopilot systems, the construction of new aircraft, and the modification of existing systems. In addition, sensor and computer systems were set up to enable atmospheric-physical measurements with high temporal resolution and accuracy on board the UAS. New and modified sensors for air temperature, water vapour content, aerosol particles were designed and tested. The measurement data was evaluated using post-processing and meteorological analysis software (named PASTA) that had to be programmed beforehand, specifically for the project.

Once the measurement systems had been set up on board various UAS, they were tested and calibrated. Since the calibration of the wind-measuring multi-hole flow probe (FHP) takes days when performed manually in the wind tunnel, the idea of a calibration robot was pursued.

The field tests were initially carried out on land at various test sites – e.g. WINSENT and WindForS (`www.windfors.de`) [1, 6, 5], and the MOL-RAO (Meteorologische Observatorium Lindenberg – Richard-Aßmann-Observatorium) of the German Meteorological Service near Lindenberg [2, 3, 4] – which were equipped with very precise meteorological towers. But also upstream and behind wind turbines, some of them off-shore types, which were erected in complex terrain for testing purposes.

In the third preparatory phase, flight strategies through an operating, full-size off-shore wind farm were elaborated, also with the help of Large-Eddy Simulations (LES) carried out by Train^{2}Wind partners. Negotiations were held with the authorities and with the operating company of an offshore wind farm in Denmark. This non-scientific part of preparing a larger field campaign was certainly a new professional aspect for the young scientists. This lengthy process had to be initiated a total of three times and failed in the end. Therefore only one short test campaign was performed at the Denmark site, but many valuable other tests and field experiments at the WINSENT site and the MOL-RAO could be analysed and let to precious scientific insights.

References

[1] Asmae El Bahlouli, Alexander Rautenberg, Martin Schön, Kjell zum Berge, Jens Bange, and Hermann Knaus. "Comparison of CFD simulation to UAS measurements for wind

flows in complex terrain: application to the WINSENT test site". In: *Energies* 12.10 (2019), p. 1992. DOI: 10.3390/en12101992.

[2] Frank Beyrich, Jens Bange, Oscar K. Hartogensis, Siegfried Raasch, Miranda Braam, Daniëlle van Dinther, Doreen Gräf, Sabrina Martin, Aline van den Kroonenberg, Arnold Moene, Bram van Kesteren, and Björn Maronga. "Towards a Validation of Scintillometer Measurements: The LITFASS-2009 Experiment". In: *Boundary Layer Meteorology* 144.1 (2012), pp. 83–112.

[3] Miranda Braam, Frank Beyrich, Jens Bange, Andreas Platis, Sabrina Martin, Björn Maronga, and Arnold F. Moene. "On the discrepancy in simultaneous observations of the structure parameter of temperature by scintillometers and unmanned aircraft". In: 158.2 (2016), pp. 257–283.

[4] Cathy Hohenegger et al. "FESSTVaL: the Field Experiment on Submesoscale Spatio-Temporal Variability in Lindenberg". In: *Bulletin of the American Meteorological Society* 104.10 (2023), E1875–E1892.

[5] K. zum Berge, A. Gaiser, A. Platis, H. Knaus, and J. Bange. "Seasonal Changes in Boundary-Layer Flow over a Forested Escarpment Measured by an Uncrewed Aircraft System". In: 186.1 (2023), pp. 69–91.

[6] Kjell zum Berge, Martin Schön, Moritz Mauz, Andreas Platis, Bram van Kesteren, Daniel Leukauf, Asmae El Bahlouli, Patrick Letzgus, Hermann Knaus, and Jens Bange. "A Two-Day Case Study: Comparison of Turbulence Data from an Unmanned Aircraft System with a Model Chain for Complex Terrain". In: 180 (2021), pp. 53–78.

In situ measurement of the turbulent atmospheric flow interaction with offshore wind farm, including entrainment and deep wind farm wakes

Matteo Bramati

The Umweltphysik group of the university of Tübingen is a pioneering institution for the deployment of Uncrewed Aerial Systems (UAS) for collecting data in the atmosphere. These systems, operated with scientific data collection of for systematic and automated meteorologic sampling are often refereed as Weather-sensing UAS [4]. With this term we refer to small flying systems, operated remotely, with a maximum take-off weight of 25 kg.

Within the Train^{2}Wind project, the EKUT.1 candidate was assigned to the task of providing *in situ* data (turbulent wind vector, temperature, pressure, humidity etc.) by performing a series of flights with such UAS. Those flights would have taken place in a common Intensive Observation Period (IOP) at the Rodsand 2 wind park in the nearby of Lolland Danemark. The UAS data would have been used for a comparison with the other Train^{2}Wind partners (LiDAR & simulations).

Fixed Wings UAS

The fixed wing aircraft of type MASC3 (Multi-purpose Airborne Sensor Carrier-3) was a well established platform already at the beginning of the EKUT.1 project [5]. It is a 4 m wingspan model weighting approximately 8 kg with a pusher engine configuration. It carries in the front a set of sensors that allow a fast sampling of the wind vector, together with pressure, temperature and humidity. This system has been already widely used for meteorological and turbulence sampling providing reliable and unique datasets [2][6].

The plan was to use the system to perform flights withing the wind farm at hub height in order to obtain consecutive sampling of air within the rows of the wind farm. Despite the considerable flight time of the MASC3 - around 1h30min - a problem arose when inspecting the takeoff/landing location: no long enough flat surface was present for the landing procedures of this aircraft. Therefore the choice was taken to operate a more modern version of the system, called MASC-V, able to take off and land vertically thanks to 4 rotors mounted vertically on the fuselage. The sensor systems would have remained the same. At first there was the idea to take off and land from the maintenance vessel that every day sails towards the wind park for routine repairs, however that possibility was quickly discarded as the space available onboard was not enough to grant safety for a 4 m wingspan UAS.

The usage of a this new system required a training plan more intense than usual. The EKUT.1 candidate prepared and organized multiple flight training days together with the colleagues at Uni Tübingen, in order to train the UAS pilots as well as to establish fixed roles for the crew members. The vehicle maintenance was a consistent part of the everyday work. Checklists for the operations, maintenance and repair has been drafted during this training days. Spe-

cial attention was paid to all those modification that would have allowed safe operations offshore: long range telemetry connection and buoyancy in case of emergency landing. Despite these quite challenging requirements, the vehicle was ready for operation for the time of the starting of the IOP in March 2023.

Rotary Wings UAS

The fixed wing UAS measurements provided by the MASC-3 would have been integrated by multi-rotor systems measurements. Differently from the fixed wing systems, multi-rotor can easily hold their position in the air providing fixed point measurements and allowing for vertical profiles. The operation of this types of aircraft is considered easier with respect to the former as they are generally of smaller size and can take off vertically, requiring minimum space [1].

The EKUT.1 candidate was indeed assigned to develop this technology from the first day of employment. Together with other colleagues of Tübingen also employed in Train^{2}Wind, he developed a system based on a commercially available frame (DJI S900). This multi-copter was employed in a first study which aimed at establishing an easily repeatable and low-cost method for calibrating the UAS itself as a wind vector sensor. The same study put the basis for a drag coefficient wind estimation method which highlighted how a bigger cross sectional area could help in enhancing the sensitivity of the multi-rotor to the incoming wind [3]. This system was successfully used to map the wake of an on-shore wind turbine as well as for performing vertical profiles up to 800 m above the ground.

This system was also planned to be deployed in the LollEx campaign, however, the only chance to use it was to takeoff and land from the maintenance vessel. Once more, however, due to the narrow space on the deck of the ship, this plan had to shift and the usage of a smaller multicopter was decided. This second system, based on the commercially available frame of the Holybro X500, was modified by EKUT.1 in order to mimic the bigger DJI S900. With only 50 cm rotor to rotor distance, this system fitted perfectly the requirements in terms of space and safety as well as the floatability in case of incident/malfunction.

The X500 system underwent an analogous calibration like the one described in Bramati, Schön, Schulz, Savvakis, Wang, Bange, and Platis [3] and was equipped with one pressure and humidity sensor (BME280, Bosch). This system was also used during the first visit to the IOP location in September 2022. Even though the purpose of this small two-days test flight was only to prove the operability of the system in a challenging environment such that of a floating platform, an initial set of data were collected and constitute now the EKUT.1 contribution to the project repository in Zenodo.

Results and Conclusions

In the end the crew from Uni Tübingen could not take part to the IOP since the flight permissions from the Danish authorities were not issued on time. Despite the maximum effort from all the people involved in the drafting and modification of the documents, the continuous

negative and unclear feedback from the Danish Aviation authorities delayed the process up to an unsustainable deadline. Therefore the only scientific contribution of EKUT.1 for the Train^{2}Wind project remains the dataset collected with the X500 multirotor and uploaded on Zenodo. Despite the unfortunate fate of the LollEx campaign for the Tübingen crew in terms of scientific results, there are several messages to take home on the topic of IOP organization.

- The location of the experiments should be identified as soon as possible in order to start early enough the flight permission procedures.
- A clear communication between the UAS crew, the project leaders, the facility managers (wind park managers) and the vessel crew is crucial.
- In the aformentioned communication it is extremely important to clarify what each entity is willing (or even allowed) to offer to the others.
- Communication between all the partners should be fast and constructive.

References

[1] Pramod Abichandani, Deepan Lobo, Gabriel Ford, Donald Bucci, and Moshe Kam. "Wind Measurement and Simulation Techniques in Multi-Rotor Small Unmanned Aerial Vehicles". In: *IEEE Access* 8 (2020), pp. 54910–54927. DOI: 10.1109/ACCESS.2020.2977693.

[2] Kjell zum Berge, Martin Schoen, Moritz Mauz, Andreas Platis, Bram van Kesteren, Daniel Leukauf, Asmae El Bahlouli, Patrick Letzgus, Hermann Knaus, and Jens Bange. "A Two-Day Case Study: Comparison of Turbulence Data from an Unmanned Aircraft System with a Model Chain for Complex Terrain". In: *Boundary-Layer Meteorology* 180.1 (2021), pp. 53–78. ISSN: 1573-1472. URL: https://doi.org/10.1007/s10546-021-00608-2.

[3] Matteo Bramati, Martin Schön, Daniel Schulz, Vasileios Savvakis, Yongtan Wang, Jens Bange, and Andreas Platis. "A Versatile Calibration Method for Rotary-Wing UAS as Wind Measurement Systems". In: *Journal of Atmospheric and Oceanic Technology* 41.1 (2024), pp. 25–43. DOI: 10.1175/JTECH-D-23-0010.1. URL: https://journals.ametsoc.org/view/journals/atot/41/1/JTECH-D-23-0010.1.xml.

[4] James O. Pinto, Debbie O'Sullivan, Stewart Taylor, Jack Elston, C. B. Baker, David Hotz, Curtis Marshall, Jamey Jacob, Konrad Barfuss, Bruno Piguet, Greg Roberts, Nadja Omanovic, Martin Fengler, Anders A. Jensen, Matthias Steiner, and Adam L. Houston. "The status and future of small uncrewed aircraft systems (UAS) in operational meteorology". In: *Bulletin of the American Meteorological Society* 102.11 (2021), E2121–E2136. DOI: 10.1175/BAMS-D-20-0138.1.

[5] Alexander Rautenberg, Martin Schön, Kjell zum Berge, Moritz Mauz, Patrick Manz, Andreas Platis, Bram van Kesteren, Irene Suomi, Stephan T. Kral, and Jens Bange. "The Multi-Purpose Airborne Sensor Carrier MASC-3 for Wind and Turbulence Measurements in the Atmospheric Boundary Layer". In: *Sensors* 19.10 (2019). DOI: 10.3390/s19102292.

[6] Martin Schön, Irene Suomi, Barbara Altstädter, Bram van Kesteren, Kjell Zum Berge, Andreas Platis, Birgit Wehner, Astrid Lampert, and Jens Bange. "Case studies of the wind field around Ny-Ålesund, Svalbard, using unmanned aircraft". In: *Polar Research* 41 (2022), pp. 1–15. DOI: 10.33265/polar.v41.7884.

Development of a robot for automatized calibration of multi-hole probes in a wind tunnel

Mosaab Sajidi and Jens Bange

Introduction and motivation

The state of the art [2, 1, 4, 6] for 3D turbulent wind vector measurements aboard fixed-wing UAS (uncrewed aircraft systems) consists of a combination of flow measurements using a multi-hole probe (usually five-hole probe FHP), attitude measurements using an inertia measurement unit (IMU), and satellite navigation (e.g. GPS). The latter two are combined e.g. using a Kalman filter to a high-resolution inertia navigation system (INS) – a technology that is nowadays available for purchase. However, the FHP principle is used almost exclusively in science by highly specialised research groups, and especially for the complex calibration of such probes, in order to achieve very high resolution and accuracy, only individual solutions exist [7, 3].

Subject of the present sub-project was the development of an automatized calibration facility for the research UAS of type 'Multipurpose Airborne Sensor Carrier' MASC-3 [5] and MASC-V (Figure 1), a vertical takeoff and landing UAS manufactured by ELEVONX. Both systems are operated by the Environmental Physics group at the University of Tübingen especially for wind-energy science.

Figure 1: Multipurpose Airborne Sensor Carrier MASC-V during vertical landing. The FHP is mounted at the tip of the nose boom, far in front of fuselage, wings, and rotors.

The calibration process for FHP at the university of Tübingen, used to be a manual, lengthy and exhausting full-day process, starting from setting up the calibration structure in a fashion where the tip of the five hole probe is coincident with the axis of the wind tunnel, and changing the angle combinations 442 times ranging from -20 to 20 degrees with a step of one or two degrees at a time.

The idea was to design a robot that does all of this automatically, and a post processing code, that fulfill the following criteria:

- designed in a manner that does not interrupt the air flow in all angular positions,
- manage to keep the FHP stable during measurement time, and
- avoiding updraft of airflow because of the airfoil,
- accurately position the FHP in the specific range of -20 to 20 degrees in both axis of rotation for an accurate calibration,
- adjust horizontally and vertically to be positioned in the center of the airflow.

Mechanical structure and electronics

From an engineering stand point, motion is the start point, rotation in the X axis, and on the Z axis (pitch and yaw). We decided on having a platform with two hold towers (Figure 2), that allow the rotational movement of the FHP, with arms holding a concave airfoil that holds the electronics and FHP itself. The platform is made of five symmetrical parts that are mounted with each other, using two aluminum load bearing, holding a tower on each end (3D printed in one fold to avoid complex structures) that hold arms and loads, and a heavy motor each, as well as counter weight to balance the platform.

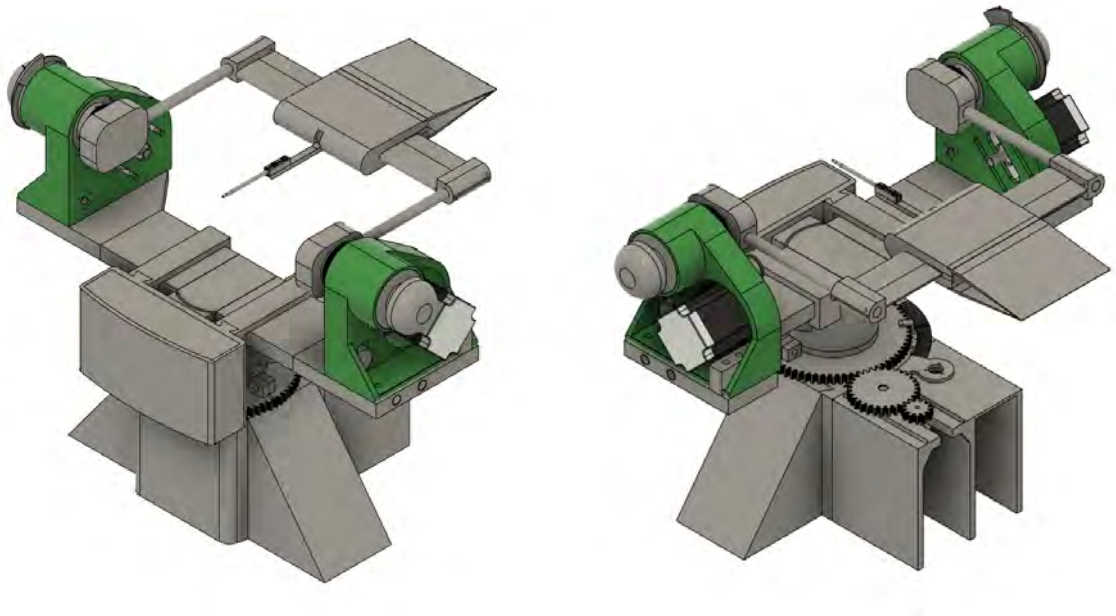

Figure 2: The wind tunnel calibration robot in its latest design version for 3D printing, from two perspectives. Software used: Fusion 360 by Autodesk, Inc. (`www.autodesk.de`).

The platform has a cylindrical form that is also made out of three different parts that are tight fitted. One of those parts is a gear that will eventually connect the platform with the base of the robot. The base is a large area sub-assembly made of four parts. One holds the platform with bearings that reduces the torque needed for moving such inertia, and another that holds the electronics just like the towers do, a motor and a rotary encoder, as well as

two side parts for tipping stability.

All this need energy transfer. On the towers, timing belts were enough for the loads in question, but on the base, a timing belt leads to enormous tension that is simply unsupported by 3D printed structures, so it resulted to the use of gears that were also 3D printed. The whole structure is mounted on a moving table that can be height adjusted with a foot pedal that can either increase or decrease the altitude of the entire robot.

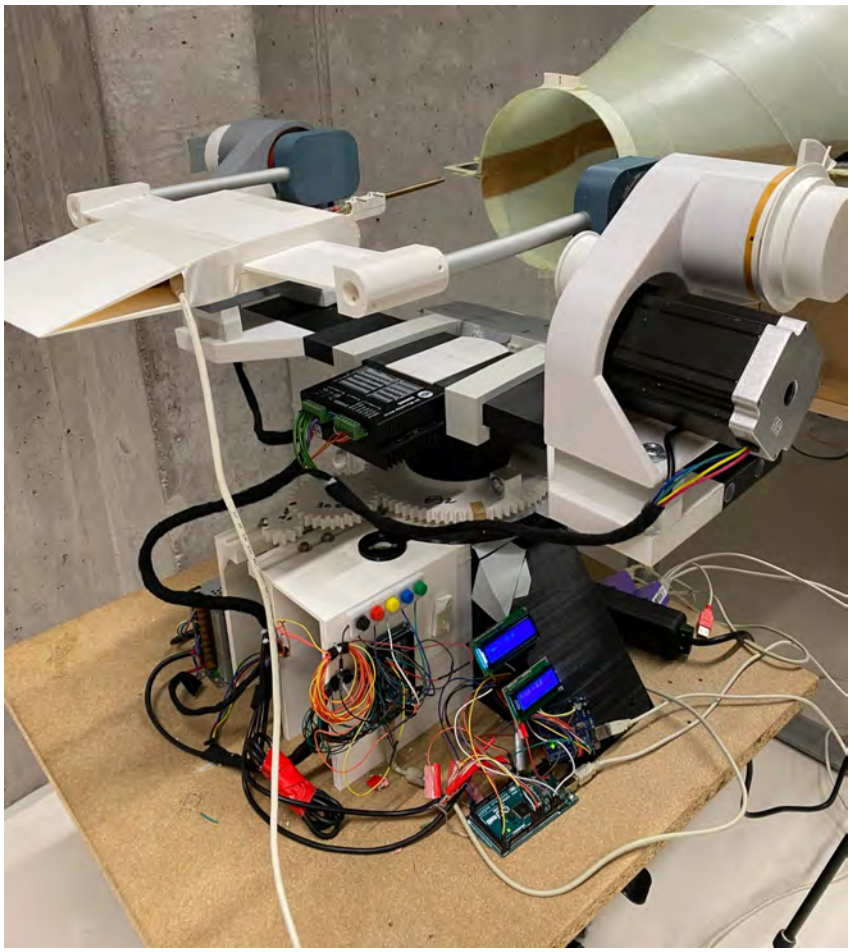

Figure 3: The current version of the robot in the wind tunnel.

This robot (Figure 3) is structured in a command circuit, a power circuit, and a data circuit. The command circuit is an Arduino that is connected to a couple of motor drivers. They send the commands for the motors to move for a certain angle taking into consideration the ratios of the gears and timing belts, also connected to buttons for manual setting to assign the 0 degree position. The power circuit consists of a power source that can provide 15 A to supply the motors through the motor drivers, offering 5 A to each motor. There are two drivers: One controlling the yaw motion and it is connected to one motor, and another driver that is connected to two different motors that are wired differently from one another, one is directly polarised and the other one is reverse polarised (they are symmetrical and they need to rotate in different directions). The data circuit is made out of two Arduinos that each is connected to their respective rotary encoder that will be linked to either the gear chain or the timing belt chain, providing data on the angle combination. This data is

live-streamed through LCD screens that show both pitch and yaw angles of the robot.

Validation

In order to validate the approach, we must first make sure that the robot is actually going to the right positions at the right step, making sure that the robot is reaching all the required positions as accurate or better as the manual calibration. Calibrations were made in the same wind speed and the same conditions (temperature, humidity, and pressure), and ran both calibrations through our post processing code.

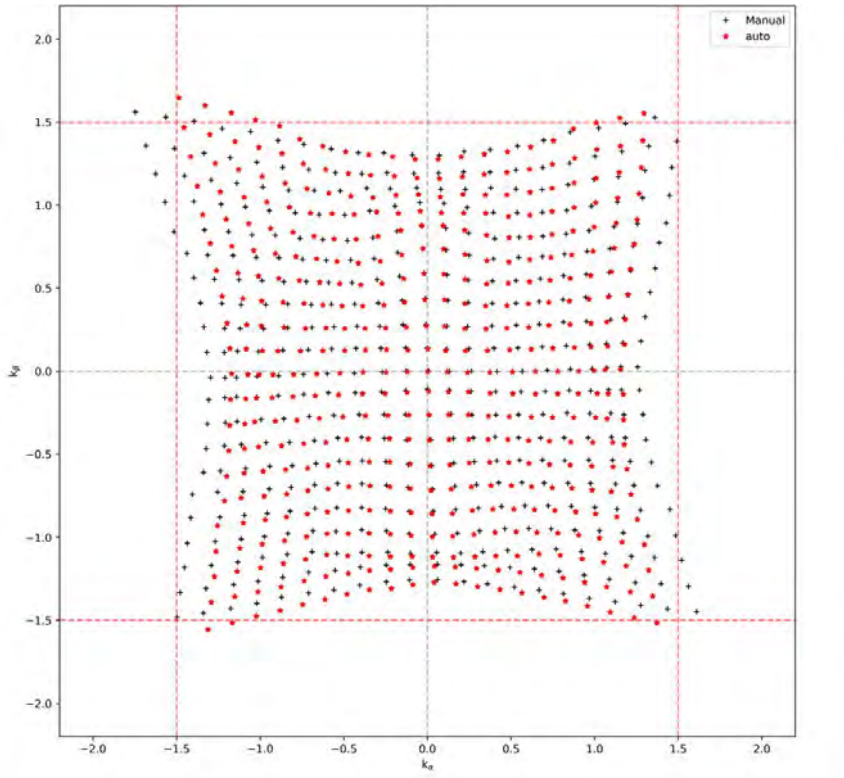

Figure 4: Comparison of the manual and the automatic calibration mesh.

The obtained polynomials of the two calibrations (Figure 4) were applied to on the same flight data set in order to calculate the corresponding true airspeeds (TAS), resulting in a mean offset of 0.014 m/s, an identical standard deviation of 0.127 m/s, with a the correlation of 0.999.

References

[1] Jens Bange, Marco Esposito, Donald H. Lenschow, Philip Brown, Volker Dreiling, Andreas Giez, Larry Mahrt, Szymon Malinowski, Alfred R. Rodi, Raymond A. Shaw, Holger Siebert, Herman Smit, and Martin Zöger. "Airborne Measurements for Environmental Research – Methods and Instruments". In: Wiley, 2013. Chap. 2: Measurement of Aircraft State, Thermodynamic and Dynamic Variables, 641 pp.

[2] Jens Bange, Joachim Reuder, and Andreas Platis. "In: T. Foken (editor) Handbook of Atmospheric Measurements". In: Springer Nature, Switzerland, 2021. Chap. 49: Unmanned aircraft systems, pp. 1333–1351. DOI: 10.1007/978-3-030-52171-4_49.

[3] Alexander Rautenberg, Jonas Allgeier, Saskia Jung, and Jens Bange. "Calibration Procedure and Accuracy of Wind and Turbulence Measurements with Five-Hole Probes on Fixed-Wing Unmanned Aircraft in the Atmospheric Boundary Layer and Wind Turbine Wakes". In: *Atmosphere* 10.3 (2019), p. 124.

[4] Alexander Rautenberg, Martin Graf, Norman Wildmann, Andreas Platis, and Jens Bange. "Reviewing Wind Measurement Approaches for Fixed-wing Unmanned Aircraft". In: *Atmosphere* 9.11 (2018), p. 422.

[5] Alexander Rautenberg, Martin Schön, Kjell zum Berge, Moritz Mauz, Patrick Manz, Andreas Platis, Bram van Kesteren, Irene Suomi, Stephan T. Kral, and Jens Bange. "The Multi-Purpose Airborne Sensor Carrier MASC-3 for Wind and Turbulence Measurements in the Atmospheric Boundary Layer". In: *Sensors* 19.10 (2019), p. 2292. ISSN: 1424-8220. DOI: 10.3390/s19102292. URL: http://www.mdpi.com/1424-8220/19/10/2292.

[6] A. C. van den Kroonenberg, T. Martin, M. Buschmann, J. Bange, and P. Vörsmann. "Measuring the Wind Vector Using the Autonomous Mini Aerial Vehicle M2AV". In: *J. Atmos. Oceanic Technol.* 25 (2008), pp. 1969–1982.

[7] N. Wildmann, S. Ravi, and J. Bange. "Towards Higher Accuracy and Better Frequency Response with Standard Multi-Hole Probes in Turbulence Measurement with Remotely Piloted Aircraft (RPA)". In: *Atmos. Meas. Tech.* 7.4 (2014), pp. 1027–1041. DOI: 10.5194/amt-7-1027-2014.

In-situ measurements of airborne sea salt in offshore wind parks with an uncrewed aircraft system

Vasileios Savvakis

Introduction

As the wind energy sector increasingly exploits offshore wind power due to its numerous benefits (lower surface roughness at sea, higher and more consistent winds, and reduced noise impact on urban centers), a matter of profound concern related to offshore wind turbine operations is corrosion [1]. A driving factor of corrosion in such structures is the presence of aerosol particles like sea salt, which can adhere to turbine blades and other components, leading to increased surface roughness and subsequent aerodynamic losses. The corrosive nature of sea salt exacerbates material degradation, potentially reducing the structural integrity and efficiency of turbines over time. Additionally to that, maintenance costs may rise due to the need for more frequent cleaning and component replacement. It has also been observed that aerosol particles may enhance cloud presence and subsequently decrease wind potential locally, which could result in lower available energy from wind turbines as a whole [2].

The goal of this specific part of the project was to develop a lightweight aerosol sensor system, for deployment on an uncrewed aerial system (UAS) with a focus mainly on aerosol particle (e.g. sea salt) concentration measurements inside offshore wind parks. To achieve this, a series of prerequisites needed to be fulfilled first, which included sensor development and validation, experimental flights, formulating a method for identifying sea salt among other aerosols and preparation of a UAS for usage in highly humid, offshore conditions. Thus, a measurement system based on an optical sensor was constructed, at the necessary weight and dimensions to fit on a multi-rotor UAS of type S900 (DJI, China). Furthermore, a novel mathematical method was conceived, for aerosol identification from the acquired data, based on their hygroscopic behavior. Within the scope of Train^{2}Wind, a measurement campaign was planned to take place in the offshore wind park Rødsand 2 (Rødby, Denmark) after the UAS and its sensors had been finalized, for data collection and consequent analysis of sea salt levels and their effect on the operation and integrity of the wind turbines.

Methodology

For the measurements, an optical particle counter (OPC) of type N3 (Alphasense, United Kingdom) was used, as it is small (7.5 x 6.0 x 6.3 cm) and light (105 g), which favors operation on an airborne platform. The OPC-N3 has a size range of 0.3 to 40 μm across 24 size channels, and outputs particulate matter (PM) types (PM1, PM2.5 and PM10) from bin counts through an internal algorithm. The sensor was equipped with a self-constructed diffusion drying system to ensure accurate measurements at conditions of high humidity. Including

its data acquisition companion computer (at a frequency of 1 Hz), the OPC system has an endurance of 2 h with its own power supply, running independently from the UAS.

The efficiency of the dryer was tested in humid conditions by hovering near a governmental air pollution station in an urban center (Mannheim, Germany), as well as by performing vertical profiles in low altitude clouds at a rural area (Lindenberg, Germany). To identify aerosol types just from OPC measurements, a new method using simultaneous measurements from two OPCs (one with a dryer and one without) was developed, which was based on the calculation of hygroscopic growth factor (GF) and hygroscopicity parameter κ as a result of the difference between ambient and dry air samples. As a preparation for offshore operations, the UAS with the sensor system was also shortly employed at a rural field site on the free flow and wake of a single onshore wind turbine (Schopfloch, Germany), performing vertical profiles from the ground and up to 120 m (above the height of the turbine) in altitude.

Due to a lengthy delay with the organization of the experimental campaign in Rødsand 2, it was eventually not possible to acquire permission for the flight operations at the area of the wind park from the Danish authorities, and the UAS was ultimately not used for that matter. However, short-term measurements from inside the wind park were performed during a two-day campaign onboard a maintenance vessel inside Rødsand 2 in September (2022), and the dual-OPC measurement method was tested for the specific identification of sea salt amounts during this time. Other than that, other kinds of measurements were performed since, and most specifically of mineral dust from the Sahara desert, notably during an intense dust event in the Mediterranean (Cyprus, April 2022) [5].

Results & Discussion

The newly constructed drying channel performed well under laboratory and outdoor conditions. Specifically, a significant decrease (from above 95 % to 41 %) in relative humidity was observed during experiments in a fog chamber before and after the measured airflow passed through the dryer, which was maintained for over 30 minutes. As the component was designed for short-term measurements with a UAS of endurance of 20 – 25 min, the dryer's performance is considered adequate for airborne operations. Results from the hovering flights near the station at Mannheim measuring (among other pollutants) all PM types during a morning of high humidity (89 – 95 %) showed significant overestimation from the OPC system on our UAS when the dryer was not in place, but all measurements were comparable when the dryer was used [4]. This further confirms the effectiveness of the dryer for measurements in high humidity, as is often the case in the marine boundary layer. Vertical profiles through a low-altitude cloud showed that the system can detect layer base (at 64 m above ground for these flights, in perfect agreement with ceilometer CHM 15k operating at the same location) and top very well, due to a sharp increase in PM10 concentrations at the altitude when the UAS entered the cloud layer [4].

Parallel OPC measurements of PM2.5 with and without a drying channel accurately predicted the type of air mass in the case of either continental and marine air, due to the dif-

ference in hygroscopic behavior of sea salt (predominant in marine air) or urban aerosols (predominant in continental air) [3]. This shows that this new approach, while certainly being an approximation to an extent, can indicate the presence of sea salt in the OPC measurements just by taking advantage of two simultaneous measurements (dry air from an OPC with a dryer, and ambient air from an OPC without a dryer). Short measurements on the maintenance vessel in Rødsand 2 showed low PM concentrations of particles mostly up to 2 μm in size during the days of measurements, possibly due to the clear weather conditions of almost no surface wind. The vertical profiles in and out of the wake of an onshore wind turbine showed relatively low aerosol levels under the bottom wake boundary, but higher peaks at nacelle height which persisted up to a distance of 6 D. These preliminary flights are not conclusive, and more measurements should be performed to further investigate this result.

Conclusions

Building on the outcomes of this work, a new approach for the estimation of sea salt levels inside offshore wind parks was developed from the combination of two novel concepts: a small-sized diffusion dryer appropriate for operation with a miniaturised OPC, and a mathematical method for air mass origin indication based on simultaneous OPC measurements from two sensors with just one dryer. The low weight and dimensions of such a system allow it to be mounted on a UAS for in-situ measurements of PM concentrations and size distributions of sea salt from any point inside and in the vicinity of the offshore wind park of interest. The uniqueness and rarity of such a dataset could prove highly useful for better model input of model simulations, as well as the understanding of the dynamics and the effects of the aerosols on the turbines themselves as well as the local weather phenomena.

References

[1] Oyewole Adedipe, Feargal Brennan, and Athanasios Kolios. “Review of corrosion fatigue in offshore structures: Present status and challenges in the offshore wind sector”. In: *Renewable and Sustainable Energy Reviews* 61 (2016), pp. 141–154.

[2] Mark Z Jacobson and Yoram J Kaufman. “Wind reduction by aerosol particles”. In: *Geophysical Research Letters* 33.24 (2006).

[3] Vasileios Savvakis, Martin Schön, Matteo Bramati, Jens Bange, and Andreas Platis. “Calculation of aerosol particle hygroscopic properties from OPC derived PM2.5data”. In: *Meteorologische Zeitschrift* (Feb. 2024), pp. -.

[4] Vasileios Savvakis, Martin Schön, Matteo Bramati, Jens Bange, and Andreas Platis. “Small-Scale Diffusion Dryer on an Optical Particle Counter for High-Humidity Aerosol Measurements with an Uncrewed Aircraft System”. In: *Journal of Atmospheric and Oceanic Technology* 41.3 (2024), pp. 205–219.

[5] Vasileios Savvakis, Martin Schön, Keri A. Nicoll, Claire L. Ryder, Alkistis Papetta, Maria Kezoudi, Franco Marenco, Jens Bange, and Andreas Platis. “In-situ observations of charged Saharan dust with an uncrewed aircraft system”. In: *Aerosol Science & Technology* (2024). Accepted, in production.

Enhancing turbulence measurements in offshore wind farms using UAS and LES

Gabriela Miranda García and Andreas Platis

Introduction

The development of offshore wind farms has significantly increased to meet renewable energy targets, but their wakes can extend several tens of kilometres downstream [9, 8, 7, 1], impacting energy production and structural loads of future farms. Traditional methods like Light Detection and Ranging (LiDAR) and meteorological towers have spatial limitations in characterizing the wind field, whereas UAS can measure turbulence over long distances.

As a UAS of type fixed wing measures the turbulent variables spatially, a minimum flight length and a minimum number of repetitive flight legs are required. Legs not exceeding the largest eddies in size insufficiently sample the dynamic wind field. This causes a systematic error by systematically under- or overestimating the turbulent wind and its standard deviation [10] and causes a random flux error. In order to estimate both errors, 'virtual UAS flights' will be modelled using Large Eddy Simulations (LES) in which the virtual UAS changes its position at each time step of the simulation, thus capturing the instantaneous wind speed. In this way, a spatial data series is obtained to calculate the momentum flux in such a heterogenous wind field, including the systematic and random flux errors according to the expression stated in [5] and [4]. Further, the virtual flights will reveal at which positions and heights the measurements shall be located depending on the atmospheric conditions and wind farm site to gain the most knowledge from the flights.

Methods

For this study, an LES simulation of the wind flow in the offshore wind farm Lillgrund was used. Lillgrund is the largest offshore wind farm in Sweden with 48 turbines located 10 km off the coast of southern Sweden. The turbines have a hub height of 65 m and a rotor diameter of 93 m. The simulation was ran in EllipSys3D [6], with equal grid spacing of 10 m and a total of 480 x 320 grid points on one plane at hub height. Conditions were considered neutral based on a precursor simulation where flow is devoloped without wind turbines. The flow development is controlled by cyclic boundary conditions on all sides, except top and bottom which had a far field velocity specified and a no-slip condition. Once the flow in the precursor is developed, the planes for the wind components u, v, w along the x, y and z axes respectively, were saved for every time step and used as inflow in the wind farm simulation, which replaced the stream-wise cyclic boundary conditions with inlet and outlet boundary conditions.

A flight path was defined over which the momentum flux was calculated using two different techniques. The first technique consisted of generating a time series of wind speed for each

of the points along the flight path. Based on these time series, the average momentum flux for that region was calculated. The second technique consisted of creating a virtual flight in which the UAS changed its position at each time step of the simulation, thus *capturing* the instantaneous wind speed. In this way a spatial data series was obtained to calculate the momentum flux. The time series was considered as the *reference* since it provided constant information about the wind speed changes at each point along the flight path. The momentum flux calculated with the UAS data series was compared with the momentum flux calculated with the *reference* for validation of the minimum flight distance of the UAS. The size of turbulent structures prevailing in the undisturbed flow and in the wake of wind turbines are different, and were studied separately.

As mentioned earlier, the validation of momentum flux calculated using UAS is done by comparing it to a *reference* which source is a time series. When calculating momentum flux using a time series it is crucial to define an appropriate time window. Studies have used the ogive method to assess the suitability of the eddy-covariance method to measure surface fluxes with different time windows [3]. The virtual flight path crosses only grid points to avoid interpolation of the wind speed data at positions outside the grid. Between each point on the path is a distance of 21 meters, which allows the virtual UAS to travel at a speed of 21 m/s, matching the speed of a real UAS. The virtual flight starts from the north end, collecting wind speed data at each point along the path and at each time step, until it reaches the opposite end. Once the UAS is in this end, the first *leg* is considered completed. Then, the UAS returns along the same leg to return to the starting point, completing the second leg. This process is repeated until a total of 20 legs are achieved. Before the UAS starts a new leg there is a lap time that varies randomly between 35 and 55 seconds, which are average values that a UAS takes for making every turn under strong winds in real conditions.

Results & Discussion

To define a time window appropriate for momentum flux calculation from a time series source, and to assess the suitability of the eddy-covariance method for surface fluxes with different time windows, the ogive function was used [2, 3]. The ogive function is a cumulative integral of the co-spectrum between the vertical wind speed (*w*) and another variable, in this case the main wind speed (*u*). The integral is calculated from the highest to the lowest frequencies in the time series. The cumulative integral of the co-spectrum of *u* and *w* equals the covariance of those two variables, therefore we can consider the values in the ogive plot as values of momentum flux. The figure shows that at high frequencies the cumulative integral of the co-spectrum is zero and as we reduce the frequency, it increases until reaching a more or less constant value from a frequency of .001 Hz or its equivalent to 15 min. The output showed that in the time domain a window of 15 min is necessary to capture the largest eddies. If a window is longer than 15 min, the momentum flux will be more or less constant and equal to -.055 $\mathrm{m^2 s^{-2}}$, and if the window is smaller it will be underestimated.

Momentum flux was calculated for different windows, with low values when the window

was below 100 m, but higher as the window size increased. When using a window size of 540 m, the momentum flux reached a plateau at -0.14 $\mathrm{m^2 s^{-2}}$. When the window size was larger the flux remained the same, which indicated that 540 m is sufficient to capture the largest eddies, and that the maximum value has been reached from this length, since from about 900 m the momentum flux decreased again to -0.12 $\mathrm{m^2 s^{-2}}$. The value in the plateau was far away from the *reference*, which means that a single repetition or leg is not enough and that more *legs* need to be averaged. Therefore, the impact of using a larger number of legs (or repetitions) on the mean momentum flux was assessed. A total of 20 legs were considered, and for each of them the momentum flux was calculated using the 540 m window size. Consecutive calculations of average momentum flux as more legs were added showed that after 11 repetitions the *reference* was reached.

A comparison with the time domain momentum flux was performed considering only the section corresponding to the wake. In addition, Root Mean Square Error (RMSE) and Mean Absolute Error (MAE) were used to evaluate the differences. In the first step, only the first leg was considered. The momentum flux was calculated using a window size of 37 m (2 x 18.6 m) and the corresponding RMSE and MAE were determined. Subsequently, the error was recalculated for more legs or repetitions with the same size window size. By increasing the repetitions to 10, it was observed that the RMSE can be reduced from .20 a .10 $\mathrm{m^2 s^{-2}}$, and the MAE from 0.158 to 0.07 $\mathrm{m^2 s^{-2}}$. The virtual flight shows accurate results only at two points close to the turbine, while in the rest of the wake area there is a considerable deviation with respect to the reference, reaching values close to or greater than zero. Therefore, the procedure was repeated for larger window sizes (3 x 18.6, 4 x 18.6, etc...). For all sizes the error was minimal when reaching 10 legs or repetitions. It was shown that the optimal window size is 5 x 18.6 m (93 m) with a MAE of 0.04 $\mathrm{m^2 s^{-2}}$ and a RMSE 0.05 $\mathrm{m^2 s^{-2}}$. This is an interesting result since 93 m coincides with the rotor diameter of the Lillgrund turbines.

Conclusions

The main conclusions drawn from the outcomes of this projects are outlined below:

- This study confirmed the differences in turbulent structure sizes in front of a wind farm and behind a wind turbine.
- The undisturbed area is characterized by large eddies that can reach sizes of 540 m.
- Calculating turbulent fluxes with a UAS under conditions like the ones used in this simulation require a minimum window size of 540 m to capture all eddies.
- The minimum time window required when measuring eddies of 540 m is 15 minutes.
- The minimum window size required to capture entrainment behind a wind turbine with a UAS is equal to the rotor diameter of the wind turbine, in this simulation it is equal to 93 m.
- The minimum time window required when measuring eddies of 93 m was 7 minutes.

References

[1] Beatriz Cañadillas, Richard Foreman, Volker Barth, Simon Siedersleben, Astrid Lampert, Andreas Platis, Bughsin Djath, Johannes Schulz-Stellenfleth, Jens Bange, Stefan Emeis, et al. "Offshore wind farm wake recovery: Airborne measurements and its representation in engineering models". In: *Wind Energy* 23.5 (2020), pp. 1249–1265.

[2] RL Desjardins, JI MacPherson, PH Schuepp, and F Karanja. "An evaluation of aircraft flux measurements of CO 2, water vapor and sensible heat". In: *Boundary Layer Studies and Applications: A Special Issue of Boundary-Layer Meteorology in honor of Dr. Hans A. Panofsky (1917–1988)* (1989), pp. 55–69.

[3] Thomas Foken, Florian Wimmer, Matthias Mauder, Christoph Thomas, and Claudia Liebethal. "Some aspects of the energy balance closure problem". In: *Atmospheric Chemistry and Physics* 6.12 (2006), pp. 4395–4402.

[4] D. H. Lenschow, J. Mann, and L. Kristensen. "How Long Is Long Enough When Measuring Fluxes and Other Turbulence Statistics". In: 11 (1994), pp. 661–673.

[5] J. Mann and D. H. Lenschow. "Errors in Airborne Flux Measurements". In: D 99 (1994), pp. 14519–14526.

[6] Jess A Michelsen. "Basis3D-a Platform for Development of Multiblock PDE Solvers: β-release". In: (1992).

[7] Andreas Platis, Marie Hundhausen, Astrid Lampert, Stefan Emeis, and Jens Bange. "The role of atmospheric stability and turbulence in offshore wind-farm wakes in the German bight". In: *Boundary-Layer Meteorology* (2021), pp. 1–29.

[8] Andreas Platis, Marie Hundhausen, Moritz Mauz, Simon Siedersleben, Astrid Lampert, Konrad Bärfuss, Bughsin Djath, Johannes Schulz-Stellenfleth, Beatriz Canadillas, Thomas Neumann, et al. "Evaluation of a simple analytical model for offshore wind farm wake recovery by in situ data and Weather Research and Forecasting simulations". In: *Wind Energy* 24.3 (2021), pp. 212–228.

[9] Andreas Platis, Simon K Siedersleben, Jens Bange, Astrid Lampert, Konrad Bärfuss, Rudolf Hankers, Beatriz Cañadillas, Richard Foreman, Johannes Schulz-Stellenfleth, Bughsin Djath, et al. "First in situ evidence of wakes in the far field behind offshore wind farms". In: *Scientific reports* 8.1 (2018), p. 2163.

[10] Manfred Wendisch and Jean-Louis Brenguier. *Airborne measurements for environmental research: methods and instruments*. John Wiley & Sons, 2013.

Development and improvement of fast response chilled-mirror hygrometer for UAS measurements

Nicholas Ceccon Libardi

Introduction and motivation

Due to its low impact on wind turbine's power output, when compared to other variables, e.g. wind speed, humidity is a variable often neglected by the wind energy community. However, humidity fluctuations in the atmosphere is a concern for other economical activities, like agriculture, where the crop productivity is directly affected by such variations in the local weather. With the development of wind energy until a couple of decades ago focusing mostly on onshore technology and the lack of noise mitigation technology, most wind farms were installed in remote areas or areas with low demographic density, making it to blend with crop fields in rural areas [1, 4]. With this large number of crops affected by wind farm wakes, measuring humidity becomes a very important activity, in order for farmers to plan ahead and lessen the effects of abrupt changes in the local weather caused by these wind farms that surround them. Moreover, the continuous growth of wind turbines rotor blades, mostly for offshore and near-shore wind farms, but not exclusively, makes this an even greater problem [2].

Figure 1: MASC with its sensorhood mounted on during flight campaign in Lindenberg, Germany. Source: B. Lammel

State-of-the-art

Current technologies suitable for UAS are able to reliably measure fluctuations in humidity up to 1 Hz, which is the case for humidity sensors based on capacitive sensor elements. This number is far from the dissipation range and for meaningful humidity measurements, the sampling frequency should be at least one order of magnitude higher. Another type of humidity sensors is the dew point mirror, or chilled-mirror hygrometer (CMH), depicted in 2. These sensors are known for their high precision at the cost of being large devices, making then unsuitable for airborne measurement. In [3], a miniature fast-response CMH is proposed for fixed-wing uncrewed aircraft systems (UAS). The device is not larger than a

(10x3x2) cm block and a such sensor is capable of measuring humidity up to 10 Hz, which is corroborated by the power spectrum of a single flight. However, the system cannot be reliably used once the Peltier element of the CMH, a main component of the measurement system, is not proven to have the characteristics necessary to measure signals up to 10 Hz. Moreover, the CMH system is affected by the different ambient conditions and its tuned PID controller can become obsolete if ambient conditions change considerably (e.g temperature and dew point).

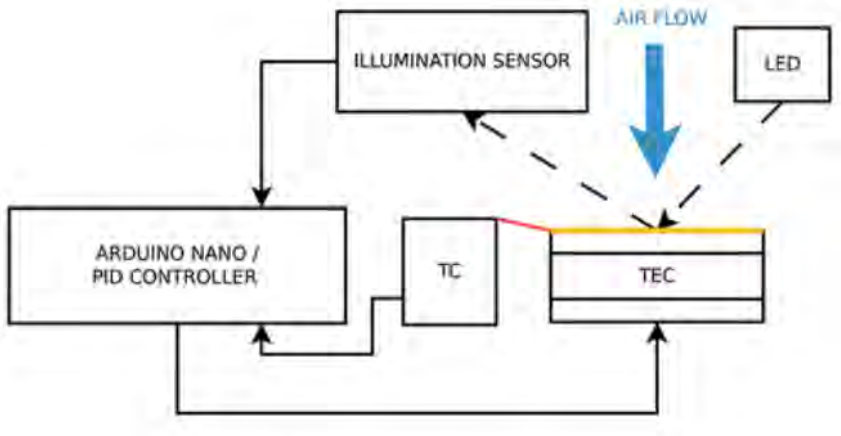

Figure 2: Schematic of the high-frequency chilled-mirror hygrometer [3].

Methodology

In this study, we focused on improving the control of the mirror temperature, which is done by a PID controller. Due to the complexity of the system and the difficult to model that is imposed by such complexity, model-free control methods are the most suitable techniques for the CMH. An example of such type of control is the PID itself. A PID controller takes as input the error between the current state and the desired state of our controlled variable, in our case the mirror temperature, and we multiply the signal by the gain K_P, the integral of the signal multiplied by K_I and the derivative of the signal multiplied by K_D, and the output will be our control action. These gains are fixed values in a standard PID, which can be tuned through different techniques to get the desired controller behaviour before deploying it. With that in mind, we implemented an adaptive PID controller [5], which is able to adjust the controller gains online, based on input information, acting as a self-tuning method during operation. To test the performance of the new controller, we used an in-house developed temperature calibration chamber and wind tunnel to simulate the change in environmental conditions. The results for the temperature chamber tests are depicted in 3 and it is clear that the new controller (A-PID) performs better in bringing the error to zero as the environmental conditions change.

Results and Discussion

To confirm the improvement shown in 3, the CMH with the new controller and the CMH with the former controller should be mounted together to the same UAS during a flight campaign for a realistic comparison. Future research should focus on the thermoelectric cooler, which lies in the core of CMH measurement system. The component should be proven to have the required dynamic characteristics to measure 10 Hz variations in the dew point sensed by the mirror. The same concern applies to the air intake, which is not guaranteed to sample the air without losing information about the humidity fluctuations or adding noise to the signal.

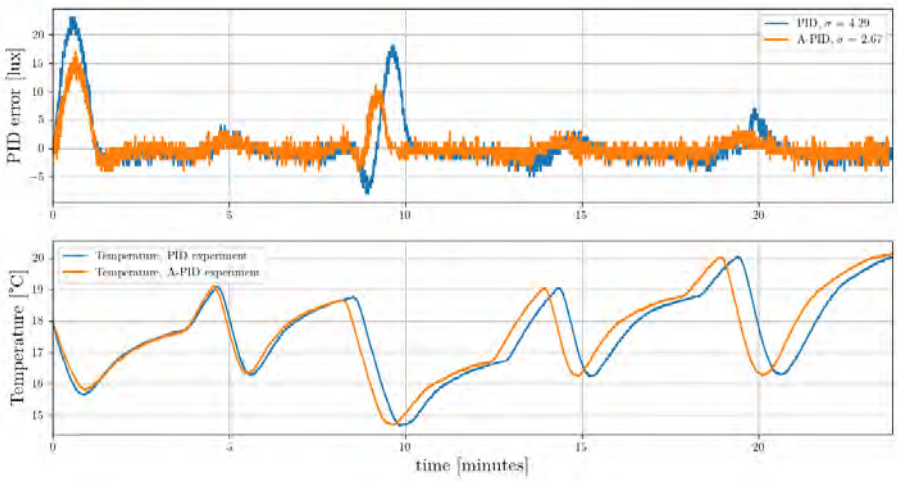

Figure 3: Comparison of the dew-point mirror temperature control using a conventional PID (PID) with tuned gains and an adaptive PID (A-PID) with changing environmental conditions.

References

[1] Kevin A. Adkins and Adrian Sescu. "Wind Farms and Humidity". In: *Energies* 15.7 (2022). ISSN: 1996-1073. DOI: 10.3390/en15072603. URL: https://www.mdpi.com/1996-1073/15/7/2603.

[2] John Stephen Haywood, Adrian Sescu, and Kevin Allan Adkins. "Large eddy simulation study of the humidity variation in the shadow of a large wind farm". In: *Wind Energy* 23.2 (2020), pp. 423–431. DOI: https://doi.org/10.1002/we.2434. eprint: https://onlinelibrary.wiley.com/doi/pdf/10.1002/we.2434. URL: https://onlinelibrary.wiley.com/doi/abs/10.1002/we.2434.

[3] Moritz Mauz, Bram Kesteren, Wolfgang Junkermann, Martin Schoen, Andreas Platis, and Jens Bange. "Miniature high-frequency chilled-mirror hygrometer for atmospheric measurements aboard fixed wing UAS". In: *Meteorologische Zeitschrift* 29 (Nov. 2020). DOI: 10.1127/metz/2020/1026.

[4] Daniel Rajewski, Eugene Takle, Julie Lundquist, Steven Oncley, Thomas Horst, Michael Rhodes, Richard Pfeiffer, Kristopher Spoth, and Russell Doorenbos. "Crop Wind Energy Experiment (CWEX): Observations of Surface-Layer, Boundary Layer, and Mesoscale Interactions with a Wind Farm". In: *Bulletin of the American Meteorological Society* 94 (May 2013), pp. 655–672. DOI: 10.1175/BAMS-D-11-00240.1.

[5] Toru Yamamoto, Kenji Takao, and Takaaki Yamada. “Design of a Data-Driven PID Controller”. In: *IEEE Transactions on Control Systems Technology* 17 (2009), pp. 29–39. URL: https://api.semanticscholar.org/CorpusID:8231642.

Development and Testing of a Multi-Rotor Drone Carrying an Ultrasonic Anemometer for Atmospheric Turbulence Investigations

Mauro Ghirardelli

Introduction

The state-of-the-art method for characterizing atmospheric boundary layer (ABL) turbulence involves in-situ measurements taken by tower- or mast-mounted sonic anemometers, which are then extrapolated over broader areas using scaling theories [6]. This approach has proven insufficient in many scenarios, particularly in the presence of non-stationary flow conditions [8, 7]. Therefore, there is a need for more flexible turbulence sampling strategies. Rotary-wing unmanned aerial vehicles (UAVs) offer a potential solution as they can be used as easily deployable and cost-effective sensor platforms [1, 5]. However, using UAVs equipped with ultrasonic anemometers is still largely unexplored. The main challenges with using rotary-wing UAVs for wind sensing are the propeller-induced flow (PIF) generated by the drone, which can significantly affect measurement accuracy, and the issue of flight stability, as research-grade sonic anemometers add considerable weight to the UAV.

Methodology

The research is divided into two main blocks: one focusing on a sensor placement study to reduce the influence of the PIF on sensor readings and the other on the development and testing of a drone-mounted ultrasonic anemometer prototype. The first part of the research was conducted by performing a parametric study using CFD simulations (Fig. 1a, 1b). These simulations investigated the values of PIF as a function of the radial distance from the fuselage of the drone [3]. Following the CFD simulations, experimental validations were conducted to ensure the accuracy of the findings. These validations included both outdoor [4] and indoor [2] experiments, where PIF was measured experimentally with LIDARs and a moving array of ultrasonic anemometers, respectively. Based on the results of the aforementioned studies, a prototype called SAMURAI-S was developed (Fig. 2a). SAMURAI-S stands for "Sonic Anemometer on a Multi-rotor UAV for Atmospheric Turbulence Investigations in a Sling Load Configuration". This design features an octocopter carrying a sonic anemometer as a payload hanging 18 meters below the main fuselage. A motion compensation algorithm was developed to compensate for the influence of the inevitable swinging of the payload on the measurements. Finally, the SAMURAI-S's reliability and measurement accuracy were tested against two sonic anemometers mounted on a 60-meter mast, showing a great level of similarity in the results (Fig. 2b).

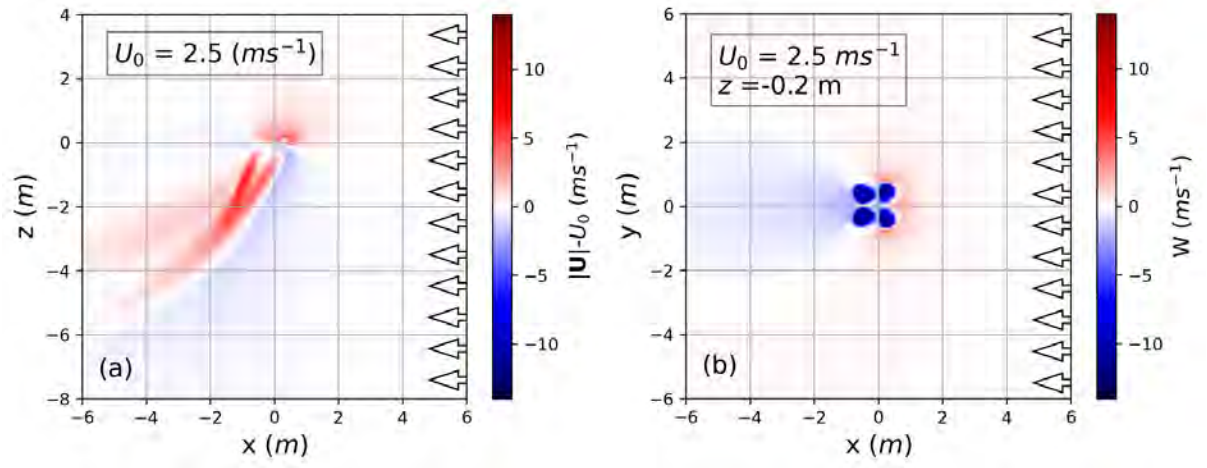

Figure 1: Examples of CFD simulation results. In both panels, the inlet velocity is $U_0 = 2.5ms^{-1}$. A simulated drone is situated at coordinates (0, 0, 0). Panel (a) shows the vertical cross-section of the horizontal flow velocity, while panel (b) depicts a cross-section 0.20 meters below the mean rotor plane of the simulated UAV, showing the vertical velocity.

Figure 2: a) Overview of the SAMURAI-S system featuring a Foxtech D130 UAV with a custom-made payload that includes an RM Young 81000 sonic anemometer. b) The system performing a validation flight close to a 60m mast.

Results and discussion

The results of this research highlight several critical aspects of PIF and the effectiveness of the SAMURAI-S system in measuring atmospheric turbulence. While PIF is more significant closer to the fuselage of the specific multicopter used in this study (an octopter with 0.71m as propeller diameter), it is significantly advected downstream with increasing background flow velocity. Moreover, it was found that PIF had a negligible influence on the free flow at distances greater than 3.7 meters below the drone in the presence of a background flow of 4 meters per second. Without background flow, it is still reduced by more than 60% within 6 meters below the drone. Additionally, the results demonstrate that while the SAMURAI-S system accurately captures the mean wind speed and turbulence characteristics along wind and crosswind directions across various atmospheric conditions, the system shows a slight tendency to overestimate vertical turbulence components, particularly at higher wind

speeds. These findings provide a solid foundation for the development and deployment of the SAMURAI-S system, ensuring its reliability and accuracy in measuring atmospheric turbulence.

References

[1] Pramod Abichandani, Deepan Lobo, Gabriel Ford, Donald Bucci, and Moshe Kam. "Wind Measurement and Simulation Techniques in Multi-Rotor Small Unmanned Aerial Vehicles". In: *IEEE Access* 8 (2020), pp. 54910–54927. DOI: 10.1109/ACCESS.2020.2977693.

[2] Alexander A. Flem, Mauro Ghirardelli, Stephan T. Kral, Etienne Cheynet, Tor Olav Kristensen, and Joachim Reuder. "Experimental Characterization of Propeller-Induced Flow (PIF) below a Multi-Rotor UAV". In: *Atmosphere* 15.3 (2024). ISSN: 2073-4433. DOI: 10.3390/atmos15030242. URL: https://www.mdpi.com/2073-4433/15/3/242.

[3] Mauro Ghirardelli, Stephan T. Kral, Nicolas Carlo Müller, Richard Hann, Etienne Cheynet, and Joachim Reuder. "Flow Structure around a Multicopter Drone: A Computational Fluid Dynamics Analysis for Sensor Placement Considerations". In: *Drones* 7.7 (2023). ISSN: 2504-446X. DOI: 10.3390/drones7070467. URL: https://www.mdpi.com/2504-446X/7/7/467.

[4] L. Jin, M. Ghirardelli, J. Mann, M. Sjöholm, S. T. Kral, and J. Reuder. "Rotary-wing drone-induced flow – comparison of simulations with lidar measurements". In: *Atmospheric Measurement Techniques* 17.9 (2024), pp. 2721–2737. DOI: 10.5194/amt-17-2721-2024. URL: https://amt.copernicus.org/articles/17/2721/2024/.

[5] Stephan T. Kral, Joachim Reuder, Timo Vihma, Irene Suomi, Kristine F. Haualand, Gabin H. Urbancic, Brian R. Greene, Gert-Jan Steeneveld, Torge Lorenz, Björn Maronga, Marius O. Jonassen, Hada Ajosenpää, Line Båserud, Phillip B. Chilson, Albert A. M. Holtslag, Alastair D. Jenkins, Rostislav Kouznetsov, Stephanie Mayer, Elizabeth A. Pillar-Little, Alexander Rautenberg, Johannes Schwenkel, Andrew W. Seidl, and Burkhard Wrenger. "The Innovative Strategies for Observations in the Arctic Atmospheric Boundary Layer Project (ISOBAR): Unique Finescale Observations under Stable and Very Stable Conditions". In: *Bulletin of the American Meteorological Society* 102.2 (Feb. 2021), E218–E243. ISSN: 0003-0007. URL: https://journals.ametsoc.org/view/journals/bams/102/2/BAMS-D-19-0212.1.xml.

[6] M. Mauder, T. Foken, M. Aubinet, and A. Ibrom. "Eddy-Covariance Measurements". In: *Springer Handbook of Atmospheric Measurements*. Ed. by Foken. Cham: Springer, 2021. Chap. 55.

[7] Fernando Porté-Agel, Majid Bastankhah, and Sina Shamsoddin. "Wind-turbine and wind-farm flows: a review". In: *Boundary-layer meteorology* 174.1 (2020), pp. 1–59.

[8] Paul Veers, Katherine Dykes, Eric Lantz, Stephan Barth, Carlo L Bottasso, Ola Carlson, Andrew Clifton, Johney Green, Peter Green, Hannele Holttinen, et al. "Grand challenges in the science of wind energy". In: *Science* 366.6464 (2019), eaau2027.

Selected publications

- For a generic overview of the project, see award-winning poster prepared by the supervisory board: Train^{2}Wind, or How Large is an Infinite Wind Farm?
- Background on the modelling approaches implemented: Database of Modelling Results
- Report on high-resolution sensors: High-resolution sensors
- Visit our website for additional information: Train^{2}Wind

Timeline of the project

1 February 2020
Official project start

February 2020
Kickoff meeting at DTU

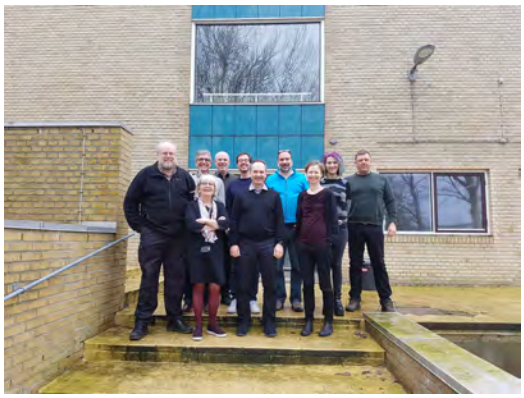

January 2022
Online project meeting

June 2022
Project meeting at DTU

June 2022
Experiment at Rødsand

September 2022
Project meeting in Rødby

May 2023
Wind Energy Science Conference in Glasgow

May 2023
Project meeting in Bergen

August 2023
Industrial workshop at DTU

March 2024
Project meeting in Tübingen

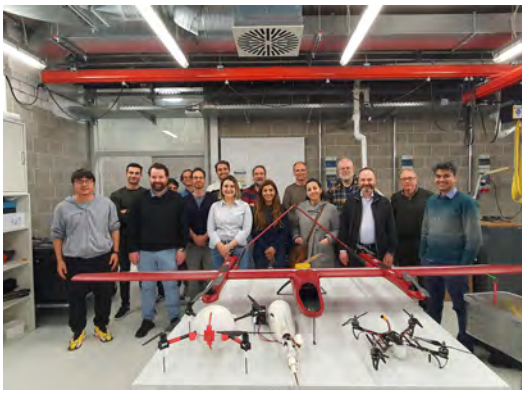

31 July 2024
Project end

Author Index